LUT
Lappeenranta
University of Technology

Niko Nevaranta

ONLINE TIME AND FREQUENCY DOMAIN IDENTIFICATION OF A RESONATING MECHANICAL SYSTEM IN ELECTRIC DRIVES

Thesis for the degree of Doctor of Science (Technology) to be presented with due permission for public examination and criticism in the Auditorium of the Student Union House at Lappeenranta University of Technology, Lappeenranta, Finland on the 7th of October, 2016, at noon.

Acta Universitatis
Lappeenrantaensis 713

Supervisor Professor Olli Pyrhönen
LUT School of Energy Systems
Lappeenranta University of Technology
Finland

Reviewers Professor Ioan Doré Landau
GIPSA-LAB (CNRS/Genoble INP/UJF), Control Department
Grenoble National Polytechnic Institute / Grenoble Alpes University
France

Dr. Tomi Roinila
Department of Automation Science and Engineering
Tampere University of Technology
Finland

Opponents Professor Ioan Doré Landau
GIPSA-LAB (CNRS/Genoble INP/UJF), Control Department
Grenoble National Polytechnic Institute / Grenoble Alpes University
France

Professor Matti Vilkko
Department of Automation Science and Engineering
Tampere University of Technology
Finland

ISBN 978-952-265-995-8
ISBN 978-952-265-996-5 (PDF)
ISSN-L 1456-4491
ISSN 1456-4491

Lappeenrannan teknillinen yliopisto
Yliopistopaino 2016

Abstract

Niko Nevaranta
Online Time and Frequency Domain Identification of a Resonating Mechanical System in Electric Drives
Lappeenranta 2016, 67 pages
Acta Universitatis Lappeenrantaensis 713
Diss. Lappeenranta University of Technology
ISBN 978-952-265-995-8, ISBN 978-952-265-996-5 (PDF)
ISSN-L 1456-4491, ISSN 1456-4491

In modern machinery, the dynamic performance of electric drives is often limited by the mechanical characteristics of the system such as flexibilities. With the growing demand for high-performance machinery, there is an increasing need for techniques to estimate mathematical models in real time that describe these mechanical systems and the possible changes in order to obtain a high-performance control. At the same time, requirements for high reliability are continuously increasing, which significantly motivates to improve system identification methods for the diagnostics and condition monitoring of mechanical parts in electric drives.

A proper real-time system identification method is of great importance in order to obtain an analytical model that sufficiently represents the most important characteristics of the identified system. Even though many identification methods have been proposed in the system identification literature, there is a strong motivation to develop computationally efficient algorithms for online frequency response estimation. Especially, online nonparametric identification could provide several opportunities for fault diagnostics and robust controller design. In this doctoral dissertation, the online system identification of a resonating mechanical system in an electrical drive is studied. The discussion covers closed-loop identification approaches, which are based on both time and frequency domain observations. The time domain identification approach employs a closed-loop output error-based identification routine. In addition, two different types of frequency domain identification approaches are proposed that are based on a time-frequency representation of signals by applying sliding-DFT and Kalman filters. It is shown that the proposed online frequency domain methods provide a good alternative to the conventional time domain online identification solutions.

Theoretical approaches are tested with experimental mechanical test setups that can be regarded as resonating two-mass systems. The experimental results confirm the feasibility of the identification methods by verifying the obtained models according to a given validation criterion, thereby showing that the system dynamics can be identified with an accuracy that makes it possible to apply the proposed approaches for online frequency response analysis.

Keywords: electrical drive, mechanical system, online identification, parameter estimation, system identification

Acknowledgments

The research documented in this doctoral dissertation was carried out over the years 2011–2016 at the Carelian Drives and Motor Centre (CDMC), which is as an independent research unit of the Laboratory of Electrical Drives Technology. The research was partially funded by ABB Drives Oy.

First, I would like to thank Professor Juha Pyrhönen, who acted as my supervisor in the earlier stage of the study, for giving me an opportunity to prepare my doctoral dissertation at LUT. I am grateful to Professor Olli Pyrhönen for the supervision of the doctoral dissertation and Dr. Markku Niemelä for his comments and guidance during this work. Dr. Tuomo Lindh deserves my sincerest thanks for the fruitful discussions concerning different aspects of the research as well as for the scientific guidance regarding various issues in this study. I also would like to thank Dr. Markku Jokinen from ABB for important discussions during the meetings. I would like to express my gratitude to Dr. Hanna Niemelä for her work to improve the language of my doctoral dissertation and articles.

The financial support of the Walter Ahlström Foundation and the Finnish Foundation for Technology Promotion is gratefully acknowledged.

Most of all, with all my heart, I extend my deepest gratitude to my wife Miia for her encouragement and patience she have had with me throughout the years. I thank my daughter Linnea for her limitless supply of bright smiles and motivating baby-babbling during the days (and nights!).

Niko Nevaranta
October 2016
Lappeenranta, Finland

“Teoriassa käytännöllä ja teorialla ei ole mitään eroa, mutta käytännössä on”

Y. Berra

Contents

List of publications

This doctoral dissertation is based on the following papers. The rights have been granted by the publishers to include the papers in dissertation.

I. Nevaranta, N., Niemelä, M., Lindh, T., Pyrhönen, O., and Pyrhönen J. (2013), "Position Controller tuning of an Intermittent Web Transport System using Off-line Identification," in *Proc. of the 15th European Conference on Power Electronics and Applications (EPE)*, pp. 1–9, Lille, France, September 2013.

II. Nevaranta, N., Parkkinen, J. Niemelä, M., Lindh, T., Pyrhönen, O., and Pyrhönen J. (2014), "Recursive identification of linear tooth belt drive," in *Proc. of the 16th European Conference on Power Electronics and Applications (EPE)*, pp. 1–8, Lappeenranta, Finland, August 2014.

III. Nevaranta, N., Parkkinen, J., Lindh, T., Niemelä, M., Pyrhönen, O., and Pyrhönen J. (2015), "Online Estimation of Linear Tooth-Belt Drive System Parameters," *IEEE Transactions on Industrial Electronics*, 2015, vol. 62, no. 11, pp. 7214–7223.

IV. Nevaranta, N., Parkkinen, J., Lindh, T., Niemelä, M., Pyrhönen, O., and Pyrhönen J. (2015), "Online Identification of a Mechanical System in the Frequency Domain with Short-Time DFT," *Modeling, Identification and Control*, 2015, vol. 36, no. 3, pp. 157–165.

V. Nevaranta, N., Derammelaere, S., Parkkinen, J., Vervisch, B., Lindh, T., Stockman, K., Niemelä, M., Pyrhönen, O., and Pyrhönen J. (2016), "Online Identification of a Mechanical System in Frequency Domain using Sliding DFT," *IEEE Transactions on Industrial Electronics*, 2016, vol. 63, no. 9, pp. 5712–5723.

VI. Nevaranta, N., Derammelaere, S., Parkkinen, J., Vervisch, B., Lindh, T., Niemelä, M. and Pyrhönen, O. (2016), "Online Identification of a Two-Mass System in Frequency Domain using a Kalman Filter," *Modeling, Identification and Control*, 2016, vol. 37, no. 2, pp. 133–147.

Nomenclature

To clarify the nomenclature used in **Publications I–VI**, some of the symbols listed below are provided with their different meanings in the respective publications, indicated by (**I**)–(**IV**).

Symbol		
A	state transition matrix	–
A	amplitude (**VI**), area (**I**), steady-state error (**I**)	–
$A(z)$	discrete-time transfer function polynomial (denominator)	–
a_0, a_1, a_2, a_3	discrete-time transfer function parameters (denominator)	–
$B(z)$	discrete-time transfer function polynomial (numerator)	–
b_0, b_1, b_2, b_3	discrete-time transfer function parameters (numerator)	–
b_s	belt damping constant (**II**), (**III**), (**V**)	Ns/m
C	measurement matrix	–
$C(z)$	transfer function of the controller	–
$C_{pc}(z)$	transfer function of the position controller	–
$C_{pos}(z)$	transfer function of the position controller	–
$C_{torq}(z)$	transfer function of the torque controller	–
$C_{vc}(z)$	transfer function of the velocity controller	–
$C_{vel}(z)$	transfer function of position controller	–
D	belt damping constant (**I**), (**IV**), (**VI**)	Ns/m
d	time delay	–
E	modulus of elasticity	N/m^2
$e(k)$	error signal	–
F	force	N
f	frequency	Hz
f_{res}	resonance frequency	Hz
$G(z)$	transfer function of a system	–
I	identity matrix	–
J	inertia	kgm^2
j	imaginary unit	–
K	Kalman gain matrix	–
K	spring constant	N/m
K_{eff}	equivalent spring constant	N/m
K_{ffv}	feed-forward gain (**I**)	1/s
K_p	velocity control gain (**I**)	1/s
K_{pc}	position control gain (**I**)	1/s
K_{vc}	velocity control gain (**II**)	1/s
k	discrete time instant, index (**V**)	–
L	gain vector	–
L_2	distance between rollers (**I**)	m
l	length	m
M	maximum peak magnitude	–

m	rate of frequency increase (**VI**)	–
m_L	mass of the cart and the load	kg
N	normal force (**I**), number of samples	N, –
N_f	number of frequencies	–
n	output noise	–
n_b	number of numerator coefficients	–
$\mathbf{P}$	covariance matrix	–
P_ffv	velocity feed-forward gain	1/s
Q_k	constant for damping (coupling dependent)	–
q	order of the system	–
R	term for cross-correlation between different signals	–
r	radius	m
r_u	excitation signal	–
$S(s)$	sensitivity function	–
$S_\mathrm{uy}(\mathrm{j}\omega)$	cross-spectral estimate between input and output signals	–
$S_\mathrm{uu}(\mathrm{j}\omega)$	auto-spectral estimate of input	–
$S_{\mathrm{r_u r_u}}(\mathrm{j}\omega)$	auto-spectral estimate of excitation signal (**VI**)	–
$S_{ww}(\mathrm{j}\omega)$	auto-spectral estimate of excitation signal (**V**)	–
s	Laplace-domain variable	–
T	torque	Nm
$T(s)$	complementary sensitivity function	–
T_i	integration time	s
T_s	sampling time	s
t	continuous time	–
u	input	–
v	velocity	m/s
$W(s)$	weighting function	–
w	excitation signal (**V**)	–
X_k	kth harmonic component	–
$\mathbf{x}$	state vector	–
x	cart position	m
y	output	–
z	time-shift operator	–

Greek alphabet

γ	coherence
δ_V	normalized Vinnocombes distance
ε	prediction error, residual
ε_max	maximum acceptable steady-state error (**I**)
ζ	damping ratio (**III**)
$\boldsymbol{\theta}$	parameter vector
θ	angular position (**I**)
λ	forgetting factor (**II**), (**III**), tuning parameter (**IV**)
μ	friction coefficient

$\boldsymbol{\varphi}$	regression vector	
φ	angular position	rad
τ	index for lag terms	
ϕ	phase	
Ω	angular velocity	rad/s
ω	angular frequency	rad/s
ω_b	bandwidth frequency (**I**)	rad/s
ω_n	natural frequency (**III**)	rad/s
ω_{res}	resonance frequency	rad/s

Subscripts

act	actual
CL	closed loop
DC	dc offset
eff	equivalent
fr	friction
im	imaginary
max	maximum
min	minimum
re	real
ref	reference
sys	system
tot	total

Abbreviations

ac	Alternating current
ARX	Autoregressive with exogenous inputs
ARMAX	Autoregressive moving average with exogenous inputs
CLOE	Closed loop output error
dc	Direct current
DFT	Discrete Fourier transform
DSP	Digital signal processor
FTR	Fourier transform regression
LS	Least squares
LTI	Linear time invariant
MIMO	Multi input multi output
OE	Output error
PI	Proportional integral
PID	Proportional integral derivative
PLC	Programmable logic controller
RLS	Recursive least squares
RPEM	Recursive prediction error method
RPLR	Recursive pseudolinear regression

PAA	Parameter adaption algorithm
PEM	Prediction error method
PMSM	Permanent-magnet synchronous motor
PRBS	Pseudo random binary signal
SDFT	Sliding discrete Fourier transform
SISO	Single input single output
XOR	Exclusive-or

1 Introduction

In many industrial and robotics applications, precise control of speed and position is essential in order to enhance quality and productivity, and to maintain high reliability. Nowadays, high-performance ac electrical drives constitute a major proportion of industrial motion control applications as they have replaced hydraulic and pneumatic actuators or dc drives in modern machinery such as robotics, machine tools, material handling, and packaging, to name but a few. Almost every motion control system includes some kind of flexibility as a result of the mechanical structure, which may set challenges for the control design, because the dynamic performance is usually reduced by the mechanical resonances of the system. With the growing demand for high-precision machinery, there is an increasing demand for techniques to estimate mathematical models that describe these elastic effects in order to obtain high-performance control. At the same time, requirements for high reliability are continuously increasing, which significantly motivates to improve methods and tools for the diagnostics and condition monitoring of mechanical systems. As the deterioration of mechanical parts over time or other unexpected changes in the system dynamics may lead to the degradation of the control performance or cause unexpected interruptions, it is important to detect the system changes as proactive maintenance before they lead to performance degradation. For these reasons, real-time system identification techniques may provide a viable solution for monitoring of the mechanical parts of a drive.

Typically, the mechanical parts of the electrical drive consist of an actuator (electric motor) and several moving or rotating masses, which are coupled together with flexible mechanical transmissions such as gearboxes, belts, or long shafts, leading to flexible structures and thereby resulting in mechanical resonances. In many industrial applications, the mechanical parts of the drive systems may have a very low resonance owing to the structure of the system such as 1) a coupling between a long shaft and a large load-side mass in rolling mills (Dhaouadi et al., 1993) and paper machines (Michael and Sacafas, 2007); 2) flexible transmission rope in elevators (Kang and Sul, 2000), or 3) flexible couplings in robotic arms (Wernholt, 2007). Often, these mechanical loads are approximated as a two- or three-mass system in order to simplify the system modeling by taking into account the dominant resonance frequencies. Even though the real mechanical system should be regarded as a complex multi-mass system in most cases, simplified two-mass or three-mass approximations have been successfully used for control design purposes to describe different systems, for example, a two-mass-system approximation in the case of rolling-mill drives (Dhaouadi et al., 1993) and conveyor drives (Hace et al., 2007), and correspondingly, a three-mass-system in the case of elevators (Kang and Sul, 2000), and other production processes such as windmills (Muyeen et al., 2007).

Naturally, the system complexity and the required model accuracy can pose challenges in terms of mathematical modeling. In general, the models can be obtained either by considering 1) physical modeling, which is essentially a theoretical approach based on physical laws and other well-established relationships; 2) system identification, which is

an experimental approach based on measurements from the system, or 3) by applying a combination of both approaches rather than by using one method only. However, in many cases, the physical models can be very complex and even impossible to obtain, because calculating the mechanical parameters can be a highly complex task, or specific 'datasheet values' are not available. For these reasons, the identification of a mechanical system in electric drives has become an increasingly important feature in different high-performance motion control applications such as a labeling machine in (Peretti and Zigliotto, 2009) or robotic arms in (Wernholt and Gunnarsson, 2006). As the control performance plays a major role in these applications, the increasing demand for high reliability significantly contributes to the improvement of methods, tools, and techniques for the identification of a mechanical system. Accurate models are essential for supervision and diagnostics purposes similarly as for mechanical design, performance simulation, and the like.

In this doctoral dissertation, the online system identification of a mechanical system in an electrical drive is studied. In this chapter, the background and motivation of the study are presented together with a short introduction to the field of system identification and general terminology. This dissertation consists of an introductory part, a summary of the journal publications, and six original publications. The introduction is divided into four chapters providing conclusions of the relevant publications.

1.1 Background of the study

Constructing mathematical models from observed data that sufficiently represent the principal dynamics of a dynamic system is a fundamental element in science. The term 'system identification' is usually applied especially when the area of control engineering is considered. Naturally, this is an important subtopic also in other fields, because a lot of the early work on identification and parameter estimation was developed by the statistics, econometrics, and time-series community. The period of 1930–1955 is widely recognized as the period of 'classical' control theory, but introduction to the system identification theory came in the 1960s by Kalman and Bucy with the development of the state-space representation for a model-based control. Subsequently, the introduction of the ARMAX (AutoRegressive Moving Average with eXogenous inputs) model by Åström and Bohlin (1965) can be regarded as a turning point in the field as it led to the predominance of the parametric prediction error identification methods (PEM) in various applications (Vassiljeva, 2012).

From 1965 to the late seventies, the model-based control was widely employed in various applications and systems by using models obtained through the developed identification techniques (Gevers, 2006). During this period, the identification was usually performed off-line using the available iterative techniques, and followed by a control design step. Soon after this, the development in the field of adaptive control (Åström and Wittenmark, 1973), (Landau, 1979), which is another example of the model-based control, produced control-goal-oriented parameter adjustment schemes that similarly focused on the

identifiability issues. Obviously, these research fields could be linked to each other as there was a close connection between iterative approaches to the identification for control and adaptive control. Because the adaptive control design is strongly connected to system estimation, the recursive nature of the applied parameter estimation techniques provided effective techniques for real-time system identification. As a result, some of the most widely recognized online parameter estimation techniques used in different servomechanisms and other applications are the extended Kalman filter (EKF) and recursive least squares (RLS) based methods.

In the seventies, the focus of the system identification studies shifted to problems related to the closed-loop identification (Gustavsson et al., 1977), and the objectives changed towards finding the best possible approximate model from a candidate set of models rather than searching for the explicit 'true' model. This period also determined the fundamental theory behind the closed-loop identification methods, which basically depend on the assumptions made of the nature of the feedback, and are thus classified as direct, indirect, or joint input-output identification methods. Some possible alternatives are for instance the refined instrumental variable method, the joint input-output method, the two-stage method, the indirect method, and the method of coprime factors; an extensive review of these methods can be found in (Landau and Karimi, 1997b), (Forssell, 1999), and (Gilson et al., 2011).

The time domain parameter identification approaches received a lot of attention because of their accuracy and straightforward presentation of the theoretical relations of systems, like transfer functions in the estimation routines, which somewhat limited the development of the frequency domain identification methods. Even though many results had already been established in the frequency domain identification (Ljung and Glover, 1981), in the nineties, significant research activity in the area led to the derivation of the theories of the 'modern' frequency domain identification (Pintelon and Schoukens, 2001). One of the main reasons behind the growth of these methods was the establishment of the robust control theories in the eighties as most of the analysis and design tools had been developed in the frequency domain. This led to the need for tools and techniques to obtain frequency domain models with uncertainty descriptions. Typically, the frequency domain spectral analysis includes calculations of a discrete Fourier transform of the measured data, which is often performed off-line. Previously, because of the limited memory and calculation capacity, these calculations were not usually desirable features for practical real-time applications, and for this reason, the online frequency domain identification methods were not as recognized as the time domain methods. Even though there are still computational limitations in some industrial applications, nowadays, online frequency domain identification methods have been adopted. Modern power electronics devices equipped with FPGA and digital signal processors (DSP) are capable of handling extensive calculations. For example, a recent study by (Cespedes and Sun, 2014) has applied online impulse-response analysis for gain-scheduling control design in order to guarantee the stability of a grid-connected inverter.

1.1.1 Identification of resonating mechanical systems

In the literature there are numerous papers describing identification techniques for various mechanical systems. In general, a mechanical system can be identified either in the off-line or online mode by time or frequency domain observations. Broadly speaking, traditional identification techniques can be divided into two main categories: nonparametric estimation methods (Heath, 2001) and parametric estimation methods (Ljung, 1987). When first faced with an unknown plant, it is often a good starting point to perform a nonparametric model identification such as a frequency response analysis. This is one of the main reasons why the frequency domain offline identification techniques are widely recognized for commissioning purposes, and they have been successfully applied to the identification of closed-loop-controlled resonating mechanical systems (Villwock and Pacas, 2008), (Wertz et al., 1999) and (Peretti and Zigliotto, 2009). The common factor of these approaches is the fact that in the commissioning state, a low-bandwidth PI controller is used, and a pseudo random binary signal (PRBS) is superposed to the controller output in order to obtain a valid result from the direct identification. Typically, in the commissioning state, the controller tuning is based on the rough assumption of the total inertia of the system under study (Schütte et al., 1997). Although the obtained frequency response of the system gives a good overview of the dynamical behavior (Ferretti et al., 2003), the offline frequency domain identification tools typically include a parameter fitting step for the tuning of controllers (Pacas et al., 2010) or for the observer design that is used for online monitoring of the plant (Bähr and Beineke, 2007). Naturally, this requires an assumption of a certain model structure to obtain a reasonable parametric model as discussed in (Yoshioka and Hanamoto, 2008).

On the other hand, the polynomial-based time domain identification approaches have also been considered for off-line commissioning purposes of resonating mechanical systems. Recent studies (Łuczak and Nowopolski, 2014) and (Saarakkala and Hinkkanen, 2013) have applied the direct identification to compare the validity of different types of discrete-time polynomial models by superposing the PRBS to the output of a low bandwidth PID-type controller. These studies have shown that the model structure of output error (OE), without a disturbance model, gives adequate results even though the data have been obtained in a closed loop, and direct identification has been applied. Similar observations have been reported in robot identification studies (Wernholt and Gunnarsson, 2006). Similarly, for online identification purposes, the polynomial-based time domain methods have been successfully applied to the direct online parameter estimation by considering their recursive form (Eker and Vural, 2003) and (Garrido and Concha, 2013).

The above-discussed studies mainly focus on the direct identification of a resonating mechanical system under closed-loop conditions, but the system identification literature also covers numerous practical examples of applying some of the well-established closed-loop identification methods. Some of methods have been successfully applied to the off-line identification of different mechanical drivelines such as the instrumental variable method for robot identification (Janot et al., 2009), the two-stage method to the

identification of a sugar crush mill (Partanen and Bitmead, 1995), the method of coprime factors (Graham and de Callafon, 2006) for a PID-controlled multi-mass system, and the simple indirect method for wind turbine identification (Novak et al., 1995). However, some of these closed-loop identification methods require extensive calculations, which have limited their usage for online identification purposes. The family of 'closed-loop output-error' (CLOE) has provided an efficient solution for online identification (Landau and Karimi, 1997a) and (Landau and Karimi, 1997b). The CLOE method has been successfully applied to the recursive identification of a flexible three-mass mechanical system (Landau and Karimi, 1997a). For a more detailed description of the OE-based identification of a flexible mechanical system in closed and open loop, see (Landau and Zito, 2011). Moreover, a more recent study (Saarakkala and Hinkkanen, 2015) has presented a modified indirect CLOE method for off-line parameter estimation of a closed-loop-controlled two-mass system.

1.2 Research methods and objective of the study

This doctoral dissertation aims at investigating closed-loop online system identification methods by which the resonating mechanical system in an electric drive can be identified when the system is excited with a persistent excitation signal. Particular attention is paid to identify the changes in the system dynamics by focusing on systems that have inherently varying resonances owing to the mechanical structure, or the resonance can change during the operation. Considering the research focus, based on an extensive literature analysis, the following research questions were set to pursue the research objectives of this doctoral dissertation:

1) *How applicable are the online system identification techniques for parameter estimation of a time-varying resonating system in electric drives?*

   a) Does the two-mass approximation sufficiently capture the essential system dynamics?

2) *How can online system identification be carried out in the frequency domain by tracking a selected band or set of frequencies using a computationally simple procedure as a possible identification approach?*

   a) Is it reasonable to monitor the region around the first resonant frequency in order to identify the dominant system dynamics?

The identification problems studied in this dissertation are treated as linear time invariant (LTI) ones and carried out in the time and frequency domains using various identification methods. The time domain identification method considered in this dissertation is based on the recursive polynomial-based closed-loop output-error method (CLOE), which is studied in the case of a parameter-varying mechanical system. It should be noted that in previous studies by (Landau and Karimi, 1997a) and (Iribas-Latour and Landau, 2013)

the feasibility of the CLOE approach has also been studied in applications with varying dynamics. In these studies, the identification problem is treated so that the local models for different operating points are estimated, whereas in this doctoral dissertation the parameter-tracking capability of the CLOE is studied.

In addition to the time domain approaches, in this doctoral dissertation, two different types of frequency domain methods are proposed for the online identification of closed-loop-controlled systems. It is shown that the proposed online frequency domain methods provide a good alternative to the conventional time domain online identification solutions. Both methods are based on a time-frequency representation of signals by applying sliding-DFT and Kalman filters. It is emphasized that in this doctoral dissertation, the proposed Kalman-filter-based identification approach is referred to as a frequency domain identification method, because the time-frequency presentation of signals using the Kalman filter can be regarded as a kind of a short-time DFT resulting in a nonparametric presentation of the frequency response. The feasibility of the SDFT-based identification approach is studied in the case of a parameter-varying two-mass system by using a multisine excitation signal, paying special attention to the detection of the position-dependent changes both in the frequency and the time domain by fitting a parametric model from the frequency domain observations. Instead, the Kalman-filter-based frequency domain identification approach is configured so that it is able to use the both multisine and chirp excitation signal for the online identification of a mechanical system on a sample-by-sample basis.

1.3 Outline of the doctoral dissertation

In this doctoral dissertation, the system identification of a mechanical system in an electrical drive is studied. The dissertation focuses on the online closed-loop identification of a mechanical load of drives that are approximated as a simple two-mass system, which sufficiently reflects the first resonance frequency, and thereby the dominant poles of the real system. In particular, the dissertation focuses on two-mass systems that have varying system dynamics.

The key focus of the dissertation is on online identification methods, the main topics being:

- Online parameter estimation of changing system parameters of a linear tooth belt drive using recursive Output-Error (OE) least-squares algorithms in an open- and closed-loop mode.
- Online direct and indirect nonparametric estimation of a selected band and set of frequencies by considering the time-frequency presentation of signals with a Kalman filter.
- Online parametric and nonparametric estimation of a changing system in the frequency domain by using a Sliding Discrete Fourier Transform (SDFT) based identification routine.

The topics are discussed in the following publications:

Publication I studies the direct off-line parameter estimation of a closed-loop-controlled two-mass system by superposing a pseudo random binary signal (PRBS) to the torque reference. A discrete time polynomial model with an OE structure is used in the time domain identification process. The identified model is applied to design a position control scheme for the system.

It is pointed out that **Publication I** is the only article in this dissertation that focuses exclusively on the off-line system identification and a model-based control design rather than on online system identification. Moreover, the two-mass-system model considered in this paper is different, because the mathematical modeling is based on the conservation of mass in a mass-flow system. It should be noted that the main focus of this doctoral dissertation is on the online identification approaches, and therefore, more emphasis is given on **Publications II**–**VI**.

Publication II addresses the direct online parameter estimation of a tooth belt drive system both in open-loop and closed-loop control. The parameters are estimated at a standstill and in the operating state by considering the algorithm that is based on a recursive output error method and applying the PRBS excitation signal. Furthermore, the off-line identification is considered in order to obtain models in different cart positions to verify the online estimated results.

It is remarked that one of the equations presented in the original publication is incorrect, and thus, the radius term r included in the left side of Equation (2) should be removed.

Publication III is a continuation of **Publication II.** It investigates the direct and indirect online parameter estimation of the tooth belt drive system under closed-loop control using a recursive closed- loop output error (CLOE) algorithm. The online-estimated values are compared with the corresponding values obtained from a simplified two-mass model, which is considered as a reference model as it provides position-dependent behavior of the parameters but neglects some of the nonidealities of the experimental test setup. Moreover, a statistical validation process is used to validate the obtained models.

Publication IV concentrates on the nonparametric identification of a mechanical system at a selected set of frequencies based on a time-frequency representation of signals with a Kalman filter. A persistent multisine excitation signal is superposed to the controller output, and the direct identification is considered. The experimental online identification results are compared with the corresponding values obtained from the online-identified frequency responses. For validation purposes, the system dynamics of the experimental test setup is varied, and a normalized Vinnicombe gap metric is used as an illustrative distance metric to compare the identified models in the desired frequency range when the system has been modified.

It is pointed out here that one of the equations presented in the original publication is incorrect, and thus, the amplitude of Equation (16) should include the square of the components.

Publication V studies the closed-loop online frequency domain identification of a mechanical system with varying dynamics; particular attention is paid to detect changes in the system dynamics. The proposed nonparametric frequency domain identification method is based on a Sliding Discrete Fourier Transform (SDFT) at a selected set of frequencies. Moreover, a Least Squares (LS) based identification criterion is applied for the estimation of a parametric model from the frequency domain observations.

Publication VI proposes an online nonparametric frequency response identification routine that is based on a Kalman filter, which is configured to perform like a short-time Fourier transform (similarly as in **Publication IV**). The approach exploits the knowledge of the excitation signal by updating the Kalman filter gains with the known time-varying frequency of a chirp signal to estimate the frequency response on a sample-by-sample basis. The paper also discusses the closed-loop system diagnostic options with the proposed method. For validation purposes, the system dynamics of the experimental test setup is varied and the changes in the anti-resonance and resonance frequencies are monitored with the proposed method.

The author of this doctoral dissertation is the principal author of **Publications I**–**VI**. In **Publications II**–**III** and **V**, the experimental tests were performed in cooperation with Mr. Jukka Parkkinen. In **Publication V**, Niko Nevaranta defined the research problem and wrote the paper in collaboration with Dr. Stijn Derammelaere. Dr. Stijn Derammelaere contributed to the work by analyzing and implementing the SDFT design used in his previous study (Derammelaere et al., 2014).

The other coauthors have participated in commenting on the papers. In addition, the author has been the principal author or coauthor in the following publications. These publications are listed here, but are not appended to this dissertation and are therefore not discussed in detail.

VII. Nevaranta, N., Niemelä, M., Pyrhönen, J., Pyrhönen O., and Lindh, T. (2012), ”Indirect tension control method for an intermittent web transport system,” in *Proc. of the 15th International Power Electronics and Motion Control Conference (EPE-PEMC)*, pp. 1–6, Novi Sad, Serbia, September 2012.

VIII. Huikuri, M., Nevaranta, N., Niemelä, M., and Pyrhönen, J. (2013), “Sensorless Positioning of a Non-Salient Permanent Magnet Linear Motor by Combining Current Angle Method and Back-EMF Estimator,” in *Proc. of the 39th Annual Conference of the IEEE Industrial Electronics Society (IECON)*, pp. 3142–3148 Vienna, Austria, November 2013

IX. Huikuri, M., Nevaranta, N., Niemelä, M., and Pyrhönen, J. (2014), "Dynamic Magnetic Circuit Modeling of Permanent Magnet Linear Motor," in *Proc. of the 16th European Conference on Power Electronics and Applications (EPE)*, pp. 1–9, Lappeenranta, Finland, August 2014.

X. Parkkinen J., Nevaranta N., Niemelä M., Lindh, T., and Pyrhönen J., "Motion Synchronization of Biaxial Linear Tooth Belt Drive System," *Int. Review of Elec. Eng. (I.R.E.E)*, Vol. X, no. X, pp. 1–8, 2016 (submitted for publication).

XI. Nevaranta N., Goubej, M., Lindh, T., Niemelä, M., and Pyrhönen, O., "Non-Parametric Frequency Response Estimation of Two-Mass-System using Kalman Filter," in *Proc. of the 18th European Conference on Power Electronics and Applications (EPE)*, pp. 1–9, Karlsruhe, Germany, September 2016. (Accepted for publication).

1.4 Summary of scientific contributions

The main scientific contributions of this doctoral dissertation are:

- Study of direct and indirect parameter estimation in the case of a varying two-mass resonant system using the recursive OE methods (**Publication II** and **III**).
- Introduction and application of the SDFT-based frequency domain method combined with the LS-based parameter fitting algorithm for indirect closed-loop identification of varying two-mass resonant system (**Publication V**). In addition, to avoid the possible instabilities and rounding errors modulated-SDFT is applied.
- Verification and testing of Kalman-filter-based frequency domain identification approach for real time nonparametric frequency response estimation (**Publication IV**).
- Design and introduction of online frequency domain identification approach, which is based on a Kalman filter that is synchronized to the instantaneous frequency of the chirp excitation signal (**Publication VI**).
- The possibility to apply the Kalman-filter-based identification approach for closed-loop diagnostics is studied in **Publication VI**.

2 System modeling

The mechanical dynamics of a rotating electrical drive can be mathematically modeled by applying Newton's second law of rotating bodies. In most cases, the multi-mass mechanical loads of an electrical drive can be approximated as two- or three-mass systems in order to simplify the overall system modeling by taking only into account the dominant resonance frequencies. As a result, the two-mass-system-based modeling has become popular in many industrial applications, and numerous advanced control methods have been proposed, for example in (Yun et al., 2013) and (Khan and Dhaouadi, 2015) in order to obtain high dynamics of the drive system.

This doctoral dissertation focuses on the identification of two-mass resonant systems. Two different types of experimental mechanical systems are considered to experimentally verify the identification methods. This chapter introduces the mechanical equations governing the physics of the experimental systems under study.

2.1 Coupled belt drive system

The two-mass resonant system shown in Fig. 2.1 is a coupled belt drive that consists of two moments of inertias (nip rollers) coupled by a flexible belt material. Different belt materials can be used to change the coupling stiffness.

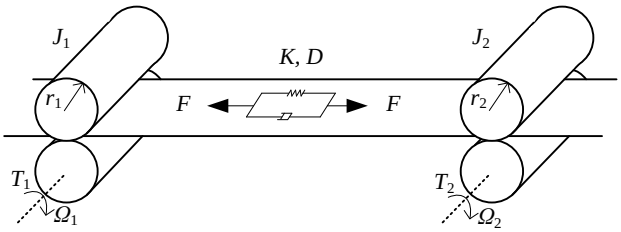

Fig. 2.1 Coupled belt drive system consisting two moments of inertias coupled by flexible belt material.

The mechanical dynamics of the investigated two-mass system depicted in Fig. 2.1 can be described by the following set of equations

$$J_1 \frac{\mathrm{d}\Omega_1}{\mathrm{d}t} = T_1 - T_{\mathrm{fr1}} + r_1 F \tag{2.1}$$

$$J_2 \frac{\mathrm{d}\Omega_2}{\mathrm{d}t} = T_2 - T_{\mathrm{fr2}} - r_2 F \tag{2.2}$$

$$F = K(r_2\Omega_2 - r_1\Omega_1) + D\left(r_2\dot{\Omega}_2 - r_1\dot{\Omega}_1\right) \tag{2.3}$$

Equations (2.1) and (2.2) are the elementary dynamic equations for rotation, where J_1 and J_2 represent the total moment of inertias of the nip rollers, Ω_1 and Ω_2 are the angular

velocities of the rollers, T_1 and T_2 are the torques developed by the electrical motors, T_{fr1} and T_{fr2} are the frictional torque components, r_1 and r_2 are the roller radii, and F represents the tension force. The dynamics of the coupling is expressed by Equation (2.3), where K is the spring constant and D is the damping constant of the belt material. The coupled belt drive system is used to verify the Kalman-filter-based online identification routine discussed in **Publications IV** and **VI**. Moreover, the same experimental system is considered in **Publication I** for validating the controller design based on the off-line identified model. It is pointed out that in **Publication VI** the experimental system includes a belt tensioner, which, in practice, changes the system dynamics over to a three-mass system. The parameters for the different two-mass system configurations discussed in this dissertation are given in Table 2.1.

Table 2.1. Parameters of the reference system studied in **Publications I**, **IV**, and **VI**

Parameter*)	**System 1**	**System 2**	**System 3**
Spring constant K [N/m]	$3.10 \cdot 10^4$	$5.75 \cdot 10^4$	$7.00 \cdot 10^4$
Damping constant D [N/m]	90	120	100
Roller 1 inertia J_1 [kgm^2]	0.032	0.032	0.018
Roller 2 inertia J_2 [kgm^2]**)	0.032	0.032	0.032
Resonance frequency [Hz]	11.1	15.1	20.4
Anti-resonance frequency [Hz]	7.8	10.7	16.6

*) Roller radii r_1 and r_2 are 0.05 m **) Value represents the total inertia

The parameters presented in Table 2.1 are regarded as the nominal reference system values for the experimental coupled belt drive system under study. These parameter values are based on material properties, experimental tests, and geometrical values. It should be noted that the parameters, especially the belt properties, are only known with some degree of confidence because of the limited information given in the manufacturer's datasheet. Based on the experimental tests, 5% uncertainty for inertial terms can be considered, and based on the belt manufacturer's tests (ISO 21181, 2005), it is reasonable to consider 10% uncertainty for the spring constant. Moreover, the datasheet value for damping constant is not available, and thus, the experimental tests and the guidelines given in (Frei et al., 1986) have been used to obtain an estimate for the damping constant.

The transfer function for the reference two mass system has been derived between the torque T_1 and the angular velocity Ω_1 using Equations (2.1)–(2.3). The frequency responses of the reference systems calculated from Table 2.1 parameters are depicted in Fig. 2.2. The main purpose of these reference models is the theoretical evaluation of the proposed identification methods. In **Publication IV**, the proposed identification approach is experimentally validated with the reference systems 1 and 2 in order to study the changes in the system dynamics. Similarly, in **Publication VI**, the experimental system is configured so that the system change corresponds to the change from the reference system 2 to 3. The parameter changes in the experimental mechanical system have been obtained by changing the belt material or by removing the upper roller of the nip roller J_1 (see Fig. 2.1).

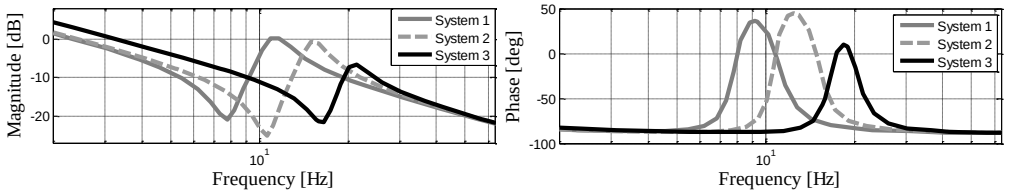

Fig. 2.2 Frequency responses of the two-mass resonant system configurations calculated from Table 2.1 parameters. The transfer function between the torque T_1 and the angular velocity Ω_1 is obtained from Equations (2.1)–(2.3).

2.2 Tooth belt drive

The other experimental system considered in this dissertation is a tooth belt drive system depicted in Fig. 2.3, which includes a linearly moving mass attached between rotational masses. Thus, the system is a varying two-mass resonant system, formed from the spring constants, which change as a function of position of the mass. Similar kinds of mechanical systems with position-dependent dynamics can be found for example in elevators (Kang and Sul, 2000) or lead-screw drives (Varanasi and Nayfeh, 2009). This experimental setup is considered in **Publications II**–**III** for the verification of the closed-loop OE identification and in **Publication V** for the SDFT-based frequency domain method.

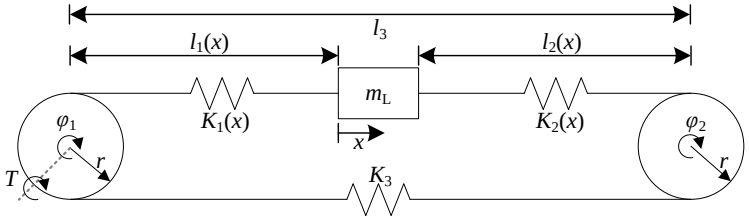

Fig. 2.3 Tooth belt drive that includes linearly moving mass attached between two belt pulleys.

The modeling of the tooth belt drive depicted in Fig. 2.3 has been discussed in **Publications III** and **V**, and thus, the linearized two-mass system approximation is discussed here in brief. The differential equations, without friction terms, of the two-mass model of the linear tooth belt axis can be defined as follows

$$\frac{J_s}{r}\ddot{\varphi} = \frac{T}{r} - b_s \cdot (r\dot{\varphi} - \dot{x}) + K_{eff} \cdot (r\varphi - x) \tag{2.4}$$

$$m_L \ddot{x} = b_s \cdot (r\dot{\varphi} - \dot{x}) + K_{eff} \cdot (r\varphi - x) \tag{2.5}$$

where J_s is the inertia of the driven end, r is the radius of the belt pulley, T is the torque developed by the motor, b_s is the position-dependent belt damping, K_{eff} is the position dependent equivalent spring constant of the axis, and m_L is the mass of the cart and the load on the axis. From Equations (2.4) and (2.5), the transfer function can be derived from the torque reference T to the motor mechanical angular velocity Ω. This leads to the

following linearized expression for the transfer function, which has a rigid part and a flexible part

$$\frac{\Omega(s)}{T(s)} = \underbrace{\frac{1}{J_s m_L s}}_{\text{Rigid part}} \underbrace{\frac{m_L s^2 + b_s s + K_{\text{eff}}}{s^2 + \frac{J_s + m_L r^2}{J_s m_L} b_s s + \frac{J_s + m_L r^2}{J_s m_L} K_{\text{eff}}}}_{\text{Flexible part}} \tag{2.6}$$

This transfer function represents a linearized system model in different operating points, which have a position-dependent equivalent spring constant expressed as

$$K_{\text{eff}}(x) = K_1(x) + \frac{K_2(x) K_3}{K_2(x) + K_3} \tag{2.7}$$

where K_3 is the spring constant of the lower part of the belt. $K_1(x)$ and $K_2(x)$ represent the position-dependent spring constants of the belt, which change as a function of $l_1(x)$ and $l_2(x)$, which are the lengths of the tooth belt between the pulleys and the cart as a function of cart position x, as illustrated in Fig. 2.3. In the mathematical model (2.4)–(2.5), the belt damping coefficient b_s has been selected using the guidelines for approximations of different flexible couplings (Frei et al., 1986). The position-dependent modeling of belt damping is further explicated in **Publication III**. It should be noted that the parameter estimation is based on the transfer function (2.6) that describes the two-mass-system approximation of the dominant resonance frequency, which can be used to represent the complete mechanical load of the electrical drive in a simplified way. A similar type of approximation is common for many different mechanical two-mass systems (Pacas et al., 2010). Moreover, the absence of static friction such as Coulomb friction effects in the model is justified as the online identification experiments are performed during operation, and zero velocity is avoided as much as possible. The parameters for the tooth belt drive system considered in this dissertation are given in Table 2.2.

Table 2.2. Parameters of the reference system studied in **Publications II**, **III**, and **V**

Symbol	Parameter	Nominal value[1)]	Variation[2)]
J_s (kgm^2)	Inertia	0.0028	–
K_{eff} (N/m)[*)]	Spring constant	$5.0 \cdot 10^5$	$4.0 \cdot 10^5 – 1.1 \cdot 10^6$
m_L (kg)	Load and cart mass	6.7	–
b_s (Ns/m)[**]	Belt damping constant	130	115 – 190
f_{res} (Hz)	Resonance frequency	61	54 – 91
l_3 (m)	Dist. between pulleys	2.14	–
r (m)	Roller radius	0.019	–

*) Tension of the belt has been set to 450 N

) Approximated with $b_s = \frac{K_{\text{eff}}}{2\pi f_{\text{res}} Q_k}$ and using $Q_k = 10$ (see **Publication III)

The values of Table 2.2 have been obtained from the manufacturer's datasheets and from the experimental laboratory tests such as the tensile strength test for the belt material. Detailed discussion about the tooth belt drive considered in this dissertation and the experimental determination of the parameters can be found in (Jokinen, 2010). In Fig. 2.4, the frequency responses of the tooth belt drive in cart positions 0.35 m, 0.8 m, and 1.4 m are depicted. From this example figure, the position-dependent system dynamics of the tooth belt drive can be observed as the resonances of the system change as a function of cart position. This position-dependent behavior is explicated in the **Publications III** and **V**. The tooth belt drive is identified both in open loop and closed loop. However, in many cases the open-loop identification is problematic (or impossible) due to the difficulties in designing of the offset torque reference without causing the system to rush and the amplitudes of the excitation should be designed so that the movement is minimized. In general, the PRBS is suitable for exciting mechanics with a limited stroke as it minimizes the movement due to excitation (Shuy and Lee, 2010).

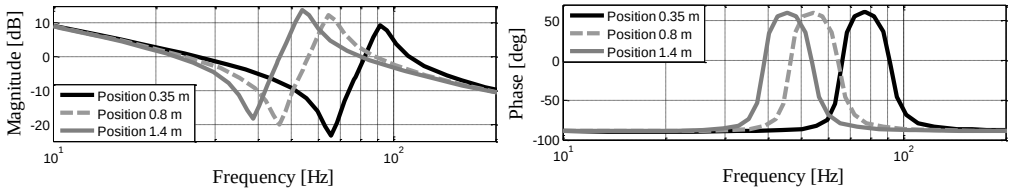

Fig. 2.4 Example frequency responses of the tooth belt drive in the cart positions 0.35 m, 0.8 m, and 1.4 by using the parameter values of Table 2.2 and the linearized transfer function (2.6).

It is worth remarking that, in **Publications III** and **V**, uncertainty of 20 percent is chosen to emphasize the changing and position dependent damping of the system. Correspondingly, 5 percent parameter uncertainty for the spring constant is considered that is based on the simplification of the effective spring constant in (2.7) and inaccuracy in the initial tension of the belt. Furthermore, for the nominal value of inertia uncertainty of 15 percent is chosen to emphasize the inertia terms, such as belt inertias, that are not fully known.

3 System Identification

The particular focus of this doctoral dissertation is on the closed-loop system identification problems with persistent excitation. This chapter discusses the online and off-line identification approaches using time and frequency domain observations and introduces the online identification approaches considered in **Publications II–VI**. Furthermore, the excitation signals and the identified model validation are discussed in brief.

3.1 Closed-loop and open-loop identification

The well-established closed-loop identification approaches are based on assumptions made of the nature of the feedback; these approaches can be classified into three subcategories. In the direct approach, the method is applied directly to the measured input $u(k)$ and output $y(k)$ signals, and the effect of the feedback controller is omitted. In this case, no (or only a few) assumptions are made on how the data was generated. On the contrary, the idea of indirect methods is to identify the closed-loop system and calculate an open-loop system using the knowledge of the feedback law (controller). The third category covers the joint input-output approaches in which typically two model structures are estimated separately by considering the input and output jointly as outputs of an augmented system, which is driven by a reference signal and noise. The estimated augmented system provides an opportunity to solve the open-loop loop model and the controller from the closed-loop experiment. Basically, in this approach, knowledge of the feedback law is not required, although a certain model structure for the controller must be known in advance. In Fig. 3.1, the direct and indirect identification configurations are shown, where $C(z)$ is the closed-loop controller, $G(z)$ is the process, $r(k)$ is the reference signal, $r_u(k)$ is the excitation signal, $u(k)$ is the input signal, and $y(k)$ is the output signal. The signals used in the identification are indicated by dashed grey arrows.

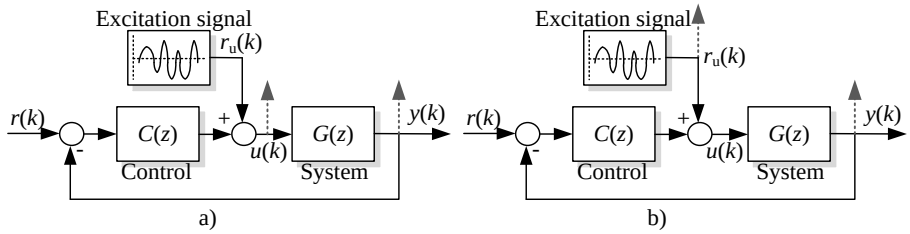

Fig. 3.1 a) Direct identification and b) indirect identification in a closed loop.

It is emphasized that the direct approach in Fig. 3.1a is only applicable for most closed-loop identification problems when prediction error methods (Ljung, 1987) or some of the subspace methods are considered, because there is usually a strong correlation between the system input $u(t)$ and the noise $n(t)$ as a result of the feedback loop. However, the direct approach can be used to obtain valid results also in the case of other identification methods, for instance, when a low-bandwidth controller (Villwock and Pacas, 2008) is used or a separate noise estimation routine is considered. Correspondingly, there are

various ways to approximate a valid system model under closed-loop conditions. Basically, in the case of indirect and joint input-output approaches, the fundamental idea is to convert the closed-loop identification problem into an open-loop one by considering the excitation signal as an input which is uncorrelated with the noise. In this doctoral dissertation, the focus is on the direct and indirect identification.

In **Publications III**, **V**, and **VI** the open-loop model $G(z)$ is indirectly solved from the transfer function

$$G(z)=\frac{G_{\mathrm{cl}}(z)}{1-C(z)G_{\mathrm{cl}}(z)} \tag{3.1}$$

where $G_{\mathrm{cl}}(z)$ is the closed-loop model describing the relation of the signals $y(k)$ and $r_{\mathrm{u}}(k)$ in Fig. 3.1. Particularly, in **Publication III** the known controller structure $C(z)$ is included in the regression vector and in **Publications V**−**VI** the open-loop model is solved from Equation (3.1).

3.2 Excitation signals

A persistent excitation condition must be met in parameter estimation to guarantee convergence of the parameters, which, in practice requires that the excitation signal should excite frequencies across the desired range with a variance as large as possible. In most cases, the input signals are limited to certain maximum allowed values, for instance the torque and velocity in electric drives. Therefore, the PRBS is preferable for this type of applications as the large variance is easily obtained by a binary signal, and it varies between two values (e.g. −1 and 1). The statistical properties of the PRBS have been discussed further in (Villwock et al., 2008). Similarly, the swept sinusoid, stepped sinusoid and the random-phase multi-sine has been widely applied in the identification of different systems. More about the properties of different excitation signals can be found for example in (Pintelon and Schoukens, 2001).

In **Publications IV**−**V**, multisine signals are considered with N_{p} samples in the period, which can be determined as

$$r_{\mathrm{u}}(t)=\sum_{k=1}^{N_f} A_{\mathrm{k}}\cos(2\pi f_{\mathrm{k}}t+\phi_{\mathrm{k}}) \tag{3.2}$$

where A_{k} are the amplitudes of each frequency component, frequencies f_{k} chosen from the grid $\{\frac{2\pi l}{N_{\mathrm{p}}}, l=1,\ldots,\frac{N_{\mathrm{p}}}{2}\text{-}1\}$, and the random phases ϕ_{k} uniformly to the interval $[0, 2\pi)$. It should be noted that, in **Publication V** the Schroeder multisine is considered, and thus, the phases are chosen as

$$\phi_k=\phi_1-\frac{\pi k}{k_{\max}}. \tag{3.3}$$

In **Publications II, III**, and **V**, because of the nonlinearities, the identification is carried out in a well-defined operating region. This means that the amplitude of the input signal is limited. The PRBS and the Schroeder multisine with a flat-amplitude spectrum (A_k = A) meets this requirement. Obviously, if the amplitude is chosen too high, the system no longer operates around the desired operation point, and nonlinearities may be dominant. It should be mentioned that in the off-line frequency domain identification literature, the nonlinear behavior of the system is usually determined by considering multisine excitation signals with different realizations of random phases in order to obtain linear dynamics of the nonlinear system. Moreover, the knowledge of the possible nonlinear distortions is obtained by calculating variances and covariance. For online identification purposes, if practical applications are considered, this would require extensive calculations and memory storage space, which is usually the main disadvantage of online DFT-based identification methods (Barkley and Santi, 2009). In addition, the fact that the Schroeder phases (3.3) are not random over k makes this type of multisine less suited for nonlinear detection. The work by (Pintelon and Schoukens, 2001) provides a useful review of the properties of different excitation signals and their usage in nonlinear distortion detection.

In **Publications V**−**VI**, a linear chirp signal is considered that can be expressed as

$$r_u(k)=A\cdot\cos(2\pi\cdot f(t)\cdot t+\phi), \tag{3.4}$$

where the time-varying frequency $f(t)$ can be written as

$$f(t)=\frac{m}{2}t+f_0, \tag{3.5}$$

where f_0 is the starting frequency, and m is the rate of frequency change over the time duration T

$$m=\frac{f_1-f_0}{T}. \tag{3.6}$$

In **Publication V**, the chirp is applied for off-line identification purposes in order to obtain a nonparametric model behavior in certain cart positions. This result is used to show that the online nonparametric frequency domain method is suitable for tracking position-dependent changes in the system. Correspondingly, in **Publication VI**, the chirp excitation signal is considered with the nonparametric Kalman-filter-based identification approach so that the known time-varying frequency (3.5) is used to update the Kalman gains. This is further discussed in Section 3.5.2.

3.2.1 Properties of the excitation signals

When comparing the basic properties of the excitation signals under consideration, it is evident that the only excitation signal that can exclusively excite the frequency band of interest is the multisine. The other signals, the chirp and PRBS, excite frequencies outside the desired band. One of the main advantages of the PRBS over other signals is that the signal is formed from sequences of rectangular pulses, which can take two different levels (binary). Basically, the pulses of the PRBS represent a kind of an approximation of a discrete-time white noise, thereby resulting in a spectral content rich in frequencies (Landau and Zito, 2011). The binary form provides computational benefits as it can be generated easily by means of shift registers with feedbacks, which reduces the memory storage requirement. In addition, the one of the main advantage of the binary signals is the low crest factor. Moreover, the binary signals provide a good spectrum for the excitation signal, but their disadvantage is that the binary sequences are mostly for linear system analysis, and hence, they are not efficient in detecting nonlinearities. Furthermore, the frequency content of the PRBS is not accurately tunable, which can be considered a minor drawback. Depending on the type of the excitation signal, the safety issues of practical mechanical applications can set certain limitations, and in most cases, the system should preferably not be excited at its resonance frequency. Especially, when sinusoidal excitation signals are applied, avoidance of the resonance region can be problematic. The risk of resonances can be circumvented to some degree when the PRBS are considered (Pacas et al., 2004).

On the other hand, in the case of basic chirp signals, the frequency is decreased or increased linearly from the initial frequency f_0 to the desired final frequency f_1. Thus, the major part of the power is equally distributed between these frequencies, which can be considered an advantage. However, the amplitude spectrum of the chirp signal is not completely flat (Pintelon and Schoukens, 2001), which basically indicates that other frequencies with a lower signal-to-noise ratio are also introduced to the signal. This has an impact on the length of the required measurement, which, again, is directly proportional to the desired accuracy. Thus, the main disadvantage of the chirp signal is that a slow sweeping is usually required for precise measurement in order to reduce errors and obtain accurate results, which prolongs the duration of the experiment. A second drawback can be found when considering identification of systems with nonlinear dynamics. The chirp signal can have a disturbing effect, because a number of other spectral lines are also excited with the frequency lines of interest. Despite these limitations, the chirp-excitation-based offline identification is widely applied for instance to the identification of the flexibilities of industrial robot manipulators (Östring et al., 2003) and (Saupe and Knoblach, 2015).

As a final conclusion, the selection of a suitable excitation signal is based on personal preference, identification method, technical limitations of the application, and many case-specific secondary selection criteria (e.g. no power outside the desired frequency band). The selection criteria for the different excitation signals under study have been further discussed in **Publications II–VI**.

3.3 Polynomial-model-based identification

The parametric identification techniques are typically based on a fixed, in advance determined structure of a mathematical relation, and the parameters of the structure are fitted to the data. Thus, the selection of a proper model structure and degree is of great importance in the case of parametric methods. In most cases, the prior knowledge of the model dynamics can be used to select the degree of the model directly, or the appropriate model degree can be, for instance, iteratively searched by analyzing the statistical properties of different candidate models (Raol et al., 2004). In this doctoral dissertation the time domain parameter estimation is based on a prior knowledge of the model structure of the systems. For instance, by transforming the continuous time transfer function (2.6) into an equivalent discrete time transfer function, we obtain

$$y(k)=\frac{B(z)}{A(z)}u(k)+n(k) \tag{3.7}$$

where the $y(k)$ is the system output, $u(k)$ is the input signal, and $n(k)$ is the output noise of the system. The numerator and denominator parts in Equation (3.7) are $B(z) = b_1 + b_2z^{-1} + b_3 z^{-2}$ and $A(z) = 1 + a_1z^{-1} + a_2 z^{-2} + a_3z^{-3}$, respectively. The output of this pulse transfer function (3.7) can be denoted as

$$y(k)=\boldsymbol{\varphi}(k)^{\mathrm{T}}\boldsymbol{\theta} \tag{3.8}$$

where $\boldsymbol{\varphi}(k)$ is the regression vector and $\boldsymbol{\theta}$ is the parameter vector, which depend on the identification configuration. In **Publication I**, the direct identification is considered with an OE model, which is based on the prediction error method (PEM). The PEM-type of identification with an OE model is valid for the direct closed-loop identification under certain assumptions (Gilson et al., 2011), and its applicability to the off-line direct identification of closed-loop-controlled resonating mechanical systems has recently been studied in (Saarakkala and Hinkkanen, 2015) and (Łuczak and Zawirski, 2015).

3.3.1 **Online identification in the time domain**

The standard RLS algorithms are well known for their low computational complexity and good numerical properties, and they have been successfully applied to the online parameter estimation of different industrial applications both in open-and closed-loop control. The basic form of the RLS algorithm can be expressed as

$$\boldsymbol{\theta}(k)=\boldsymbol{\theta}(k-1)+\mathbf{L}(k)\varepsilon(k) \tag{3.9}$$

$$\varepsilon(k)=y(k)-\boldsymbol{\varphi}(k)^{\mathrm{T}}\boldsymbol{\theta}(k-1) \tag{3.10}$$

$$\mathbf{L}(k)=\frac{\mathbf{P}(k-1)\boldsymbol{\varphi}(k)^{\mathrm{T}}}{\lambda+\boldsymbol{\varphi}(k)^{\mathrm{T}}\mathbf{P}(k-1)\boldsymbol{\varphi}(k)} \tag{3.11}$$

$$\mathbf{P}(k)=\frac{1}{\lambda}\left(\mathbf{P}(k-1)-\frac{\mathbf{P}(k-1)\boldsymbol{\varphi}(k)\boldsymbol{\varphi}(k)^{\mathrm{T}}\mathbf{P}(k-1)}{\lambda+\boldsymbol{\varphi}(k)^{\mathrm{T}}\mathbf{P}(k-1)\boldsymbol{\varphi}(k)}\right) \tag{3.12}$$

where $\boldsymbol{\theta}$ is the unknown parameter vector, $\mathbf{L}(k)$ is the gain vector, $\varepsilon(k)$ is the prediction error, $y(k)$ is the measured output, $\boldsymbol{\varphi}(k)$ is the regression vector, $\mathbf{P}(k)$ indicates a covariance matrix, and λ is the forgetting factor $(0<\lambda\leq 1)$. Typically, these real-time estimation problems have been solved by using direct closed-loop parameter estimation methods, where the influence of the feedback controller is omitted (Garrido and Concha, 2013). In some cases, this can lead to biased parameter estimates. Motivated by the features of the closed-loop output-error (CLOE) recursive algorithm in (Landau and Karimi, 1997a) in **Publication III**, the indirect closed-loop method uses the known excitation signal and structure of the controller in the regression vector. Obviously, the standard RLS form (3.9)–(3.12) is the same for the recursive pseudolinear regression (RPLR) that is used as the parameter adaption algorithm (PAA) in the CLOE-based identification. The basic form of the CLOE algorithm is based on the utilization of the known controller $C(z)$ in the regression vector with the closed-loop predictor $\hat{y}(k)=\boldsymbol{\varphi}(k)^{\mathrm{T}}\boldsymbol{\theta}(k)$ as follows

$$\hat{u}(k)=-C(z)\hat{y}(k)+r_{\mathrm{u}}(k). \tag{3.13}$$

The method has been successfully applied to the real-time parameter estimation of closed-loop-controlled three-mass flexible transmission systems (Landau and Karimi, 1997a), and more recent studies (Saarakkala and Hinkkanen, 2015) have presented a modified CLOE method for off-line parameter estimation of a two-mass system. However, in **Publication III** the system has time-varying parameters, and thus, the recursive algorithm under consideration includes a forgetting factor in order to obtain good tracking properties.

3.4 Off-line nonparametric methods

Most of the nonparametric identification methods apply the frequency domain characteristics of the system, and usually no (or few) prior assumptions are made with respect to the model structure. The spectral and correlation analyses, for instance (Villwock and Pacas, 2008) and (Barkley and Santi, 2009), are well-known examples of identification methods that can be regarded as nonparametric. Basically, in the correlation analysis, time domain observations are used, whereas the spectral analysis is a frequency domain method. Moreover, other identification methods such as the step-response-based approaches in the continuous- or discrete-time domain can also be referred to as nonparametric methods. Evidently, in the case of frequency-response-based methods, it is typically required that the measured data are available in the frequency domain. However, the measured data are usually acquired as a record of time series, and thus, in order to perform a signals analysis, the time domain signals must be converted into the frequency domain by applying some transformation technique.

In general, the frequency response of a linear system with an input signal $u(t)$ and an output signal $y(t)$ can be expressed by the ratio of the cross-spectral estimate of the input and the auto-spectral estimate of the input and output as

$$\hat{G}(\mathrm{j}\omega) = \frac{S_{uy}(\mathrm{j}\omega)}{S_{uu}(\mathrm{j}\omega)}. \tag{3.14}$$

This transformation can be achieved in different ways (Villwock and Pacas, 2008), but it results in extra calculations, and its accuracy is highly dependent on the chosen transformation method (Saarakkala, 2014). Moreover, the frequency domain observations can be applied to estimate a parametric model, but the calculation burden increases further as an additional parameter-fitting algorithm is needed. As a conclusion, the nonparametric identification methods are usually nonrecursive and require extensive calculations, implying that the identification must often, be performed by off-line data processing.

Compared with the off-line time domain approaches, there are, however, several advantages in the estimation of parametric models by fitting the frequency domain data. Obviously, the main advantages include the data reduction as a large number of time domain samples can be replaced by a small number of spectral lines (Pintelon et al., 1994), and the use of a periodic excitation signal provides an opportunity to perform the estimation only at the frequencies where it is available. Moreover, the effect of noise is reduced as a large amount of data is compressed into a number of frequency points, and noisy (nonexcited) frequency lines are eliminated. These aspects are used extensively and relatively easily in most modern off-line frequency domain nonparametric identification methods (Pintelon and Schoukens, 2001). The primary disadvantage of the frequency domain analysis is the required calculations of the discrete Fourier transform of the measured data. These calculations are not usually desirable features for real-time applications, which has, limited their usage in online frequency domain identification. For online identification purposes, the monitoring of a system at a selected set or band of frequencies is a desirable feature. When the behavior of these frequencies has to be tracked in real time, it is worth considering a DFT algorithm that provides benefits in the terms of computational efficiency and real-time performance.

In this doctoral dissertation, the off-line frequency domain identification approach (Villwock and Pacas, 2008), which is based on the Welch method, is used as a benchmark method to compare and validate the online frequency domain identification methods studied in **Publications V–VI**. More specifically, in **Publication VI**, the LS-based parameter-fitting algorithm of Levenberg and Marquardt is applied for the parameter estimation of a two-mass system.

3.5 Online identification in the frequency domain

For online identification purposes, the recursive time domain parameter estimation methods have received the most attention as they have been shown to overcome many of

the drawbacks of classical frequency domain techniques in terms of closed-loop issues, accuracy, computational cost, and memory storage requirements. As a result, the online identification in the frequency domain is not widely recognized in the system identification literature that focuses on the problems related to the closed-loop identification. Naturally, some nonparametric methods have been proposed for real-time frequency response estimation, for instance, in (Holzel and Morelli, 2011) where a real-time recursive Fourier transform regression (FTR) has been suggested for linear model identification. The method is based on the selection of the band of frequencies that covers the frequency range of interest and the LS-based fitting criterion is used for the estimation of the unknown parameters. However, the method is only applicable to systems for which the full state can be measured (or otherwise observed) since it is an equation error based method (Raol et al., 2004). Another method has been introduced in (Olivier, 1994), where a Fourier-Laguerre series is proposed for the open-loop identification of a linear system. However, this method can be also regarded as a parametric identification method, as in practice, it require initial selection of the model complexity. Furthermore, a recent study by (Barkley and Santi, 2009) have applied nonparametric cross-correlation identification method for real-time loop transfer function identification of a dc-dc converter. Even though the authors have used an FPGA board with an additional memory block for experimental validation, the method requires extensive calculations and memory storage space, which set certain limitations to its applicability. However, it is pointed out that the modern power electronics devices equipped with FPGA and digital signal processors (DSP) are capable of handling extensive computations that enable the efficient use of online frequency-domain identification methods and adaptive control (Cespedes and Sun, 2014).

The online frequency domain identification methods studied in this doctoral dissertation are the SDFT and the Kalman-filter-based short-time DFT, which are not well-recognized methods in the system identification literature, but they have been successfully applied for other purposes. For example, the SDFT algorithm has been used for the prognosis of power electronics devices or for fault diagnostics of electric motors (Abed et al., 2001) by tracking of a prior-known fault frequency. On the contrary, the Kalman filter approach discussed in thesis has been applied for tracking the harmonics components in the power system voltage and current waveforms (Girgis et al., 1991) and (Kamwa et al., 2014).

3.5.1 Sliding discrete Fourier transform

The SDFT is well known as a simple but effective technique for real-time spectral analysis, and it has been successfully used in some industrial applications, for instance, for sensorless control (Derammelaere et al., 2014) or fault diagnostics (Abed et al., 2001). The SDFT relies on the fact that at each new time instant n, only one measurement sample is added to the sum, and only the oldest measurement sample is removed from the window as illustrated in Fig. 3.3.

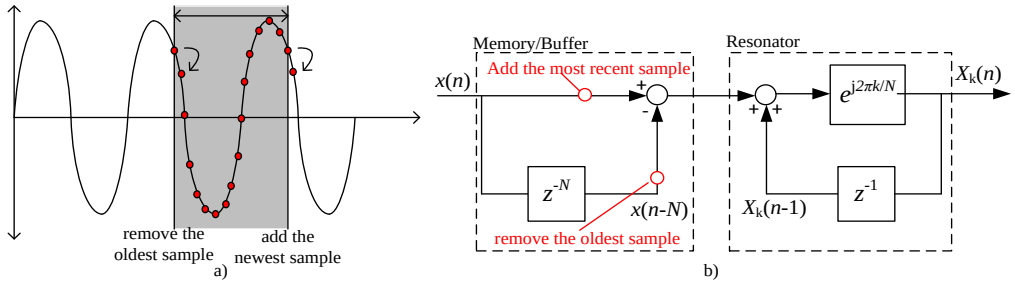

Fig. 3.2 a) Principle of the SDFT and b) the SDFT implementation. At each new time instant the last sample $x(n)$ is added and the oldest sample $x(n–N)$ is removed from the window. The derivation of the SDFT is given in Appendix B.

The SDFT has not been widely applied for real-time identification purposes, and only a few relevant studies can be found in the system identification literature (LaMaire et al., 1987) and (Hashimoto and Ishida, 1999). It should be noted that both of these studies apply the SDFT for identification for control purposes, and more specifically, for the adaptive control, whereas **Publication V** exclusively concentrates on the identification issues of a closed-loop servomechanism when the SDFT is applied. Thus, the main focus of **Publication V** is to show that the SDFT can be effectively used to the nonparametric frequency domain identification in real-time using a short record of data in the sliding window. Moreover, for validation purposes the LS-based identification criterion is applied for the estimation of a parameter vector $\boldsymbol{\theta}$ that corresponds to the model structure (3.7)

$$\boldsymbol{\theta}=\left(\boldsymbol{\Phi}^{\mathrm{T}}\boldsymbol{\Phi}\right)^{-1}\boldsymbol{\Phi}^{\mathrm{T}}\boldsymbol{\Psi}, \tag{3.15}$$

where $\boldsymbol{\Phi} = \left[\boldsymbol{\varphi}_{nR}\ \boldsymbol{\varphi}_{nI}\right]^{\mathrm{T}}_{2\cdot i\times(2\cdot q+1)}$ is the matrix of the real and imaginary equation pairs of a third order (q = 3) model

$$G(e^{\mathrm{j}\omega_n T_\mathrm{s}})=X_n+\mathrm{j}Y_n \tag{3.16}$$

for the frequencies $n = 1\ldots i$, denoted as

$$\begin{aligned}\boldsymbol{\varphi}_{nR} = \big[&\cos(0\omega_n T_s)\ \cos(\omega_n T_s)\cdots\cos(q\omega_n T_s)\ -X_n\cos(0\omega_n T_s)\\ &+Y_n\sin(0\omega_n T_s)\cdots-X_n\cos(q\omega_n T_s)+Y_n\sin(q\omega_n T_s)\big]^{\mathrm{T}}\end{aligned} \tag{3.17}$$

$$\begin{aligned}\boldsymbol{\varphi}_{nI} = \big[&\sin(0\omega_n T_s)\ \sin(\omega_n T_s)\cdots\sin(q\omega_n T_s)\ -X_n\sin(0\omega_n T_s)\\ &-Y_n\cos(0\omega_n T_s)\cdots-X_n\sin(q\omega_n T_s)-Y_n\cos(q\omega_n T_s)\big]^{\mathrm{T}}.\end{aligned} \tag{3.18}$$

Finally, the matrix $\boldsymbol{\Psi}$ represents the real and imaginary components of the equation pairs

$$\boldsymbol{\Psi} = \begin{bmatrix} X_n\cos(q\omega_n T_\mathrm{s}) - Y_n\sin(q\omega_n T_\mathrm{s}) \\ X_n\cos(q\omega_n T_\mathrm{s}) - Y_n\sin(q\omega_n T_\mathrm{s}) \end{bmatrix}_{2\cdot i\times 1}^{\mathrm{T}}. \tag{3.19}$$

This type of a parameter estimation routine results in an iterative least-squares solution in the frequency domain. It should be noted that a well-chosen weighting function $W(e^{\mathrm{j}\omega_n T_\mathrm{s}})$ could be used to improve the quality of the estimates, for instance, by using the denominator coefficient $A(e^{\mathrm{j}\omega_n T_\mathrm{s}})$ of the previous estimation. Obviously, the LS-type parameter estimation routine is preferable for off-line identification purposes, but it is considered in **Publication V** in order to show the applicability of the SDFT-based nonparametric identification routine. Moreover, the structure of the matrices (3.15) for the frequency domain observations can be chosen differently; for instance in (Hashimoto and Ishida, 1999), the nonparametric model is combined with the known controller structure in order to adapt the controller parameters.

3.5.2 Time-frequency representation of signals using a Kalman filter

Basically, the standard Kalman filter solution is an extension of the recursive least squares parameter (RLS) estimation method (3.9)–(3.15). Traditionally, the Kalman-filter-based online identification tools proposed in the literature such as (Schütte et al., 1997) and (Perdomo et al., 2013) can be considered parametric time domain methods. This is due to the fact that the proposed methods takes explicitly into account prior knowledge about the system dynamics, and in most cases, this information is based on the use of a parametric model obtained from off-line identification. However, in this doctoral dissertation, particularly, in **Publications IV** and **VI**, the proposed Kalman-filter-based identification approach is referred to as a frequency domain identification method, because the time-frequency presentation of signals using the Kalman filter can be regarded as a kind of a short-time DFT resulting in a nonparametric presentation (3.16) of the frequency response. The Kalman-filter-based short-time DFT can be obtained by considering the following simplified state-space representation

$$\begin{aligned} \mathbf{x}(k+1) &= \boldsymbol{\Phi}(\mathrm{k})\mathbf{x}(k) + \mathbf{w}(k) \\ z(k) &= \mathbf{H}\mathbf{x}(k) + \mathbf{v}(k), \end{aligned} \tag{3.20}$$

where $\mathbf{x}(k)$ is the state vector, $\boldsymbol{\Phi}(k)$ is the state transition matrix, $\mathbf{H}(k)$ is the measurement matrix and $z(k)$ is the output of the Kalman filter. $\mathbf{v}(k)$ and $\mathbf{w}(k)$ are the measurement and model error vectors, respectively. For the state estimation problem, the following Kalman filter solution can be written

$$\hat{\mathbf{x}}(k+1) = \boldsymbol{\Phi}(k)\hat{\mathbf{x}}(k\text{-}1) + \mathbf{K}(k)[z(k) - \mathbf{H}\hat{\mathbf{x}}(k-1)], \tag{3.21}$$

where $\mathbf{K}(k)$ is the Kalman gain. In Publications **IV** and **VI**, the Kalman filter under study can be regarded as a kind of a fixed-coefficient state observer with predetermined stability characteristics. Thus, the Kalman filter gain is selected as

$$\mathbf{K}(k)=\frac{\mathbf{\Phi}(k)\mathbf{H}^{\mathrm{T}}(k)}{\mathbf{H}(k)\mathbf{H}^{\mathbf{T}}(k)+\lambda} \tag{3.22}$$

where λ is the tuning parameter. The derivation of (3.22) is further discussed in **Publication VI**. The following state vector is considered to estimate a *n*th frequency component ω_{n}

$$\mathbf{x}(k)=\begin{bmatrix} x_{\mathrm{real}}(k) \\ x_{\mathrm{imag}}(k) \end{bmatrix} \tag{3.23}$$

where $x_{\mathrm{real}}(k)$ and $x_{\mathrm{imag}}(k)$ are the real and imaginary components of the signal that can be estimated by considering the following transition matrix

$$\mathbf{\Phi}(k)=\begin{bmatrix} \cos(T_{\mathrm{s}}\cdot\omega_n) & \sin(T_{\mathrm{s}}\cdot\omega_n) \\ -\sin(T_{\mathrm{s}}\cdot\omega_n) & \cos(T_{\mathrm{s}}\cdot\omega_n) \end{bmatrix} \tag{3.24}$$

where T_{s} is the sample time. From the viewpoint of system identification, the signal component representation with a Kalman filter provides an opportunity to recursively estimate the frequency contents of the signals. In **Publication IV**, the Kalman-filter-based fixed-coefficient state observer depicted in Fig. 3.3a is used for the online identification of a closed-loop-controlled two-mass system by using a multisine excitation signal. Moreover, in **Publication VI**, a similar observer is considered**,** but the state transition matrix, and thus, the Kalman gain, is updated with the known time-varying frequency (3.22) as depicted in Fig. 3.3b.

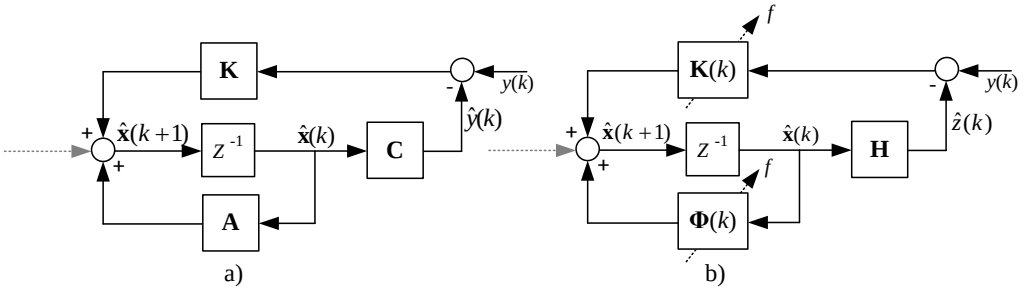

Fig. 3.3 Examples of the Kalman filter configurations: a) fixed coefficient state observer considered in the **Publication IV** for tracking of multisine excitation signal. b) State observer for tracking of a swept sinusoid considered in **Publication VI**.

The fundamental theory behind the Kalman-filter-based short-time DFT was initially proposed by Bitmead et al. (1986), and after that, it has been applied for online system identification (Parker and Bitmead, 1987) and diagnostics purposes (Jenssen and Zarrop, 1994). These methods have been successfully used for the frequency response identification of open-loop and closed-loop systems using a multisine excitation signal. Basically, in **Publication IV** for the tracking of a multisine excitation signal, the state-space realization of the Kalman filter requires a large block-diagonal form for the selected

set of frequencies. Obviously, the fixed Kalman filter gain sets the tracking properties for all frequencies as the same (Bitmead et al., 1986). However, a more recent study by Goubej (2015) has used an improved approach of (Bitmead et al., 1986) for real-time identification of a mechanical three-mass system so that the frequency components of the observer are weighted differently.

It is emphasized that one of the main targets of this doctoral dissertation is to study the applicability of the proposed Kalman-filter-based identification routines under operating conditions that somewhat correspond to the commissioning state, that is, a soft controller is considered. For this reason, in **Publications IV**–**VI**, the direct identification approach is considered, which, in practice provides valid results only when the signal generator injects a high-frequency excitation compared with the closed-loop bandwidth. Obviously, the indirect identification approaches avoid problems with correlation of the input and output signals, and thus, are preferable if the proposed identification routine is applied, for instance, to performance assessment of control loops. In **Publication VI** it is shown in brief that the indirect identification with the Kalman filter is also applicable to determine the open-loop frequency response from the closed-loop experiments.

3.6 Validation

Model validation is one of the most important steps in the system identification. Especially, when considering system identification from the viewpoint of control design, usually the main objective is to find the best possible approximate model in a given class and according to a given criterion rather than to search for the 'true' model. Obviously, an exact system model is optimal for all kind of applications, but in practical identification cases, the task is to approximate a 'true' system, and hence, the target application should be used to estimate the quality of the model. Naturally, if the identified model is used for controller design, it is more important to achieve the control performance goals than the distinctive quality of the model. This is the main reason why the closed-loop identification criterion is usually determined as a function of the desired closed-loop controller performance criterion. Usually, simple models can be successfully used, for instance, to design a high-performance control, but the critical part of the identification is to find which terms or dynamics should be included in the model that sufficiently captures the essential system behavior. In **Publication I**, the identified OE model is used for a cascaded position controller design, which is then compared with the design obtained with the reference model. Basically, in this example case, the validation process is completed through the obtained controller performance, which shows that the identification improves the system model.

3.6.1 **Residual analysis**

The well-known validation tool is the residual analysis, which is based on statistical properties of the residuals $\varepsilon(k)=y(k)-\hat{y}(k)$ which is shown in Fig. 3.5.

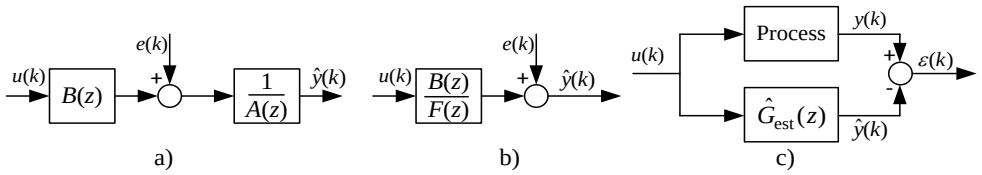

Fig. 3.4 a) ARX model structure, b) OE model structure, and c) validation by residual analysis (see **Publications III** and **V**). note: in the publications, $A(z)$ and $B(z)$ are used to denote the numerator and denominator, respectively.

The auto-correlation test is commonly applied to evaluate the whiteness of the residuals

$$R_{\varepsilon}(\tau) = \frac{1}{N}\sum_{k=1}^{N} \varepsilon(k)\varepsilon(k-\tau) \tag{3.25}$$

but for the OE model considered in **Publications II**–**III**, the emphasis of the residual analysis is on the cross-correlation

$$R_{\varepsilon,u}(\tau) = \frac{1}{N}\sum_{k=1}^{N} \varepsilon(k)u(k-\tau) \tag{3.26}$$

since noise is not included in the OE structure, and thus, the modeling focuses on the dynamics of system rather than on the disturbance properties (Ljung, 2010). For the same model class, the cross-correlation between the residual and the delayed prediction model output sequence can be used to evaluate the model (Landau et al., 2011)

$$R_{\varepsilon,y}(\tau) = \frac{1}{N}\sum_{k=1}^{N} \varepsilon(k)\hat{y}(k-\tau)\,. \tag{3.27}$$

In general, the whiteness test is used to evaluate the goodness of the identified model by evaluating the residual autocorrelation function (3.25), which should remain within a specified confidence interval in order to pass the uncorrelation test of the residuals. Correspondingly, the cross-correlation in the residual analysis should show the uncorrelation of the past inputs, thereby resulting in stochastically verified parameter estimates. The confidence interval considered in **Publications III** and **V** corresponds to a 3% level of significance of the hypothesis test for a Gaussian distribution, and thus, a stochastically valid model should verify the condition $|R(\tau)| \leq 2.17/\sqrt{N}$. To a certain extent, these confidence intervals are reasonable, but as a result of modeling and non-Gaussian error, it is usually preferable to consider the practical limit $|R(\tau)| \leq 0.15$ (Landau et al., 2016). Moreover, in (Landau et al., 2011) it has been proposed that the online-estimated model is valid if the positive lag values verify the condition $\tau = 1,2,\ldots, \max(n_a, n_b+d)$. One reason to emphasize the positive lags during the model validation is the possible influence of feedback in the system, which may result in a correlation for negative lags. For this reason, it should be noted that for model validation purposes, the

possible correlation in negative lags is not a reason to reject the obtained model (Ljung, 2010).

The results of the model validation are discussed in **Publications III** and **V**. It is pointed out that the parametric models obtained with the identification methods are different in the general model class, but the same validation test can be used for a practical comparison. The second observation should be made on the fact that the system under study has time-varying parameters, which leads to certain limitations in the validation procedure. It is worth pointing out that the term ‘statistical properties’ can be slightly misleading when this type of a model validation procedure is applied to a continuously time-varying system. However, the dynamics of the tooth belt drive system is studied in a well-defined operating range and the independent validation data have been collected under approximately same circumstances as the identification data, and thus, the basic behavior of the system can be assumed to be the same. Thus, it can be assumed that, at least to a certain extent, the tests can be used, especially when the validity of different local models is tested in a well-defined operating area for instance in a narrow position interval.

4 Results

The research work produced several results. In this chapter, the experimental verification of the identification methods are discussed and the summary of the research results are presented.

First, the configurations of both the experimental tests setups under study are introduced. Furthermore, it is described how the identification experiments were conducted. After that, the most important findings and conclusions of the research results is presented in the form of short summary. Finally, a comparison of the online identification methods is made and perspectives from the viewpoint of controller design via system identification is discussed in brief.

4.1 Experimental verification

The coupled-belt drive system, shown in Fig. 4.1a, is studied in **Publications I**, **IV** and **VI**, whereas the tooth belt-drive system, shown in Fig. 4.1b, is considered in **Publications II**, **III** and **V**.

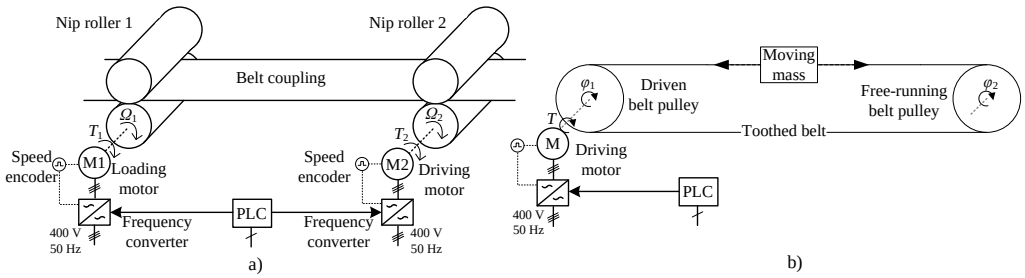

Fig. 4.1 Experimental two mass resonant systems: a) coupled belt drive system and b) tooth belt-drive system.

In the case of coupled belt drive system depicted in Fig. 4.1a, the rollers are driven by frequency-converter-supplied permanent magnet synchronous motors (PMSM), and a programmable logic controller (PLC) is used for data acquisition and to implement the excitation signals, PI controller, and references. The other experimental test system depicted in Fig. 4.1b is a linear tooth belt drive with a limited stroke, which includes a moving mass attached between the belt pulleys. The other pulley is driven by a frequency-converter-supplied PMSM, and the other pulley is free-running. A programmable logic controller (PLC) is used for data acquisition and to implement the excitation and reference signals, but the frequency converter (ASCM1) which have a commercial motion control software is used to implement the cascade position control. The used motion profiles are created in the PLC and fed to the frequency converter at every 500 μs. In both experimental systems, the angular velocity is measured with an absolute encoder mounted on the driving motor. The technical data of the experimental test setups are given in Appendix A.

In this doctoral dissertation, the system in Fig. 4.1a is considered to be an electromechanical system with free movement so that the other nip roller is treated as a driven one, and the other is used as a load to set the tension of the belt. Thus, the system is operated at the desired constant nonzero velocity, and the identification is carried out so that the excitation signal is added to the torque reference signal after the system has been stabilized to the desired velocity. An illustrative example of the velocity, torque and excitation signals during the identification experiment are shown in Fig. 4.2a when the PRBS has been superposed to the velocity controller output. Correspondingly, in the case of the tooth belt drive, the application provides linear motion over a limited stroke, and therefore, identification must be performed within a limited operating range. Consequently, the experiments become more complicated as smooth motion profile must be designed and an adequate position control is required during the tests. Similar restrictions can be found from some of the robot joint (Wernholt and Gunnarsson, 2006) and feed-drive system (Kim and Chung, 2005) identification problems, where the freedom of motion is similarly limited. Example of identification experiment in the case of tooth belt drive system is shown in Fig. 4.2b when the system is excited with multisine during trapezoidal motion profile.

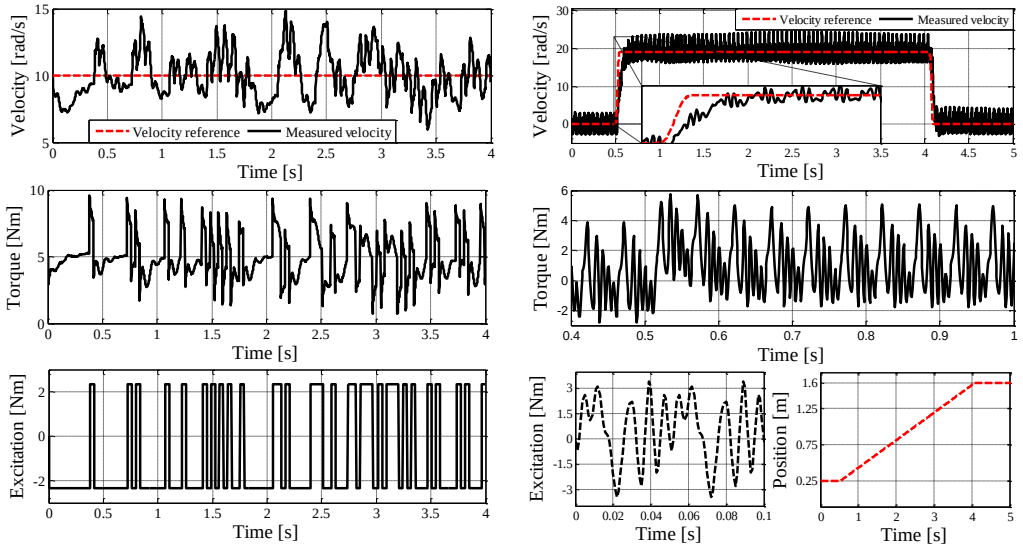

Fig. 4.2 References and signals during the identification experiment of: a) coupled belt drive using PRBS and b) tooth belt drive using multisine excitation signal.

The measured signals shown in Fig. 4.2 are given as an illustrative example in order to clarify the difference in the identification experiments carried out with the tests setups under study. In the case of the coupled belt drive with free movement, the closed-loop identification experiments are carried out at nonzero velocity, that is, by operating the system at 10 rad/s when the belt is pre-tensioned to 50 N. Whereas in the case of the tooth belt drive trapezoidal motion profiles are considered and the zero velocity is avoided as

much as possible, in order to mitigate the effect of the nonlinear friction to the estimation result. The limitations of the identification experiments with the tooth belt drive are further discussed in **Publications II**–**III** and **V**.

In the practical experimental verification, the maximum length PRBS is the only signal that has been generated online in the PLC by using XOR-ports-based shift register. The multisines and the chirp excitation signals were designed and prepared in Matlab, and subsequently stored in the PLC. Depending on the identification method, the measured input or the known excitation signal are used with the measured output to estimate frequency response directly or indirectly from the closed-loop experiments. In order to obtain valid results from the identification, the offset components of the signals corresponding to the operating point has been removed or considered in the estimation routine. Moreover, the identification experiments have been carried out several times in order to verify the proposed identification methods and to obtain independent data for validation purposes.

4.2 Summary of the key results

In this section the most important findings and conclusions of the research results are presented in the form of short summary. At first, the Kalman-filter-based online identification methods and experimental results obtained with the coupled belt drive are discussed. This experimental test setup, with various mechanical configurations, has been considered for both online and offline identification purposes and widely discussed in **Publications I**, **IV** and **VI**. For this reason, only the key findings are discussed in brief in this section. Thus, the both Kalman-filter-based online identification approached are studied in the case of the mechanical system configuration 2 of Table 2.1. Three different excitation signals; the PRBS, multisine and chirp are considered for the determination of frequency responses. In the case of the multisine and chirp, the Kalman-filter-based approaches are applied for online nonparametric frequency response estimation, whereas, the PRBS is used to obtain offline post-processed frequency response.

In Fig. 4.3 the online estimated frequency responses are compared with the offline-identified frequency response. The frequency responses has been directly estimated from the closed-loop experiments. Evidently, the online-identified frequency responses are in a good correspondence with the offline-identified one although small discrepancies can be noticed, as expected. This result is important as it clearly validate the applicability of the proposed Kalman-filter-based identification approaches for real-time frequency response estimation at a selected band frequencies. Moreover, the time-frequency presentation of signals using the Kalman filter can be regarded as a kind of a short-time DFT resulting in a nonparametric presentation of the frequency response. Such a presentation has its advantages, such as compactness and computational simplicity, when considering online identification of a closed-loop-controlled mechanical system at a selected band of frequencies. Furthermore, the presentation also provide several

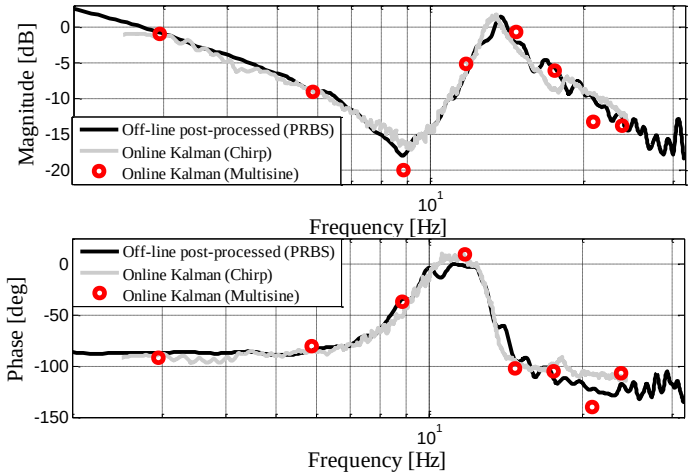

Fig. 4.3 Online estimated frequency responses using the Kalman-filter-based identification approaches compared to the offline post-processed frequency response.

opportunities to closed-loop diagnostics as was discussed in **Publications IV** and **VI**. The changes in the mechanical system could be observed by applying the nonparametric form to calculate Vinnicombe's gap between to models in **Publication IV**. Moreover, the online estimated Nyquist curve in **Publication VI** provided the opportunity to calculate the controller performance- and system-related parameters by considering different distances in the Nyquist plot.

The tooth belt drive was used to validate the closed-loop parameter estimation routines; the recursive time domain OE methods and the SDFT-based frequency domain identification approach. In the case of the OE methods the system was excited with the PRBS whereas in the case of the SDFT the Schroeder multisine was considered. Besides the fundamental differences between the identification methods and the excitation signals, the identification experiments have been carried out differently in **Publications II**–**III** and **V**. Thus, it is more preferable to discuss the key findings of these **Publications** separately.

4.2.1 Publications II and III

The direct and indirect recursive OE methods were studied in the case of a closed-loop-controlled parameter-varying mechanical system in **Publications II** and **III**. Because, **Publication III** was a direct continuation of research work done in **Publication II**, thereby the key results of the both studies are summarized here. The online and offline OE methods were applied for direct parameter estimation in **Publication II** in order to monitor the changes in the mechanical system. The identification problem was treated as LTI system identification in a well-defined operating range and the two mass system approximation of the dominant frequency (2.6) was considered as a model structure in the estimation routines. The identification experiments has been carried out similarly as depicted in Fig. 4.2b, but a constant velocity of 0.06 m/s profile is used and the PRBS

was superposed to the torque reference. In **Publication III** the same identification problem was considered, but the parameter estimation was carried out indirectly. In Fig. 4.4 the directly and indirectly estimated parameters from the measurements are shown with the reference model. The uncertainty related to the reference system parameters are shown with the shaded area.

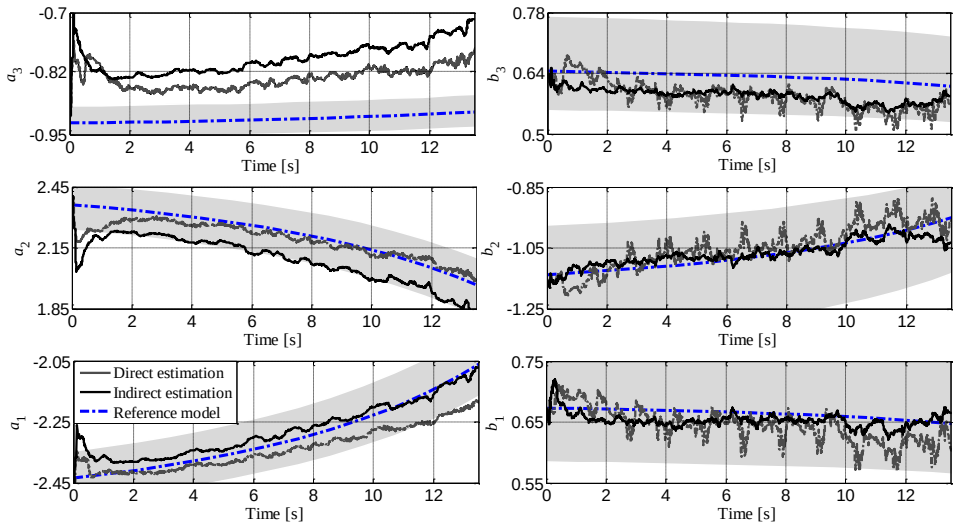

Fig. 4.4 Indirectly and directly estimated system parameters compared to the reference model parameters.

Fig. 4.4 summaries the key findings related to the online identification results discussed in **Publications II** and **III.** It can be concluded that the directly and indirectly estimated parameters are in a satisfactory agreement with the parameter behavior of the reference model, and evidently, the position depended behavior can be captured by the two mass model structure. It can be also observed that indirectly estimated numerator parameters are smoother than the directly estimated ones, because the use of closed-loop predictor (3.13) improve the identification in closed-loop conditions. Even though, the directly and indirectly estimated parameters are in a good agreement with the reference model, the residual analysis with cross correlation tests (3.26) and (3.27) is applied for validation purposes. The cross correlation based validation for directly and indirectly estimated parameters are shown in Fig. 4.5.

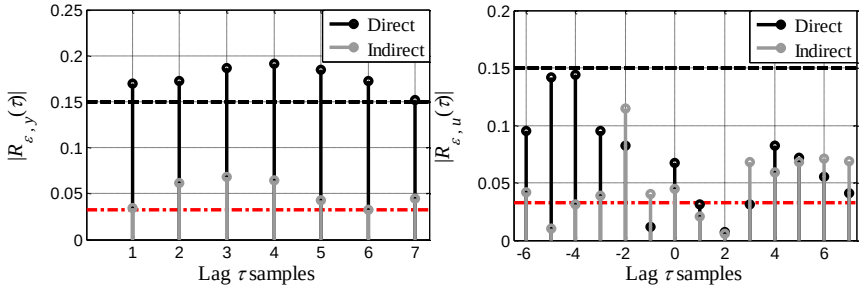

Fig. 4.5 Validation of the directly and indirectly estimated parameters with cross correlation analysis.

The validation result in Fig. 4.5 indicates that the indirect parameter estimation outperforms the direct estimation routine. The cross correlation values remains under the practical confidence limit 0.15 and are close to the 97% confidence limit. The 97% confidence limit have been determined as $2.17/\sqrt{L}$, where L = 4500 which represents the number of the samples considered in the cross validation.

As a final conclusion, the experimental results and the validation tests show that the indirect closed-loop identification method is feasible for estimating parameters of parameter varying system. As applied, the model estimation captures the changing parameters of the system and position dependent system dynamics can be clearly observed. Even though linear identification methods are utilized, the obtained parameter values show an acceptable agreement with the reference model and the validation data, and thus, the proposed indirect closed-loop identification method is feasible for online estimation of the tooth drive parameters.

4.2.2 **Publication V**

The SDFT-based online frequency domain identification routine was studied in **Publication V**. The Schroeder multisine with a frequency range of 20 Hz to 120 Hz with a frequency resolution of 5 Hz was considered as an excitation signal and the SDFT was applied to indirect nonparametric frequency domain identification. The identification experiments were carried out as depicted in Fig. 4.2b and a constant velocity of 0.38 m/s profile was used. Moreover, the frequency domain observations were used to fit parametric model by using LS-based identification routine (3.15)–(3.19) in order to validate the proposed method. In Fig. 4.6 the estimated parameters are shown with the reference model.

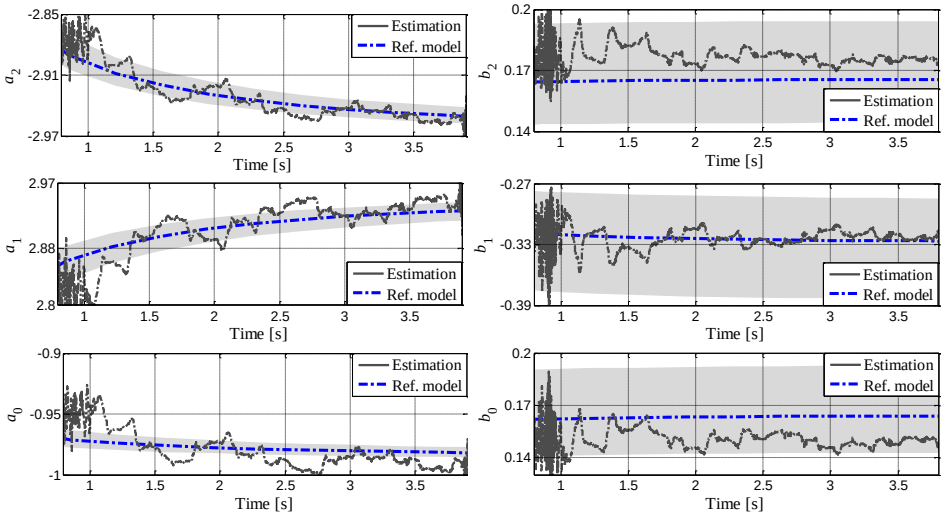

Fig. 4.6 Online estimated system parameters compared to the reference model parameters.

In Fig. 4.6 it can be concluded that the LS-estimation captures the changing parameter behavior from the frequency domain observation. However, it is worth remarking that the online parameter estimation routine is considered in a narrow frequency band and a separate noise model is not estimated, and thus, for these reasons discrepancies can be expected. By applying the cross correlation based validation tests (3.26) and (3.27), the estimated parameters can be evaluated. The cross correlation based validation tests for the estimated parameters are shown in Fig. 4.7. The number of the samples L = 3000 has been considered in the cross validation.

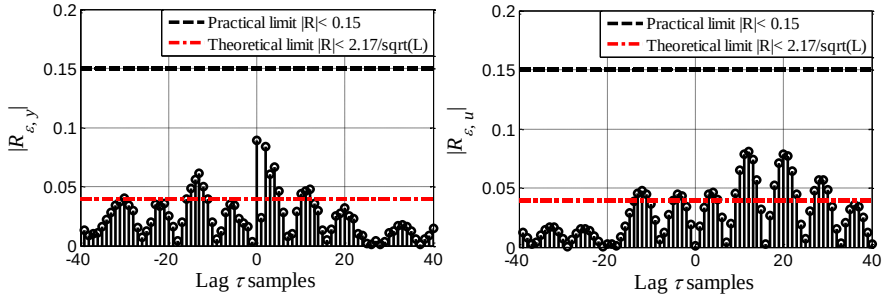

Fig. 4.7 Validation of the estimated parameters with cross correlation analysis.

The result in Fig. 4.7 show that the cross correlations are close to the $2.17/\sqrt{L}$ confidence limit, thus indicating that the estimated parameters are valid in terms of cross-correlation based residual analysis. As a final conclusion, the SDFT-based identification routine is applicable to track parameter varying system in the frequency domain. This observation was further validated by comparing the online identified magnitudes with the corresponding offline identified frequency points in **Publication V**.

4.3 Comparison of the online identification approaches

Throughout this study, the frequency and time domain identification approaches that were conducted in the course of this research have been described; now, some comparison must be made regarding these. Besides the fundamental differences that are due to the different categories into which these approaches fall, there are also other significant discrepancies, which make a direct comparison somewhat impractical. Hence, it is preferable to discuss different selection criteria from the viewpoint of advantages and disadvantages that should be considered when a specific identification approach is chosen for a practical industrial application.

Firstly, when considering the SDFT and Kalman-filter nonparametric identification approaches discussed in **Publications IV** and **V**, the main advantage of these approaches is that they can be tuned in advance based on the frequency components of the multisine signals. Preferably, this initialization requires prior knowledge of the system dynamics. In addition, the SDFT removes the bias and drift from the data, and basically does not require any other initialization than a user-specified set of frequencies to define the resonators and window size. However, an obvious drawback is the increased

computational burden when a large number of frequency components are included in the excitation signal. Similarly, the fixed state observer form of the Kalman filter also suffers from the same computational drawback, and , requires an initial selection for the tuning parameter, which sets the desired tracking properties for the filter. When these methods are applied to the identification of an electromechanical system, it can be assumed that they are, at least to a certain degree, applicable to provide a nonparametric frequency response estimate in a computationally efficient manner by using recursive computations to obtain a DFT as was shown in **Publications IV** and **V**. Thus, if only a limited frequency range is to be identified, the online frequency domain approach can be more preferable compared with the time domain methods. This is also an important aspect from the perspective of fault diagnostics.

The frequency domain observations can be applied with arbitrarily chosen frequencies to estimate a parametric model, but the computational burden increases further as an additional parameter-fitting algorithm is needed, as it is reported in **Publication V**. It is evident that if a parametric model has to be estimated online, the technical limitations related to the memory and calculation capacity of the practical application can favor the well-known efficient time domain methods with a low computational complexity such as the recursive CLOE method discussed in **Publication III**. Even though the recursive time domain methods require somewhat more initialization such as selection for the model complexity, the well-known fact that these methods can, in practice, function with an extremely low excitation is an appreciated property when practical mechanical applications are considered (Landau and Zito, 2011).

In **Publication VI,** a nonparametric Kalman-filter-based identification approach was proposed to estimate the frequency response in real time. The main drawback of this method is that it has to be synchronized to the frequency of the excitation signal, which has instantaneous frequency variation over time, for instance, the chirp. This property also introduces the second disadvantage of the method, that is, a slow sweeping is essentially required for a precise measurement. However, the chirp has an important advantage as it can be narrowed to the desired band of frequencies, which is the main contributor to the feasibility of the approach. Thus, the approach can be applied to identify and monitor different frequency regions of an electromechanical system in a frequency-by-frequency manner. The computational complexity of the method is low because only a few states are estimated simultaneously.

As a final conclusion, it can be stated that there is no single selection criterion that can be used to decide which identification method discussed in this dissertation is the most feasible one for mechanical applications, and which would always lead to a good and valid identified model. For example, in the case of many practical parameter estimation problems, it is necessary to reconsider the excitation conditions, the applied estimation algorithm, or the experimental conditions in order to obtain acceptable results. Moreover, in this dissertation, the applicability of the proposed identification methods was validated with experimental resonating systems, but when applied to a practical industrial

application, the final purpose of use, safety issues, and the technical limitations direct the selection.

4.4 Discussion

This doctoral dissertation focused on the online identification of the dominant dynamics of resonating mechanical systems, with a specific objective to identify a predefined frequency band around the first resonance frequency of the system. Especially, the proposed nonparametric frequency domain identification approaches were suitable for this purpose by exciting the system with an excitation signal containing a predefined set of frequencies. However, when considering the system identification problems from the viewpoint of the controller design, the main target is to build a parametric representation of the system by considering a prior-determined model structure that is estimated from the collected input/output data. In most cases, estimated and validated simple models can be successfully used to design a high-performance control, but the critical part of the identification is to find which terms or dynamics should be included in the model that sufficiently capture the essential system behavior. In this section, this topic is discussed from the perspective of neglected system dynamics. Certain aspects related to the controller design through identification are discussed in brief.

4.4.1 Relation of neglected system dynamics to control design

In many industrial motion control applications, the control law of preference is a simple P-position control cascaded with a PID velocity loop combined with feedforward terms (Jokinen, 2010). In this doctoral dissertation, the experimental identification and control design validation have been carried out by using electrical drives with commercial motion control software, and therefore, the cascade control structure has been under consideration. With this type of a controller structure, some design compromises have to be made with the performance, for example in the case of resonating systems, because all the closed-loop poles cannot be freely placed (Jokinen, 2010). In **Publication I**, the position cascade controller with the velocity feedforward was designed based on the reference and identified model by loop shaping. In the controller design, the sensitivity $S(s)=\left(1+C(s)\cdot G(s)\right)^{-1}$ and complementary sensitivity $T(s) = C(s)\cdot G(s)\cdot S(s)$ transfer functions with the weights were applied to obtain the performance criteria. However, in practice, several modeling errors associated with the parametric structure are expected to occur as a result of the neglected high-frequency system dynamics such as possible higher resonance modes, actuator or sensor lags, or measurement noise. These unmodeled dynamics limits the achievable bandwidth and may have an adverse effect on the performance and stability of the controller.

For resonating two-mass systems, various model-based controller design methods have been proposed in the literature such as different pole-placement assignment techniques for a two-degree-of-freedom PI controller (Zhang and Furusho, 2000), (Szabat and Orlowska-Kowalska, 2007). Especially, when using an identified model for the controller

design, it has been shown that pole placement combined with a loop-shaping technique improves the control design stability (den Hamer et al., 2005). Obviously, neglecting the high-frequency dynamics of the system can be justified to a certain degree, but it is of importance in the controller design. These frequency regions should be considered in the controller design procedure by shaping the input sensitivity function $S(s)\cdot G(s)$, and thus, the relation between the input and output disturbance of the system in order to improve the stability of the control loop. Correspondingly, the output sensitivity function $S(s)\cdot C(s)$, the relation between system input and output disturbance, is related to the robustness and disturbance rejection properties of the closed-loop control. These sensitivities should also be considered in the controller design for instance by introducing predefined fixed parts for the controller. As an example, a work by (Landau and Zito, 2011) provides practical guidelines to use sensitivity functions for the pole placement controller design based on identified models.

4.4.2 Identification in closed loop

The closed-loop identification approaches proposed in this dissertation were studied under operating conditions that approximately correspond to the commissioning state; that is, a soft controller was considered. **Publication I** was the only article appended to the dissertation that discussed the controller design by system identification. On the other hand, **Publications II−VI** exclusively studied the applicability of online identification methods for the identification of resonating mechanical systems. It obvious that a low bandwidth controller, which does not significantly damp the resonance mode of the system, is essentially required to achieve good estimates in the range of frequencies that are of interest. This is usually the first step in order to achieve an initial model for the control design. After the control design step, the closed-loop identification should be performed again with the designed controller to obtain higher precision for the critical frequency regions. For instance, with the time domain methods discussed in this dissertation, this can be achieved by filtering the excitation signal $r_u(k)$ through the output sensitivity function (Landau et al., 2011). This introduces an option to use control goal objective-oriented identification, and thus, provides an opportunity to redesign the controller or monitor the closed-loop performance. The frequency domain identification methods discussed in this work could be used for similar purposes

5 Conclusions and further study

This doctoral dissertation studied various online identification techniques for the identification of a mechanical system in electrical drives. The discussion covered a closed-loop time domain identification approach that is fundamentally based on the recursive parameter estimation with an OE-structure as well as nonparametric frequency domain approaches that are based on the time-frequency representation of signals using SDFT and Kalman filters. All the discussed methods relied on different persistent excitation signals, and thus, the considered excitation inputs included continuous sine sweep (chirp), pseudo random binary signal (PRBS), and multisines. Moreover, the dissertation focused on the online identification of a mechanical load of electric drives having dynamics that can be approximated as a two-mass system. The studied identification methods were verified by two different experimental test setups; with a coupled belt drive and tooth belt drive. The experimental results show that the studied closed-loop identification methods are applicable for estimating parameters of a servomechanism with a limited stroke as well as of an electro-mechanical actuator with free movement.

First, by considering the time domain online identification methods studied in **Publications II**–**III**, a polynomial-model-based identification method was applied. It was shown that the estimated two-mass model can be treated as a best linear approximation of the mechanical coupling in a certain operating point, and thus, the essential system dynamics in different cart positions can be online identified. This means that the two-mass-system approximation of the dominant resonance frequency can be used to represent the complete mechanical load of the drive in a simplified way.

Moreover, **Publication IV** and **VI** proposed a nonparametric methods to estimate the frequency response of a closed-loop-controlled servomechanism in real time using a Kalman-filter-based identification routine. The discussion also covered the closed-loop system diagnostics options with the proposed method in brief. The advantages of this type approach compared to well-established standard identification methods include: simpler calculations and the recursive form, which does not require storage of the whole experiment record and the possibility of detection of changes in computationally efficient manner. The main drawback is the rapid changes in the excitation signal that can introduce transients to the system which can distorts the frequency response measurement, as the proposed Kalman filter method assumes a steady state response to a constant frequency harmonic signal from its definition. Thus, as a result in **Publication VI**, the longer duration of the experiment is essential in order to obtain reliable results, and hence, a slow frequency sweeping is required. Nevertheless, this type of identification routine may be applied for the identification of changes in the desired band of frequencies, which is desirable feature from the viewpoint of diagnostics.

Finally, **Publication V** discussed and evaluated the application of the SDFT for indirect nonparametric frequency domain identification of a closed-loop-controlled mechanical system with varying system dynamics. The paper showed that the nonparametric behavior

of the frequencies of interest can be effectively identified and tracked in the frequency domain by using a short record of data in the sliding window. Because this results in a nonparameteric characterization of dynamic system, it provides several opportunities to diagnostics and supervision purposes such as fault detection, as well as for real-time dynamic modelling required by self-tuning control algorithms. The paper also showed that the parameters of the simplified two-mass system approximation can be obtained from the frequency domain observations by considering a Least-Squares (LS) based identification criterion for the estimation of a parametric model. Similar type of linear model estimation routine from the nonparametric frequency response observations has been successfully applied for nonlinear flight application in (Holzel and Morelli, 2011). Thus, the method proposed here could provide interesting opportunities for the monitoring of changing resonating mechanical systems for instance in a wind mill application.

In the course of the study, certain topics of further interest have arisen in the case of the studied online identification methods.

5.1 Suggestions for future work

Even though a linear identification method was applied in **Publications II**–**III**, the obtained parameter values show an acceptable agreement with the reference model, and thus, the proposed indirect closed-loop identification method is valid for online estimation of the tooth belt drive parameters. However, for this specific application, the nonlinearities could be parameterized and introduced in the regression vector. Moreover, even though the model validation gave stochastically valid parameter estimates the bias could be reduced by filtering the input and output using the estimated denominator polynomial.

Obviously, the main drawback using the LS algorithm in **Publication V** for parameter estimation from the viewpoint of online identification is the increased computational burden in conjunction with the number of frequency points considered in the estimation. This issue is considered in the future research by applying a recursive form of the LS algorithm for the parameter estimation so that the resonator outputs of the SDFT are used in a frequency-by-frequency manner. However, this implies an undesirable feature as the estimation is basically delayed, and thus, limits its usefulness for certain applications, yet, but could be feasible to detect system changes for diagnostics purposes.

In **Publication VI**, it is evident that the identification method requires further improvement, for instance, the selection of the Kalman filter gain for different frequency regions in conjunction with a swept excitation signal amplitude design. Moreover, the state-space representation could be extended to the observer form so that the states of the corresponding signals and the transfer functions associated with the relation of these signals could be estimated simultaneously. This observer form could be useful for diagnostics purposes and change detection.

As a final suggestion, the future research work dealing with the topic of controller design should include the implementation and testing of advanced controllers that are updated or their performance is monitored with a real-time identification method. The frequency domain identification methods discussed in this dissertation could provide several opportunities for an advanced controller. Firstly, the uncertainties and modelling errors can be directly interpreted in the frequency domain, which are important metrics of robustness. The nonparametric presentation with uncertainties could allow an advanced controller structure with a robust learning scheme or adaptation that compensates for the errors with different adaptation weights for the identified frequencies. Obviously, the price of these opportunities is the large computational load of the required frequency domain calculations.

References

Abed, A., Weinachter, F., Razik, H., and Rezzoug, A. (2001). Real-time implementation of the sliding DFT applied to on-line's broken bars diagnostics. In: *Proc. IEEE IEMDC*, pp. 345–348, Jun. 2001.

Barkley, A. and Santi, E. (2009). Improved online identification of a DC-DC converter and its control loop gain using cross-correlation methods. *IEEE Transactions on power electronics*, vol. 24, no. 8, pp. 2021–2031, Aug. 2009.

Beineke, S., et al. (1998). Identification of nonlinear two-mass systems for self-commissioning speed control of electric drives. In: *Proc. IECON*, pp. 2251–2256, 1998.

Bitmead, R., Tsoi, A.C., and Parker, P.J. (1986). A Kalman filtering approach to short-time fourier analysis. *IEEE Trans. Acoust., Speech, Signal Process*, vol. 34, no. 6, pp. 1493–1501, 1986.

Bähr, A. and Beineke, S. (2007). Mechanical resonance damping in an industrial servo drive. In: *Proc. of EPE*, pp. 1-10, Aalborg, Denmark, 2007.

Cespedes, M. and Sun, J. (2014). Adaptive control of grid-connected inverters based on online grid impedance measurements. *IEEE Transactions on sustainable energy*, vol. 5, no. 2, pp. 516–523, Apr. 2014.

den Hamer, A.J., Angelis, G.Z., van de Molengraft, M., and Steinbuch, M. (2005). A practical loop-shaping approach for pole-placement in mechatronics systems. In: *Proc: IEEE Conf. on Control Applications*, pp. 394–399, Aug. 2005.

Derammelaere, S., et al. (2014). Load angle estimation for two-phase hybrid stepping motors. *IET Electric power applications*, pp. 257–266, vol. 8, no. 7, 2014.

Dhaouadi, R., Kubo, K., and Tobise, M. (1993). Two-degree of freedom robust speed controller for high-performance rolling mill drives. *IEEE Transactions on industrial applications*, vol. 29, no. 5, pp. 919–923, Oct. 1993.

Eker, I. and Vural, M. (2003). Experimental online identification of a three-mass mechanical system. In: *IEEE CCA Conf.*, vol. 1, pp. 60–65, Jun. 2003.

Ferretti, G., Magnani, G., and Rocco, P. (2003). Load behaviour concerned PID control for two-mass servo systems. In: *Proc. of the 20013 IEEE/ASME Int. Conf. on Advanced Intelligent Mechatronics*, pp. 821–826, 2003.

Forssell, U. (1999). *Closed-loop Identification: Methods, Theory and Applications*. Doctoral thesis, Linköping Studies in Science and Technology, Dissertations, No. 566, Linköping University, Sweden.

Frei, A., Grgic, A., Heil, W., and Luzi, A. (1986). Design of pump shaft trains having variable-speed electric motors. In: *International Pump Symposium*, Houston, TX, pp. 33-44, May, 1986.

Garrido, R. and Concha, A. (2013). An algebraic recursive method for parameter identification of a servo model. *IEEE/ASME Transaction on Mechatronics*, vol. 18, no. 5, pp. 1572–1580, Oct. 2013.

Garrido, R. and Concha, A. (2014). Inertia and friction estimation of a velocity-controlled servo using position measurement. *IEEE Transactions on industrial electronics*, vol. 61, no. 9, pp. 4759-4770, Sep. 2014.

Gevers, M. (2006). A personal view of the development of system identification. *IEEE Control Systems Magazine*, vol. 26, no. 6, pp. 96–105, Dec. 2006.

Gilson, M., Garnier, H., Young, P.C., and Van den Hof, P.M.J. (2011). Optimal instrumental variable method for closed-loop identification. *IET Control Theory and Applications*, vol. 5, no. 11, pp. 1147–1154, 2011.

Girgis, A., Bin Chang, W., and Makram, E. (1991). A digital recursive measurements scheme for on-line tracking of power system harmonics. *IEEE Transactions on Power Delivery*, vol. 6, no. 3, pp. 1153-1160, July 1991.

Goubej, M. (2015). Kalman filter based observer desgin for real-time frequency identification in motion control systems. In: *Proc. 18th Conf. on Process control*, pp. 79–84, 2015.

Graham, M.R. and de Callafon, R.A. (2006). Linear regression method for estimating approximate normalized coprime plant factors. In: *14th IFAC Symp. on System Identification*, Newcastle, Australia, pp. 1–6, 2006.

Gustavsson, I., Ljung, L., and Söderström, T. (1977). Identification of processes in closed loop - identifiability and accuracy aspects. *Automatica*, vol. 13, no. 1, pp. 59–75, 1977.

Hace, A., Jezernik, K., and Sabanovic, A. (2007). SMC with disturbance observer for a linear belt drive. *IEEE Transactions on industrial electronics*, vol. 54, no. 6, pp. 3402–3412, Dec. 2007.

Hashimoto, T. and Ishida, Y. (1999). An application of time delay estimation by ANNs to frequency domain I-PD controller. In: *Proc. Int. Joint. Conf. on Neural Networks*, pp. 2164–2167, Washington, USA, 1999.

Heath, W.P. (2001). Bias of indirect non-parametric transfer function estimates for plants in closed loop. *Automatica*, vol. 37, no.10, pp. 1529–1540.

Holzel, M. and Morelli, E. (2011). Real-time frequency response estimation from flight data. In: *Proc. AIAA Atmospheric Flight Mechanics Conference*, pp. 1–26, 2011.

Iribas-Latour, M. and Landau, I.D. (2013). Identification in closed-loop operation of models for collective pitch robust controller design. *Wind Energy*, vol. 16, no. 3, pp. 383–399, 2013.

ISO:21181:2005 (2013). Light conveyor belts -- Determination of the relaxed elastic modulus. *2013 revised ISO Standard*.

Janot, A., Vandanjon, P.O., and Gautier, M. (2009). Identification of robots dynamics with the instrumental variable method. In: *IEEE Int. Conf. on Robotics and Automation*, Kobe, Japan, pp. 1762–1767, 2009.

Jenssen, A. and Zarrop, M. (1994). Frequency domain change detection in closed loop. In: *Proc. Int. Conf. in Control*, pp. 676–680, 1994.

Jokinen, M. (2010). *Centralized motion control of a linear tooth belt drive: Analysis of the performance and limitations*. Doctoral thesis, Acta Universitatis Lappeenrantaensis No. 407, Lappeenranta University of Technology, Finland.

Kalman, R.E. and Bucy, R.S. (1961). New results in linear filtering and prediction theory. *Trans. ASME series D, Journal of Basic Engineering*, vol. 83, pp. 95–108, 1961.

Kamwa, I., Samantaray, S.R., and Joos, G. (2014). Wide frequency range adaptive phasor and frequency PMU algorithms. *IEEE Transactions on smart grid*, vol. 5, no. 2, pp. 569-579, March 2014.

Kang, J.-K. and Sul, S.-K. (2000). "Vertical-vibration control of elevator using estimated car acceleration feedback compensation". *IEEE Transactions on industrial electronics*, vol. 47, no. 1, pp. 91–97, Feb. 2000.

Khan, I.U. and Dhaouadi, R. (2015). Robust control of elastic drives through immersion and invariance. *IEEE Transactions on industrial electronics*, vol. 61, no. 7, pp. 1572–1579, March 2015.

Kim, M.-S. and Chung, S.-C. (2005). A systematic approach to design high-performance feed drive systems. *Int. Journal of Machine tools and Manufacture*, vol. 45, pp. 1421–1435.

LaMaire, R., Valanani, L., Athans, M., and Gunter, S. (1987). A frequency-domain estimator for use in adaptive control systems. In: *Proc. American Control Conf.*, pp. 238–244, Minneapolis, USA, 1987.

Landau, I.D. (1979). *Adaptive control: The model reference approach*. Marcel Dekker, New York, 1979.

Landau, I.D., Airimitoaie, T.B., Castellanos-Silva, A., and Constantinescu (2016). *Adaptive and robust active vibration control - Methodology and Tests*-. Springer-Verlagen, London, 2016.

Landau, I.D. and Karimi, A. (1997a). An output-error recursive algorithm for unbiased identification in closed loop. *Automatica*, vol. 33, no. 5, pp. 933–938, May 1997.

Landau, I.D. and Karimi, A. (1997b). Recursive algorithms for identification in closed loop: A unified approach and evaluation. *Automatica*, vol. 33, no. 8, pp. 1499–1523, Aug. 1997.

Landau, I.D., Lozano, R., M'Saad, M., and Karimi, A. (2011). *Adaptive Control: Algortihms, Analysis and Applications*. Springer-Verlagen, London, 2011.

Landau, I.D. and Zito, G. (2011). *Digital Control Systems: Design, Identification and Implementation*. (pp. 279–315 and pp. 375–397), Springer-Verlagen, London, 2011.

Ljung, L. (1987). *System identification: Theory for the user*. Pretice-Hall, Englewood Cliffs, NJ, 1987.

Ljung, L. (2010). *System identification toolbox: User's guide*. Natick, MA: Mathworks, 2010.

Ljung, L. and Glover, K. (1981). Frequency domain versus time domain methods in system identification. *Automatica*, vol. 17, no. 1, pp. 71–76, 1981.

Łuczak, D. and Nowopolski, K. (2014). Identification of multi-mass mechanical systems in electric drives. In: *Proc. of 16th Int. Conf. on Mechatronics*, pp. 275–282, 2014.

Łuczak, D. and Zawirski, K. (2015). Parametric identification of multi-mass mechanical systems in electrical drives using nonlinear least squares method. In: *Proc. IECON*, pp. 4046–4051,Yokohama, Japan, Nov. 2015.

Michael, C.-A. and Sacafas, A.-N. (2007). Dynamic and Vibration Analysis of a Multimotor DC Drive system with Elastic Shafts Driving a Tissue Paper Machine. *IEEE Transactions on industrial electronics*, vol. 54, no. 4, pp. 2033–2046, Aug. 2007.

Muyeen, S.M., et al. (2007). Comparative study on transient stability analysis of wind turbine generator system using different drive train models. *Renewable Power Generation*, vol. 1, no. 2, pp. 131–141, March 2007.

Novak, P., Ekelund, T., Jovik, I., and Schmidtbauer (1995). Modeling and control of variable-speed wind-turbine drive-system dynamics. *IEEE Control systems*, vol. 15, no. 4, pp. 28-38, 1995.

Olivier, P.D. (1994). Online system identification using Laguerre series. *IEE Proc. Control Theory Applications*, vol. 141, no. 4, pp. 249–254, July 1994.

Pacas, M., Villwock, S., and Eutebach, T. (2004). Identification of the mechanical system of a drive in the frequency domain. In: *IEEE IECON*, vol. 2, pp. 1166-1171, Nov. 2004.

Pacas, M., Villwock, S., Szczupak, P., and Zoubek, H. (2010). Methods for commissioning and identification in drives. *Int. Journal for Computation and Mathematics in Electrical and Electronic Engineering*, vol. 29, no. 1, pp. 53–71, 2010.

Parker, P. and Bitmead, R. (1987). Adaptive frequency response identification. In: *Proc. 28th Conf. on Decision and Control*, pp. 348–353, 1987.

Partanen, A.G. and Bitmead, R.R. (1995). The application of an iterative identification and controller design to a sugar cane crushing mill. *Automatica*, vol. 31, no. 11, pp. 1547–1563, 1995.

Perdomo, M., Pacas, M., Eutebach, T., and Immel, J. (2013). Identification of variable mechanical parameters using extended Kalman filters. In: *9th IEEE Int. Symp. on Diagnostics for Electric Machines, Power Electronics and Drives (SPEMPED)*, pp. 377–383, 2013.

Peretti, L. and Zigliotto, M. (2009). Identification of mechanical load for electrical drives commissioning - Labelling machine case study. In: *Proc. EUROCON*, pp. 797–803, May. 2009.

Pintelon, R., et al. (1994). Parametric identification of transfer functions in the frequency domain – A survey. *IEEE Transactions on automatic control*, vol. 39, no. 11, pp. 2245–2260, Nov. 1994.

Pintelon, R. and Schoukens, J. (2001). *System identification - A Frequency Domain Approach*. Wiley-IEEE Press, Piscataway.

Raol, J.R., Girija, G., and Singh, J. (2004). *Modelling and Parameter Estimation of Dynamic Systems*. IEE control engineering series 65, London, 2004.

Saarakkala, S. (2014). *Identification and speed control design of resonating mechanical systems in electric drives*. Doctoral thesis, Aalto University, Helsinki, 2014, ISBN 978-952-60-5826-9.

Saarakkala, S. and Hinkkanen, M. (2013). Identification of two-mass mechanical systems in closed-loop speed control. In: *Proc. of 39th Annual Conf. of IEEE Ind. Elect. Soc. (IECON)*, pp. 2905–2910, Wien, Austria, Nov. 2013.

Saarakkala, S. and Hinkkanen, M. (2015). Identification of two-mass mechanical systems using torque excitation: Design and experimental evaluation. *IEEE Transactions on industry applications*, vol. 51, no. 5, pp. 4180–4189, Sep./Oct. 2015.

Saupe, F. and Knoblach, A. (2015). Experimental determination of frequecy response function estimates for flexible joint industrial manipulators with serial kinematics. *Mechanical systems and signal processing*, vols. 52–53, no. 4, pp. 60–72, Feb. 2015.

Schütte, F., Beineke, S., Rolfsmeir, A., and Grotstollen, H. (1997). Online identification of mechanical parameters using extended Kalman filters. In: *Proc. IEEE-IAS Annual meeting*, pp. 501–508, 1997.

Shuy, K.-K. and Lee, Y.-Y. (2010). Identification of electro-mechanical actuators within limited stroke. *Journal of Vibration and Control*, vol. 16, pp. 1737–1761, May 2010.

Szabat, K. and Orlowska-Kowalska, T. (2007). Vibration suppression in a two-mass drive system using PI speed controller and additional feedback - Comparative study. *IEEE Transactions on industrial electronics*, vol. 54, no. 2, pp. 1193–1206, April 2007.

Varanasi, K.K. and Nayfeh, A.S. (2009). The dynamics of lead-screw drives: Low order modeling and experiments. *ASME Jour. Dyn. Syst., Meas., Control*, vol. 126, pp. 388–396, June 2009.

Vassiljeva, K. (2012). *"Restricted Connectivity Neural Networks based Identification for Control"*. Doctoral thesis, Tallinn University of Technology, Estonia, 2012, ISBN 978-9949-23-294-9.

Wernholt, E. (2007). *Multivariable Frequency-Domain Identification of Industrial Robots*. Doctoral thesis, Linköping Studies in Science and Technology, Dissertations, No. 1138, Linköping University, Sweden.

Wernholt, E. and Gunnarsson, S. (2006). Nonlinear identification of a physically parameterized robot model. In: *14th IFAC Symp. on Ident. and System Paramet. Estima.*, vol. 39, no. 1, pp. 143-148, 2006.

Wertz, H., et al. (1999). Computer aided commissioning of speed and position control for electrical drives with identification of mechanical load. In: *Proc. of 34th IAS Annual meeting*, vol. 4, pp. 2372–2379, 1999.

Villwock, S., et al. (2008). Influence of the power density spectrum of the excitation signal on the identification of drives. In: *IEEE IECON*, Orlando, FL, pp. 1252–1257, Nov. 2008.

Villwock, S. and Pacas, M. (2008). "Application of the Welch-Method for the identification of two- and three-mass-systems". *IEEE Transactions on Industrial Electronics*, vol. 55, no. 1, pp. 457–466, Jan. 2008.

Yoshioka, Y. and Hanamoto, T. (2008). Estimation of a Multimass System Using the LWTLS and a Coefficient Diagram for Vibration-Controller Design. *IEEE Transactions on industrial applications*, vol. 44, no. 2, pp. 566–574, March/April 2008.

Yun, J.N., Su, J., Kim, Y.I., and Kim, Y.C. (2013). Robust disturbance observer for two-ineartia system. *IEEE Transactions on Industrial Electronics*, vol. 60, no. 7, pp. 2700–2710, Jul. 2013.

Zhang, G. and Furusho, J. (2000). Speed control of two-inertia system by PI/PID control. *IEEE Transactions on industrial electronics*, vol. 47, no. 3, pp. 603–609, June 2000.

Åström, K.J. and Bohlin, T. (1965). Numerical identification of linear dynamic systems from normal operating records. *IFAC Symposium on Self-tuning Systems*.

Åström, K.J. and Wittenmark, B. (1973). On self tuning regulators. *Automatica*, vol. 9, no. 2, pp. 185–199, March, 1973.

Östring, M., Gunnarsson, S., and Norrlöf, M. (2003). Closed-loop identification of an industrial robot containing flexibilities. *Control engineering practice*, vol. 11, pp. 291–300. 2003.

Appendix A: Technical data for the test setups

In this appendix, the technical data related to the components of the experimental setup are given.

Table A.1: Technical data for the coupled belt drive test setup.

PMSM	**BSM 100N–2250 AD** (*Baldor*)
Rating plate	300 V, 50 Hz, 1200 rpm, 2.54 kW
Moment of inertia (motor)	0.0022 kgm^2
Absolut encoder (multi-turn) ppt count	2048
Frequency converter	**ASCM1–04AM–016A–4** (*ABB*)
Voltage (supply)	380–480 V
Current (supply)	17–19.8 A
Frequency (supply)	48–63 Hz
Voltage (output)	0–100 % of supply voltage
Current (rated output)	16 A
Frequency (output)	0–500 Hz
Belt material I	**HNB–12E** (*Habasit*)
Thickness	2.4 mm
Mass of belt (belt weight):	2.8 kg/m^2
Width	25 mm
Length	2600 mm
Tensile force for 1 % elongation (static, after relaxation)*	20 N/mm, 11 N/mm
Belt material II	**NHM–10EKBV** (*Habasit*)
Thickness	2.1 mm
Mass of belt (belt weight):	2.5 kg/m^2
Width	25 mm
Length	2600 mm
Tensile force for 1 % elongation (static, after relaxation)*	8 N/mm, 5.5 N/mm

* Habasit Standard SOP3-155 / EN ISO21181

Fig. A.1 Dimensions of the rubber-coated rollers of the coupled belt drive.

Table A.2: Technical data of the tooth belt drive test setup.

PMSM	**CFM90M** (*SEW*)
Rating plate	288 V, 150 Hz, 3000 rpm, 4.55 kW
Moment of inertia (motor)	0.0027 kgm^2
Absolut encoder (multi-turn) ppt count	2048
Frequency converter	**ASCM1–04AM–024A–4** (*ABB*)
Voltage (supply)	380–480 V
Current (supply)	20.2 A
Frequency (supply)	48–63 Hz
Voltage (output)	0–100 % of supply voltage
Current (rated output)	24 A
Frequency (output)	0–500 Hz
Tooth belt guide	**DGE–ZR–RF–40** (*Festo*)
Dist. between pulleys	2.14 m
Max. stroke	1.6 m
Max. added mass (load)	30 kg
Max. torque	12.1 Nm
Max. velocity	10 m/s
Max. acceleration	50 m/s^2
Repeat accuracy	±0.1 mm
Cart length	0.44 m
Cart mass	2.7 kg

Appendix B: Derivation of the SDFT

At discrete time instant n the kth harmonic components $X_k(n)$ within a period of N samples can be expressed as

$$X_k(n)=\sum_{l=0}^{N-1} x(n-(N-1)+l)\mathrm{e}^{-\mathrm{j}k\left(\frac{2\pi}{N}\right)l} \tag{B.1}$$

The Fourier component $X_k(n)$ at time instant n can be expressed as

$$X_k(n)=x(n-(N-1))+x(n-(N-1)+1)e^{-\mathrm{j}k\left(\frac{2\pi}{N}\right)}+x(n)e^{-\mathrm{j}k\left(\frac{2\pi}{N}\right)(N-1)} \tag{B.2}$$

By considering the same form to the previous component $X_k(n\text{-}1)$ following is obtained

$$X_k(n-1)=x(n-N)+x\big(n-(N-1)\big)e^{-\mathrm{j}k\left(\frac{2\pi}{N}\right)}+x(n-1)e^{-\mathrm{j}k\left(\frac{2\pi}{N}\right)(N-1)} \tag{B.3}$$

Moreover, by subtracting (B.3) from (B.2)

$$X_k(n)=(X_k(n-1)-x(n-N))e^{\mathrm{j}k\left(\frac{2\pi}{N}\right)}+x(n-1)e^{-\mathrm{j}k\left(\frac{2\pi}{N}\right)(N-1)} \tag{B.4}$$

By considering the notation

$$e^{\mathrm{j}k\left(\frac{2\pi}{N}\right)}=e^{-\mathrm{j}k\left(\frac{2\pi}{N}\right)(N-1)} \tag{B.5}$$

thus the (B.4) can be rewritten as

$$X_k(n)=(X_k(n-1)+x(n)-x(n-N))e^{\mathrm{j}k\left(\frac{2\pi}{N}\right)} \tag{B.6}$$

Thus, at each time instant n the only the last sample $x(n)$ is added and the oldest sample $x(n\text{-}N)$ is removed from the window.

Publication IV

Nevaranta, N., Parkkinen, J., Lindh, T, Niemelä, M., Pyrhönen, O. and Pyrhönen J.

"Online Identification of a Mechanical System in the Frequency Domain with Short-Time DFT"

Modeling, Identification and Control, vol. 36, no. 3, pp. 157–165

Modeling, Identification and Control, Vol. 36, No. 3, 2015, pp. 157–165, ISSN 1890–1328

Online Identification of a Mechanical System in the Frequency Domain with Short-Time DFT

N.Nevaranta J.Parkkinen T.Lindh M.Niemelä O.Pyrhönen J.Pyrhönen

Department of Electrical Engineering, Lappeenranta University of Technology, FI-53851 Lappeenranta, Finland.
E-mail: {Niko.Nevaranta,Jukka.Parkkinen,Tuomo.Lindh,Markku.Niemela,Olli.Pyrhonen,Juha.Pyrhonen}@lut.fi

Abstract

A proper system identification method is of great importance in the process of acquiring an analytical model that adequately represents the characteristics of the monitored system. While the use of different time-domain online identification techniques has been widely recognized as a powerful approach for system diagnostics, the frequency domain identification techniques have primarily been considered for offline commissioning purposes. This paper addresses issues in the online frequency domain identification of a flexible two-mass mechanical system with varying dynamics, and a particular attention is paid to detect the changes in the system dynamics. An online identification method is presented that is based on a recursive Kalman filter configured to perform like a discrete Fourier transform (DFT) at a selected set of frequencies. The experimental online identification results are compared with the corresponding values obtained from the offline-identified frequency responses. The results show an acceptable agreement and demonstrate the feasibility of the proposed identification method.

Keywords: Kalman filter, Nonparametric estimation, Online identification, Short-time DFT, Two-mass system

1 Introduction

The identification of a mechanical system in electric drives has become an increasingly important feature in different high-performance motion control applications such as robotics, machine tools, material handling, and packaging, to name but a few. As the control performance plays an important role in these applications, the increasing demand for high reliability significantly motivates to improve the methods, tools, and techniques for the diagnostics and condition monitoring of a mechanical system. The deterioration of mechanical parts over time or other unexpected changes in the system dynamics may lead to degradation of the control performance. These adverse effects can cause unexpected interruptions to the production processes, for example, in material handling. Thus, it is important to detect the system changes as proactive maintenance before they lead to performance degradation, which could eventually lead to production losses. For these reasons, different system identification techniques for the condition monitoring of mechanical parts are viable methods to enhance the reliability of electrical drives.

In the literature there are numerous papers describing identification techniques for different mechanical systems. In general, a mechanical system can be identified either in the offline or in online mode by time- or frequency-domain observations. Broadly speaking, traditional identification techniques can be divided into two main categories: nonparametric estimation methods (Villwock and Pacas, 2008), (Wang et al., 2011), (Ruderman, 2014) and parametric estimation methods (Saarakkala and Hinkkanen, 2013). For commissioning purposes, frequency-domain offline identification techniques are widely recognized, and they have been

doi:10.4173/mic.2015.3.3

successfully applied to parameter estimation of different mechanical systems in closed-loop control (Beineke et al., 1998), (Beck and Turschner, 2001). Correspondingly, other studies have considered the closed-loop time-domain identification of mechanical systems for parameter estimation and control design purposes (Saarakkala and Hinkkanen, 2013), (Nevaranta et al., 2013), (Calvini et al., 2015). Especially, recent advances in time-domain prediction error approaches (Toth et al., 2012) have mitigated the closed-loop issues. Some of these methods have been successfully applied to online parameter estimation by considering their recursive form (Nevaranta et al., 2015), (Garrido and Concha, 2013). For online identification purposes, recursive time-domain parameter estimation methods have received the most attention as they have been shown to overcome many of the drawbacks of classical frequency-domain techniques in terms of closed-loop issues, accuracy, computational cost, and memory storage requirements.

Despite the above theoretical development, there are hardly any studies available on the issues related to the use of frequency-domain techniques for online system identification. As the computational capacity has increased, the real-time frequency domain techniques could introduce attractive features for example for the online monitoring of a mechanical system at a selected set of frequencies. In (Morelli, 2000), a real-time equation error method based on finite Fourier transform in the frequency domain is used for linear model identification. Another approach has been reported in (Jenssen and Zarrop, 1994), where a recursive Kalman filter is configured to perform like a Fourier transform (Bitmead et al., 1986). These methods are regarded as a short-time discrete Fourier transform. In (LaMaire et al., 1987), (Kurita et al., 1999) adaptive frequency domain online identification based control law have been proposed. Furthermore, other frequency domain identification methods used in real-time have been reported in (Barkley and Santi, 2009). However, these methods have high memory storage requirements for data acquisition (Kurita et al., 1999) or take an iterative form (Barkley and Santi, 2009).

Even though several studies have applied different online and offline methods to identify the dynamics of the mechanical parts, to the authors knowledge, none of the previous studies have discussed or considered online identification of a mechanical system in the frequency domain. In practice, the advantages of frequency domain techniques based on a Fourier transform are that the bias and drift are removed from the measured data. Secondly, by using a priori knowledge of the expected frequency range, that is, a selected set of frequencies of the excitation signal, the data to be analyzed can be easily reduced. Motivated by the features of the short-time DFT algorithm in (Jenssen and Zarrop, 1994), (Bitmead et al., 1986), (Kamwa et al., 2014), the objective of this paper is to study online nonparametric identification of the frequency response in selected frequency points and monitoring of a velocity-controlled two-mass-system in a closed-loop control. In particular, the main idea of using the short-time DFT for identification purposes presented in (Jenssen and Zarrop, 1994) is considered, but here the theory is supported by measurement results, and the identification is carried out in a different manner. The direct identification is considered by using the measured input and output signals.

This paper studies an example case of the frequency-domain online identification of a two-mass-system. The system under study is a coupled belt system with mechanical dynamics consisting of two moments of inertias coupled by flexible belt material. The online identification is performed by exciting the system with a multi-sine excitation signal and using a short-time DFT. In the approach, nonparametric identification is performed at a selected set of frequencies that are chosen from the offline-identified frequency response and prior knowledge of the system dynamics. For validation purposes, the system dynamics of the experimental test setup is varied by changing the belt material in the system. Furthermore, the normalized Vinnicombe gap metric is used as an illustrative distance metric in order to compare offline- and online-identified models in the desired frequency range when the system has been modified.

The contents of the paper are organized as follows. First, a mathematical model of the flexible belt system under consideration is developed and introduced in Section 2. After that, the online identification procedure for the mechanical system under study is introduced in Section 3. Finally, the experimental test setup is presented and identification results are shown and analyzed in Section 4. Section 5 concludes the paper.

2 Model of the Two-mass-system

The investigated two-mass-system is a coupled belt system with mechanical dynamics consisting of two moments of inertias coupled by flexible belt material as depicted in Figure 1. The dynamics of the mechanical system in Figure 1 can be described by the following set of equations

$$J_1 \frac{d\Omega_1}{dt} = T_1 - T_{\mathrm{fr1}} + r_1 F \tag{1}$$

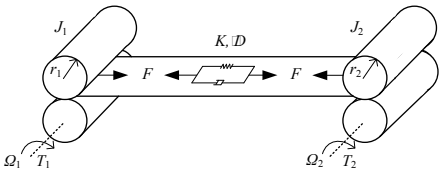

Figure 1: Flexible two-mass-system

$$J_2 \frac{d\Omega_2}{dt} = T_2 - T_{\mathrm{fr}2} - r_2 F \tag{2}$$

$$F = K(r_2\Omega_2 - r_1\Omega_1) + D(r_2\dot{\Omega}_2 - r_1\dot{\Omega}_1) \tag{3}$$

Equations (1) and (2) are the elementary dynamic equations for rotation, where J is the moment of inertia, is the angular velocity, T is the torque, T_{fr} is the frictional torque component, r is the roller radius, and F represents the tension force. The dynamics of the coupling is expressed by (3), where K is the spring constant and D is the damping constant of the belt material. In this paper, the dynamics of the two-mass-system is modified in order to show the applicability of the proposed identification method. The reference models for the system under study are calculated from the material properties and the geometrical values presented in Table 1. The reference models are used to compare the experimentally identified models. It is pointed out that the original parameters of the experimental test setup, especially the belt properties, are only known with some degree of confidence.

3 Short-Time DFT

The standard method for spectrum analysis is the discrete Fourier transform, which, in practice, requires an N array of samples. For real-time implementation, a recursive Kalman filter can be configured to perform like a Fourier transform (Bitmead et al., 1986). Thus, the short-time DFT can be obtained by using the following simplified state-space representation

$$\mathbf{x}(k+1) = \mathbf{A}\mathbf{x}(k) \tag{4}$$

$$y(k) = \mathbf{C}^{\mathrm{T}}\mathbf{x}(k)$$

where the matrices $\mathbf{A}$ and $\mathbf{C}^{\mathrm{T}}$ for the nth frequency component ω_{n} are written as

$$\mathbf{A}_{\mathrm{n}} = \begin{bmatrix} 1 & 0 & 0 \\ 0 & \cos(T_{\mathrm{s}}\omega_{\mathrm{n}}) & \sin(T_{\mathrm{s}}\omega_{\mathrm{n}}) \\ 0 & -\sin(T_{\mathrm{s}}\omega_{\mathrm{n}}) & \cos(T_{\mathrm{s}}\omega_{\mathrm{n}}) \end{bmatrix} \tag{5}$$

$$\mathbf{C}_{\mathrm{n}} = \begin{bmatrix} 1 & 1 & 0 \end{bmatrix} \tag{6}$$

Table 1: Parameters of reference systems

Parameters	Ref. system A	Ref. system B
K[N/m]	$5.75{\cdot}10^4$	$3.10{\cdot}10^4$
D[Ns/m]	100	90
J_1[kgm^2]	0.032	0.032
J_2[kgm^2]	0.032	0.032
f_{res}[Hz]	15.1	11.1

where T_{s} is the sample time. Thus, the state vector consists of the DC offset and the real and imaginary components of the signal at the frequency ω_{n}, and it is described by

$$\begin{bmatrix} x_{\mathrm{dc}}(k+1) \\ x_{\mathrm{re}}(k+1) \\ x_{\mathrm{im}}(k+1) \end{bmatrix} = \begin{bmatrix} 1 & 0 & 0 \\ 0 & \cos(T_{\mathrm{s}}\omega_{\mathrm{n}}) & \sin(T_{\mathrm{s}}\omega_{\mathrm{n}}) \\ 0 & -\sin(T_{\mathrm{s}}\omega_{\mathrm{n}}) & \cos(T_{\mathrm{s}}\omega_{\mathrm{n}}) \end{bmatrix} \begin{bmatrix} x_{\mathrm{dc}}(k) \\ x_{\mathrm{re}}(k) \\ x_{\mathrm{im}}(k) \end{bmatrix} \tag{7}$$

The equation for the output is given as

$$y(k) = \begin{bmatrix} 1 & 1 & 0 \end{bmatrix} \begin{bmatrix} x_{\mathrm{dc}}(k) \\ x_{\mathrm{re}}(k) \\ x_{\mathrm{im}}(k) \end{bmatrix} \tag{8}$$

The second and third element of the state vector $\mathbf{x}(k)$ consist of a frequency component and its derivative. Thus, the output $y(k)$ formed from the real part of the signal components. The Kalman filter solution for the state estimation problem can be written as

$$\hat{\mathbf{x}}(k+1) = \mathbf{A}\hat{\mathbf{x}}(k) + \mathbf{K}(k)(y(k) - \mathbf{C}^{\mathrm{T}}\hat{\mathbf{x}}(k)) \tag{9}$$

where $y(k)$ is the measured signal and the Kalman gain $\mathbf{K}(k)$

$$\mathbf{K}(k) = \frac{\mathbf{A}\mathbf{P}(k)\mathbf{C}^{\mathrm{T}}}{\mathbf{C}^{\mathrm{T}}\mathbf{P}(k)\mathbf{C} + r} \tag{10}$$

where r represents variance in the measurement. The covariance matrix $\mathbf{P}(k)$ is calculated as

$$\mathbf{P}(k) = \mathbf{A}\mathbf{P}(k-1)\left[\mathbf{I} + \frac{\mathbf{C}\mathbf{C}^{\mathrm{T}}\mathbf{P}(k-1)}{\mathbf{C}^{\mathrm{T}}\mathbf{P}(k-1)\mathbf{C} + r}\right]\mathbf{A}^{\mathrm{T}} \tag{11}$$

As the covariance matrix is updated, the optimal gain has a time-varying nature. For practical purposes, fixing the covariance matrix at $\mathbf{P} = \epsilon\mathbf{I}$ gives the steady-state values of the Kalman gain vector, which can be calculated offline as

$$\mathbf{K}(k) = \frac{\mathbf{A}\mathbf{C}}{\mathbf{C}^{\mathrm{T}}\mathbf{C} + \frac{r}{\epsilon}} \tag{12}$$

This expression gives a filter expression that is a fixed coefficient state observer with predetermined stability characteristics (Kamwa et al., 2014). Furthermore, this

form gives a simple tuning rule for the gain: the gain only depends on the ratio r/ϵ as the known matrices $\mathbf{A}$ and $\mathbf{C}$ are calculated beforehand. Thus, the choice of ϵ directly influences the tracking and error covariance; for instance, a small value gives slow tracking and a small error covariance. The ratio of r and ϵ is defined as

$$\lambda = \frac{r}{\epsilon} \tag{13}$$

This form provides an opportunity to use only one tuning parameter λ in the filter design. The state-space realization can be modified so that more than one frequency component can be considered at the same time by using the block-diagonal representation

$$\mathbf{A} = \begin{bmatrix} \mathbf{A}_1 & 0 & 0 & 0 \\ 0 & \mathbf{A}_2 & 0 & 0 \\ 0 & 0 & \ddots & 0 \\ 0 & 0 & 0 & \mathbf{A}_\mathrm{n} \end{bmatrix} \tag{14}$$

and correspondingly, the output matrix has the form

$$\mathbf{C}^\mathrm{T} = \begin{bmatrix} 1 & 0 & 1 & 0 \cdots & 1 & 0 \end{bmatrix} \tag{15}$$

As the signal is in a complex form, the amplitude of the nth component can be calculated by

$$|x^{(n)}| = \sqrt{x_\mathrm{re}^{(n)} + x_\mathrm{im}^{(n)}} \tag{16}$$

3.1 Estimating with Short-time DFT

In order to show the tracking properties and the influence of the tuning parameters of the Kalman filter, the following signal is considered as an example

$$y(t) = 2 + 1.3\sin(30\pi t) + 1.7\sin(80\pi t) + e(t) \tag{17}$$

where $e(t)$ is the disturbance in the signal that consists of a Gaussian noise part and three sine components with frequencies [26, 54, 72]π. The amplitude for the disturbance is set to 0.25. The Kalman filter is tuned to track frequencies $\omega_{1\text{-}7}$ = [20, 24, 30, 36, 60, 70, 80]π that include both the sine components of the signal (17) and the other components close to the disturbance frequencies. Figure 2 a) shows the estimated amplitudes for the frequencies $\omega_{1\text{-}7}$. Moreover, Figure 2 b) depicts the tracking properties in the case of a second sine component of (17) when the tuning parameter λ is varied. It can be noticed in Figure 2 a) that the amplitudes of the desired frequency components of (17) are estimated correctly under disturbances. Furthermore, the amplitudes of the other frequencies considered in the Kalman filter design as well as in $e(t)$ are estimated near zero. In Figure 2 b), the effect of the

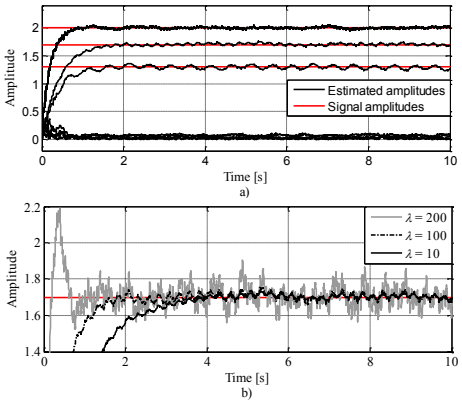

Figure 2: a) Estimated amplitudes of the signal (λ = 100) and b) tracking properties when the tuning parameter λ is varied.

tuning parameter λ is clear: when λ increases, the error in the estimate increases, but the tracking is faster. These results show that the desired frequency components can be tracked by the proposed method.

4 Experimental Results

In the experimental evaluation, a mechanical system consisting of two nip rollers coupled by a flexible belt is considered. Both of the rollers are directly coupled to BSM100N-2250AD permanent magnet synchronous motors manufactured by Baldor. The motors are controlled with high-performance ABB ACSM1 frequency converters. The velocity feedback signals are measured using high-resolution absolute encoders. An AC500 programmable logic controller (PLC) by ABB is used to implement the process controllers and the excitation signals. The experimental test setup is illustrated in Figure 3.

4.1 Offline Identification

In this paper, the offline identification is considered for two specific purposes. Firstly, based on the offline identification results, the desired set of frequency points to be monitored by the online method are selected, and thus, the frequency contents of the excitation signal are obtained. Secondly, the dynamics of the experimental system is identified in order to have a more realistic model for comparison.

The experimental offline identification tests are carried out in the nominal operation point of the system at a velocity of 10rad/s when the belt tension was set

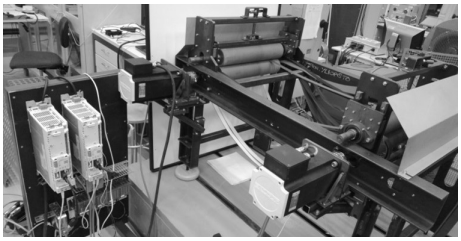

Figure 3: a) Experimental system applied in the laboratory measurements. Both of the rollers are driven by Baldor BSM100N-2250AD permanent magnet synchronous motors and controlled by ABB ACSM1 frequency converters

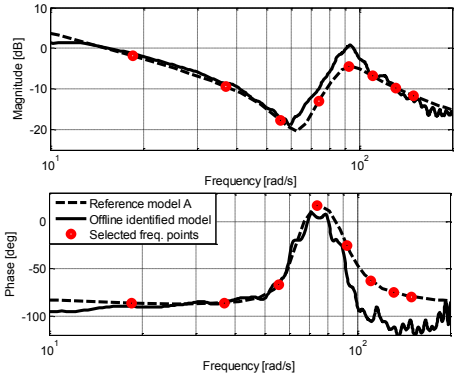

Figure 4: a) Offline-identified phase and magnitude response compared with the mathematical model (reference model A). The red dots are the selected frequencies to be monitored by the proposed online method.

to 50 N. The identification of the controlled system is carried out so that the system dynamics is excited with a pseudo random binary signal (PRBS) with 7-register and amplitude changes between the values -2.3 Nm and 2.3 Nm. The velocity is controlled by a closed-loop PI control, and the excitation signal is added to the output of the controller. By using a low-bandwidth controller, the system dynamics can be identified without losing principal information (Villwock and Pacas, 2008), (Garrido and Concha, 2013), (Garrido and Concha, 2014). In Figure 4, the experimentally identified phase and magnitude responses are compared with the frequency response of reference model A of Table 1. The offline-estimated nonparametric model is in a satisfactory agreement with the reference two-mass model. Even though there are small discrepancies between the models, the characteristics of the two-mass-system are evident in the measured phase and magnitude responses. It is pointed out that the direct comparison of the offline-identified model with the reference model of the mechanical system is difficult as the original parameters are only known with some degree of confidence. Nevertheless, the identification result is in a satisfactory agreement with the mathematical model.

As stated above, for online identification purposes, the monitoring of the mechanical system at a selected set of frequencies is a desirable feature. Based on the a priori assumption of the system dynamics and the offline identification result, the selected frequency points to be monitored are illustrated by red dots in Figure 4. The selected set includes eight frequency components close to the resonance frequency from 2.9 Hz to 23.9 Hz with a frequency resolution of 3Hz.

4.2 Estimation of Measured Output

Periodic signals are considered in this paper with N_p samples in the period, and in particular, with a random phase multisine signal, which can be written as

$$r_{\mathrm{u}}(t) = \sum_{n=1}^{N_{\mathrm{f}}} A_{\mathrm{k}} \cos(2\pi f_{\mathrm{k}} t + \phi_{\mathrm{k}}) \tag{18}$$

where N_{f} is the number of frequencies, A_{k} are the amplitudes of each frequency component, f_k are the frequencies chosen from the grid $\frac{2\pi l}{N_p}$,l=1,...,$\frac{N_p}{2}$-1 and random phases uniformly at an interval between 0 and 2π. The signal contains frequencies in the frequency range of 2.9 to 23.9 Hz with the frequency resolution of 3 Hz, and the amplitudes are chosen as one. The frequency response is only estimated at the excited frequencies. Figure 5 e) shows an example of a multisine signal amplitude in the frequency domain.

In order to illustrate the short-time DFT for online identification, the system is first excited with a different multisine excitation signal as illustrated in Figure 5. As the output of the Kalman filter is formed from the estimated states (8), it represents an estimation of the measured signal $y(k)$ calculated from the DC offset and real components. Similar type of an estimation problem for identifying the amplitudes of a harmonic signal has been considered in (San-Millan and Feliu, 2015). In this paper, the estimation properties of the Kalman filter are considered in the case of measured velocity. It is worth mentioning that the amplitude of the excitation signal has been intentionally set high for illustrative purposes. In Figure 5 a)-d), the measured velocity is compared with the estimated output. The excitation signal contains different frequencies as depicted in Figure 5 e). In Figure 5 a), the system is excited with an excitation signal with

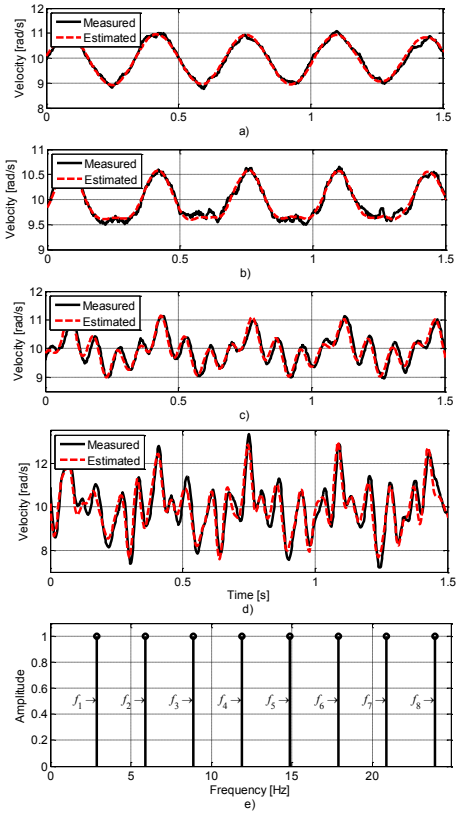

Figure 5: Estimated velocity compared with the measured velocity. a) The system is excited with f_1, b) with f_1 and f_2, c) with f_1-f_4, and d) with f_1-f_8. e) The frequency contents of the multisine signal with a frequency range of 2.9 Hz to 23.9 Hz with a frequency resolution of 3Hz.

only one frequency f_1, in Figure 5 b) with two frequencies f_1 and f_2, Figure 5 c) with four frequencies f_1-f_4, and in Figure 5 d) with eight frequencies f_1-f_8.

It can be seen in Figure 5 that the estimated signals are in a satisfactory agreement with the measured signal. Especially, in the cases a)-c), there are only slight discrepancies between the signals caused by the noise in the measurement and the small eccentricity of the roller. In Figure 5 d), the largest estimation error can be detected in the case when the excitation signal contains more frequencies; nevertheless, the estimated signal behavior agrees well with the measured one. As a conclusion, the excited frequencies can be clearly observed with the Kalman filter, thus indicating that the short-time DFT can be obtained.

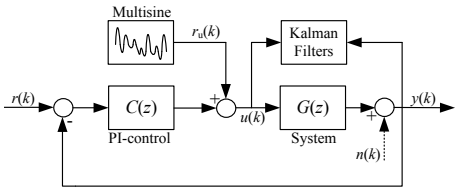

Figure 6: Scheme of the closed-loop identification.

4.3 Online Identification

First, the experimental test setup with reference parameters A (see Table 1) is considered. The system is excited with a multisine signal as depicted in Figure 5 e). The velocity is controlled with a low bandwidth PI controller, and the online estimation is performed directly by using the measured input $u(k)$ and the output signals $y(k)$ by Kalman filters as illustrated in Figure 6. The tuning parameter of the Kalman gain is chosen as $\lambda = 100$. It is pointed out that the effect of the feedback controller is now omitted as a low-bandwidth controller is used. By using (16), the amplitudes of the desired frequencies can be calculated. Thus, the ratio of the output magnitudes to the input magnitudes can be used for the estimation of the frequency response at the excited frequencies. In Figure 7, the online-estimated frequency response points are compared with the frequency responses of the offline-identified model and the reference model. Although there are slight differences between the reference frequency response and the estimated frequency points, the form of the resonance frequency can be clearly seen from the online estimated result. However, the online estimation result shows similar behavior as the offline-identified frequency re-

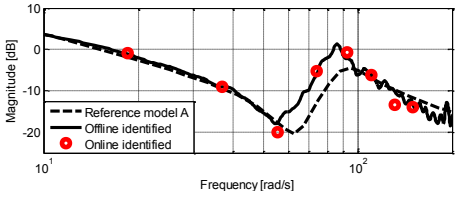

Figure 7: Online-identified frequency response points compared with the frequency response of reference model A and the offline-identified model. The red dots are the identified points with the proposed online method.

sponse, as it was expected. Moreover, we can see that the frequency component f_7 has the largest error compared with the reference and offline-identified models. However, these results are not directly comparable because of the fundamental difference between the excitation signals and the estimation methods. Nevertheless, the online estimation result is in a good agreement with the offline-identified model. Evidently, the online-identified nonparametric models in different frequency points describe the system behavior and validate the accuracy of the proposed estimation method.

4.4 Changes in the System Dynamics

The results in Figure 7 show that the dynamics of the two-mass system in the chosen frequency points can be identified directly by using Kalman filters that perform like a Fourier transform. In order to further verify the online method, the system dynamics of the experimental test setup is varied by changing the belt material between the rollers. Thus, in this paper, the modified system is regarded as reference system B with a different resonance frequency (see Table 1). In Figure 8, the online-estimated frequency points of both systems are compared with the offline-identified frequency responses. It can be observed in Figure 8 that the dynamics of the system has changed. Even though the change is small, it is enough to demonstrate that the resonance of the system has changed, which can be clearly noticed from the offline-identified frequency responses. More importantly, the same change can also be observed from the online-estimated frequency points. Especially, the change can be seen from the frequency points f_3 and f_4 that are close to the resonance and antiresonance frequencies of both systems. Furthermore, it can be noticed that the online-identified frequency component f_7 has the largest error compared with the offline-identified model in both magnitude response results. Moreover, the online-identified phase responses show more error compared with the offline-identified ones. Nevertheless, the online-identified results are in a satisfactory agreement with the offline-identified ones, thereby indicating that the short-time DFT can be applied to online identification. The characteristics of the two-mass system are evident in the online-identified amplitude and phase responses.

4.5 Distance Between the Identified Models

Typically, in order to measure the distance between the transfer function models of linear time invariant (LTI) systems, different gap metrics are used. The Vinnicombe metric (v-gap metric) between two plants

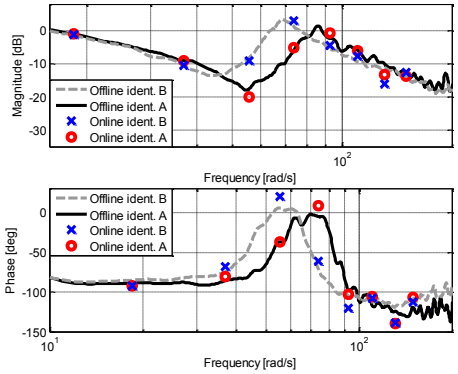

Figure 8: Online-identified frequency response points when the system is changed. The black solid line represents offline-identified system A and the dashed line system B.

$G_{\mathrm{A}}(\mathrm{j}\omega)$and $G_{\mathrm{B}}(\mathrm{j}\omega)$ is defined by (Vinnicombe, 1993)

$$\Psi\left[G_{\mathrm{A}}, G_{\mathrm{B}}\right] = \frac{\left|G_{\mathrm{A}}(\mathrm{j}\omega) - G_{\mathrm{B}}(\mathrm{j}\omega)\right|}{\left(1 + \left|G_{\mathrm{A}}(\mathrm{j}\omega)^2\right|\right)^{\frac{1}{2}}\left(1 + \left|G_{\mathrm{B}}(\mathrm{j}\omega)^2\right|\right)^{\frac{1}{2}}} \tag{19}$$

The v-gap distance is determined as

$$\delta_{\mathrm{v}}\left(G_{\mathrm{A}}, G_{\mathrm{B}}\right) = \left|\left|G_{\mathrm{A}}(\mathrm{j}\omega), G_{\mathrm{B}}(\mathrm{j}\omega)\right|\right|_{\infty} \tag{20}$$

for the frequencies $0 \leq \omega \leq \pi f_{\mathrm{s}}$ with the normalized limits $0 \leq \delta_{\mathrm{v}} < 1$. In other words, a frequency-based comparison of two systems can be obtained. By considering a known controller $C(\mathrm{j}\omega)$ and a system model $G(\mathrm{j}\omega)$, a complementary sensitivity function can be written

$$T(\mathrm{j}\omega) = \frac{G(\mathrm{j}\omega)C(\mathrm{j}\omega)}{1 + G(\mathrm{j}\omega)C(\mathrm{j}\omega)} \tag{21}$$

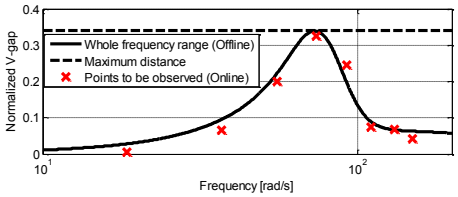

Figure 9: Frequency-based Vinnicombe gap. The solid black line is the distance of the offline-identified system models, and the dashed line is the maximum distance between them. The distances of the online-identified models at a selected set of frequencies are indicated by crosses.

In general, the v-gap metric can be used to compare the stability conditions of a controller designed for a certain plant against a set of system models. However, in this paper, the v-gap metric is only used as an illustrative distance metric in order to compare offline- and online-identified models when the system has been changed. The solid black line in Figure 9 illustrates the frequency-based v-gap of the of system models that are built from the known controller and the offline-identified model (21). It can be seen in Figure 9 that the change in the distance between the systems is noticeable as the gap of the systems is higher in the frequency region near the resonances. Furthermore, it can be noticed that the frequency region after the resonance has a small gap between the systems. In practice, this shows that there is uncertainty in the identification. Thus, in the case of parametric identification of two-mass system dynamics, this would correspond to an error in the inertial parameters. Nevertheless, the distance metric clearly shows the system changes when the resonance of the system is varied. The online frequency domain identification yields nonparametric models in the form of $G(\mathrm{j}\omega_\mathrm{n})$ at a selected set of frequencies, thereby leading to an option to monitor system changes in the desired frequency points. In Figure 9, the same distance metrics have been calculated for the online-identified nonparametric models similarly as in the case of the offline-identified ones. It can be observed in Figure 9 that the distance calculated by using online-identified frequency points indicates the same change in the dynamics as the offline result. More importantly, even though the online-identified frequency response in Figure 8 shows some error in different points, the distance of these points in Figure 9 is in a good agreement. Moreover, the advantage of the online frequency domain identification is the nonparametric model form that can be used, without loss of generality, to monitor changes in desired frequency points rather than within the whole frequency range. However, the Vinnicombe gap can be problematic distance metric, especially when considering robust controller design for system with resonances, because large distance is easily formed from the differences in the resonances. On the other hand, using the gap-metric as an online change indicator in interesting frequency points such as -3 dB closed-loop bandwidth point could lead to possibility of monitor changes of control performance.

5 Conclusions

In this paper, an online nonparametric frequency domain identification method has been presented that can be used to monitor a mechanical system at a selected set of frequencies. It is based on a Kalman filter that performs like a Fourier transform. By using the a priori knowledge of the expected frequency range, the filter can be tuned in advance to track the desired frequency components. The method was verified by experimental measurements, which confirmed the applicability of the proposed method. The results were validated by comparing the offline-identified frequency response and the online-identified frequency points. Furthermore, the experimental test setup was changed to further verify the method with different resonances. The results show acceptable agreement, thus indicating that the proposed method is suitable for the online frequency domain nonparametric identification of a mechanical system. The future work will focus on the closed-loop identification with special reference to the influence of the controller and noise on the estimation result. Moreover, by considering the adaptive form in the proposed Kalman filter, the identification could be carried out with different excitation signals for instance with a sine sweep, thereby providing the opportunity to use a simple state-space form for one frequency component.

References

Barkley, A. and Santi, E. Improved online identification of a dc-dc converter and its control loop gain using cross-correlation methods. *IEEE Trans. on Power. Elect.*, 2009. 24(8):2021–2031. doi:10.1109/TPEL.2009.2020588.

Beck, H.-P. and Turschner, D. Commissioning of a state controlled high powered electrical drive using evolutionary algorithms. *IEEE/ASME Trans. Mechatronics*, 2001. 6(2):149–154. doi:10.1109/3516.928729.

Beineke, S., Wertz, H., Schütte, F., Grotstollen, H., and Fröhleke, N. Identification of nonlinear two-mass systems for self-commissioning speed control of electrical drives. *in Proc. IEEE IECON*, 1998. pages 2251–2256. doi:10.1109/IECON.1998.724071.

Bitmead, R., Tsoi, A. C., and Parker, P. J. A kalman filtering approach to short-time fourier analysis. *IEEE Trans. Acoust., Speech, Signal Process*, 1986. 34(6):1493–1501. doi:10.1109/TASSP.1986.1164989.

Calvini, M., Carpita, M., Formentini, A., and Marchesoni, M. Pso-based self-commissioning of electrical motor drives. *IEEE Trans. Ind. Electron*, 2015. 62(2):768–776. doi:10.1109/TIE.2014.2349478.

Garrido, R. and Concha, A. An algebraic recursive method for parameter identification of a servo model. *IEEE/ASME*

Trans. Mechatronics, 2013. 18(5):1572–1580. doi:10.1109/TMECH.2012.2208197.

Garrido, R. and Concha, A. Inertia and friction estimation of a velocity-controlled servo using position measurements. *IEEE Trans. Ind. Electron.*, 2014. 61(9):4759–4770. doi:10.1109/TIE.2013.2293692.

Jenssen, A. and Zarrop, M. Frequency domain change detection in closed loop. *in Proc. Int. Conf. in Control*, 1994. pages 676–680. doi:10.1049/cp:19940213.

Kamwa, I., Samantaray, S. R., and Joos, G. Wide frequency range adaptive phasor and frequency pmu algorithms. *IEEE Trans. Smart Grid.*, 2014. 5(2):569–579. doi:10.1109/TSG.2013.2264536.

Kurita, Y., Hashimoto, T., and Ishida, Y. An application of time delay estimation by anns to frequency domain i-pd controller. *in Proc. Int. Joint Conf. on Neural Networks*, 1999. pages 2164–2167. doi:10.1109/IJCNN.1999.832723.

LaMaire, R., Valavani, L., Athans, M., and Gunter, S. A frequency-domain estimator for use in adaptive control systems. *in Proc. American Control Conf.*, 1987. pages 238–244.

Morelli, E. A. Real-time parameter estimation in frequency domain. *Jour. of Guidance, Contr. and Dynamics*, 2000. 23(5):812–818.

Nevaranta, N., Niemelä, M., Lindh, T., Pyrhönen, O., and Pyrhönen, J. Position controller tuning of an intermittent web transport system using offline identification. *in Proc. EPE*, 2013. pages 1–9. doi:10.1109/EPE.2013.6631785.

Nevaranta, N., Parkkinen, J., Niemelä, M., Lindh, T., Pyrhönen, O., and Pyrhönen, J. Online estimation of linear tooth-belt drive system parameters. *IEEE Trans. Ind. Electron*, 2015. 0(0):1–10. doi:10.1109/TIE.2015.2432103.

Ruderman, M. Tracking control of motor drives using feedforward friction observer. *IEEE Trans. Ind. Electron*, 2014. 61(7):3727–3735. doi:10.1109/TIE.2013.2264786.

Saarakkala, S. and Hinkkanen, M. Identification of two-mass mechanical systems in closed-loop speed control. *in Proc. IEEE IECON*, 2013. pages 2905–2910. doi:10.1109/IECON.2013.6699592.

San-Millan, A. and Feliu, V. A fast online estimator of the two main vibration modes of flexible structures from biased and noisy measurements. *IEEE/ASME Trans. Mechatronics*, 2015. 20(1):93–104. doi:10.1109/TMECH.2014.2304302.

Toth, R., Laurain, V., Gilson, M., and Garnier, H. Instrumental variable scheme for closed-loop lpv model identification. *Automatica*, 2012. 48(9):2314–2320. doi:10.1016/j.automatica.2012.06.037.

Villwock, S. and Pacas, M. Application of the welch-method for the identification of two- and three-mass-systems. *IEEE Trans. Ind. Electron*, 2008. 55(1):457–466. doi:10.1109/TIE.2007.909753.

Vinnicombe, G. Frequency domain uncertainty and the graph topology. *IEEE Trans. Automatic Cont.*, 1993. 38(9):1371–1383. doi:10.1109/9.237648.

Wang, Z., Zou, Q., Faidley, L., and Kim, G. Y. Dynamics compensation and rapid resonance identification in ultrasonic-vibration-assisted microforming system using magnetostrictive actuator. *IEEE/ASME Trans. Mechatronics*, 2011. 16(3):489–497. doi:10.1109/TMECH.2011.2116032.

Publication VI

Nevaranta, N., Derammelaere, S., Parkkinen, J., Vervisch, B., Lindh, T, Niemelä, M., and Pyrhönen, O.

"Online Identification of a Two-Mass System in the Frequency Domain using a Kalman filter"

Modeling, Identification and Control, vol. 37, no. 2, pp. 133–147

Modeling, Identification and Control, Vol. 37, No. 2, 2016, pp. 133–147, ISSN 1890–1328

Online Identification of a Two-Mass System in Frequency Domain using a Kalman Filter

Niko Nevaranta [1] Stijn Derammelaere [2] Jukka Parkkinen [1] Bram Vervisch [2] Tuomo Lindh [1] Markku Niemelä [1] Olli Pyrhönen [1]

[1] *Department of Electrical Engineering, Lappeenranta University of Technology, FI-53851 Lappeenranta, Finland. E-mail: {Niko.Nevaranta,Jukka.Parkkinen,Tuomo.Lindh,Markku.Niemela,Olli.Pyrhonen,Juha.Pyrhonen}@lut.fi*

[2] *Department of Electrical Energy Systems and Automation, Ghent University Campus Kortrijk, BE-8510 Kortrijk, Belgium. E-mail: {Stijn.Derammelaere, Bram.Vervisch}@ugent.be*

Abstract

Some of the most widely recognized online parameter estimation techniques used in different servomechanism are the extended Kalman filter (EKF) and recursive least squares (RLS) methods. Without loss of generality, these methods are based on a prior knowledge of the model structure of the system to be identified, and thus, they can be regarded as parametric identification methods. This paper proposes an on-line non-parametric frequency response identification routine that is based on a fixed-coefficient Kalman filter, which is configured to perform like a Fourier transform. The approach exploits the knowledge of the excitation signal by updating the Kalman filter gains with the known time-varying frequency of chirp signal. The experimental results demonstrate the effectiveness of the proposed online identification method to estimate a non-parametric model of the closed loop controlled servomechanism in a selected band of frequencies.

Keywords: Kalman filter, Non-parametric estimation, Online identification, Short-time DFT, Two-mass system

1 Introduction

System identification techniques for the diagnostics and condition monitoring of a mechanical system are key tools to enhance the reliability of electrical drives. An adequate system identification technique is of great importance in the process of acquiring a mathematical model that sufficiently represents the essential system dynamics. In terms of how the collected input output data are transformed into a mathematical model, the methods proposed for identification of mechanical systems can be broadly speaking divided into two main categories: parametric identification (Ljung, 2010) and non-parametric identification techniques (Heath, 2001). Moreover, the identification can be performed in offline or in online mode by time- or frequency-domain observations.

Different time-domain methods based on a least squares criterion are commonly used in off-line identification of mechanical systems in open-loop (Nevaranta et al., 2014) or closed-loop control (Saarakkala and Hinkkanen, 2015). Similarly, for online identification purposes, some of these methods have been successfully applied to online parameter estimation by considering their recursive form (Nevaranta et al., 2015a). One of the most widely recognized tools for estimating parameters of the mechanical system online is the extended Kalman filter (EKF) method (Schutte et al., 1997), (Perdomo et al., 2013). Basically this technique is an extension of the recursive least squares parameter (RLS) estimation method, which is also widely used for online identification in different applications. Broadly speaking, these methods can be regarded as parametric identification techniques, because they are usually

doi:10.4173/mic.2016.2.5

based on fixed, a priori determined, structure of mathematical relation, and thus, the parameters of structure are fitted to the data. In the case of non-parametric identification, typically no (or few) assumptions are made with respect to the model structure. The well-established non-parametric frequency-domain identification methods (Heath, 2001),(Villwock and Pacas, 2008), (Schoukens et al., 2012) are non-recursive, and based on the availability of the whole data record required to perform the necessary calculations. This implies that the identification must, in practice, be performed using offline or batch data processing.

Despite the theoretical development of offline frequency-domain identification methods, there are only a few studies available on the issues related to the use of non-parametric techniques for online identification purposes. In (Barkley and Santi, 2009) a non-parametric cross-correlation identification method is proposed for loop transfer function identification in closed loop. The method provides accurate frequency response estimates, but it requires a large amount of data processing and memory storage space. In (LaMaire et al., 1987) a less time-consuming identification method has been presented that applies sliding window to calculate Discrete Fourier Transformation (DFT) to fit parametric model for identification for control purposes, but in practice, the method is not stable (Duda, 2010). In addition, frequency-domain approaches that are based on adaptive neural networks have been proposed for adaptive control (Kurita et al., 1999), (Yen, 1997). Furthermore, in (Holzel and Morelli, 2011) a real-time equation error method based on a finite Fourier transform in the frequency domain has been suggested for linear model identification. Another method has been introduced in (Olivier, 1994), where a Fourier-Laguerre series is proposed for the open-loop identification of a linear system. However, these methods can be regarded as parametric identification methods as they require initial selection of the model complexity.

Motivated by the features of the Kalman-filter-based short-time DFT identification routines proposed in (Parker and Bitmead, 1987), (Nevaranta et al., 2015b) for frequency response identification of open-loop and closed-loop systems using a multi-sine excitation signal, the objective of this paper is to study the same routine in the case of a swept chirp excitation signal. In particular, the main idea of using the Kalman filter for estimating time-varying signals in a complex form is considered, but here the knowledge of the time-varying frequency of the excitation signal is used to update Kalman gains. This provides an opportunity to use a simple state space realization for tracking a selected band of frequencies of a swept excitation signal instead of large block-diagonal form (Jenssen and Zarrop, 1994) for a selected set of frequencies of a multi-sine signal. It is worth pointing out that in recent studies by (Goubej, 2015), (Goubej et al., 2013), (Kshirsagar et al., 2016) a similar type of identification routines has been considered, but in practice, the method in (Goubej, 2015) is different as considered in this paper, because in (Goubej, 2015) the block-diagonal form is used to estimate harmonic content of the swept excitation signal. Moreover, (Kshirsagar et al., 2016) considers Least Mean Squares (LMS) based adaptive filter structure, and the persistent excitation signal is superposed to the position reference of the closed-loop system, whereas in this paper, the swept excitation is added to the output of closed-loop controller and a Kalman filter is used.

The method proposed in this paper can be regarded as an online frequency response estimation routine that is based on an instantaneous estimation of the system response. The performance of the proposed method is verified by an experimental closed-loop controlled servomechanism, and the obtained online identification results are compared with the corresponding offline post-processed spectral transfer function estimates. While the main focus of this paper is on the non-parametric online identification, the closed-loop system diagnostic options with the proposed method are also discussed in brief. The diagnostics is based on the identified open-loop system model that is used to calculate the loop transfer function with the known controller.

The contents of the paper are organized as follows. Section 2 discusses the problem statement and the tracking of the chirp signal with the Kalman filter. Section 3, the mechanical system under study is introduced and the proposed non-parametric identification method is studied by simulations. Section 4 shows experimental identification results, and the system monitoring opportunities of the proposed method are discussed in short. Section 5 concludes the paper.

2 Problem Statement

In general, different systems can be identified either in open loop or closed loop by considering transfer function estimates that are formed by the ratios of auto- and cross-spectral estimates. This type of frequency-domain identification is a well-established and common approach for different systems under very general excitation conditions (Heath, 2001). In the open-loop case, the spectral transfer function estimate can be formed by taking the ratio of the cross-spectral estimate between input and output $\hat{S}_{\mathrm{uy}}(e^{\mathrm{j}\omega})$ with the auto-spectral estimate of the input $\hat{S}_{\mathrm{uu}}(e^{\mathrm{j}\omega})$; thus, the frequency re-

sponse estimate becomes

$$\hat{G}(e^{j\omega}) = \frac{\hat{S}_{uy}(e^{j\omega})}{\hat{S}_{uu}(e^{j\omega})} \tag{1}$$

The spectral estimates can be obtained in different ways (Villwock and Pacas, 2008), but in general, Eq. (1) gives a good approximation of the real system $G(e^{j\omega})$ based on the assumption that the measurement noise $n(k)$ and the input are uncorrelated, meaning that $S_{un}(e^{j\omega}) = 0$. This type of frequency response estimator Eq. (1) has been successfully used in the identification of a closed-loop controlled system by setting the controller bandwidth relatively low (Beineke et al., 1998) (Villwock and Pacas, 2008). However, when noise is affecting the system input $u(k)$, the method can give poor frequency response estimations if a separate noise model estimation is not included in the estimation routine.

In this paper, the closed-loop system shown in Figure 1 is considered, where $G(z)$ is the unknown linear transfer function of the system to be identified, and $C(z)$ is the known linear transfer function of the controller. The closed-loop controlled system is considered a stable linear time-invariant (LTI) system, which is excited by a known excitation signal $r_u(k)$, and an unknown noise signal $n(k)$ affects the system output $y(k)$. The measured output $y(k)$ can be expressed as

$$y(k) = G(z)u(k) + n(k) \tag{2}$$

where $u(k)$ is the measured input of the system. The closed-loop system can be expressed, without a reference signal $r(k)$, as follows

$$\begin{aligned} y(k) &= G(z)S(z)r_u(k) + S(z)n(k) \\ u(k) &= S(z)r_u(k) - C(z)S(z)n(k), \end{aligned} \tag{3}$$

where $S(z)$ is the sensitivity transfer function

$$S(z) = \frac{1}{1 + C(z)G(z)} \tag{4}$$

By using the following notation $G_{cl}(z)=G(z)S(z)$ and considering the relation between $y(k)$ and $r_u(k)$ in Eq. (3), the open-loop transfer function can be expressed as

$$G(z) = \frac{G_{cl}(z)}{1 - G_{cl}(z)C(z)} \tag{5}$$

Thus, the open-loop transfer function can be indirectly solved from the closed-loop spectral transfer function estimate that is formed from the cross-spectral estimate between output and excitation signals $\hat{S}_{yr_u}(e^{j\omega})$ and auto-spectral estimate of the excitation signal $\hat{S}_{r_u r_u}(e^{j\omega})$

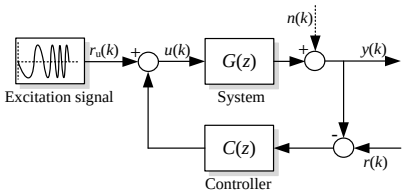

Figure 1: Closed-loop controlled system. The swept excitation signal is superposed to the controller output.

$$\hat{G}_{cl}(e^{j\omega}) = \frac{\hat{S}_{yr_u}(e^{j\omega})}{\hat{S}_{r_u r_u}(e^{j\omega})} \tag{6}$$

The main advantage of the indirect identification method is that the open-loop model $\hat{G}(e^{j\omega})$ can be correctly estimated even without estimating any noise model (Heath, 2001). The frequency-domain identification schemes Eq. (1) and Eq. (6) are well established and commonly applied to the identification of different systems. The primary disadvantage of the frequency domain analysis includes the required calculation of a discrete Fourier transform of the measured data, which is often performed offline. Basically, in the case of offline data processing, the computation time do not impose any limitations, since all the input-output data are collected prior to analysis. These calculations are not usually desirable features for online estimation procedures that deals with real-time updates when new data is available during the operation. Therefore, the issue of computational requirements for estimation becomes important. For online identification purposes, the monitoring of the mechanical system at a selected set or band of frequencies is a desirable feature. When the behaviour of these frequencies has to be tracked in real time, it is worth considering a non-parametric identification algorithm that provides benefits in the terms of computational efficiency and real-time performance. This paper proposes a Kalman-filter-based frequency domain identification method that is synchronized to the instantaneous frequency of the chirp excitation signal.

2.1 Time-Frequency Representation of Signals using a Kalman Filter

For real-time implementation, a recursive Kalman filter can be configured to perform like a sample-by-sample-based Fourier transform (Bitmead et al., 1986). The

short-time DFT can be obtained by considering the following simplified state-space representation

$$\begin{aligned} \mathbf{x}(k+1) &= \mathbf{\Phi}(k)\mathbf{x}(k) + \mathbf{w}(k) \\ z(k) &= \mathbf{H}\mathbf{x}(k) + \mathbf{v}(k) \end{aligned} \tag{7}$$

where $\mathbf{x}(k)$ is the state vector, $\mathbf{\Phi}(k)$ is the state transition matrix, and $\mathbf{H}(k)$ is the measurement matrix. $\mathbf{v}(k)$ and $\mathbf{w}(k)$ are the measurement and model error vectors. The following Kalman filter solution can be written for the state estimation problem

$$\hat{\mathbf{x}}(k) = \mathbf{\Phi}(k)\hat{\mathbf{x}}(k-1) + \mathbf{K}(k)[z(k) - \mathbf{H}\hat{\mathbf{x}}(k-1)] \tag{8}$$

where $\mathbf{K}(k)$ is the Kalman gain vector

$$\mathbf{K}(k) = \frac{\mathbf{\Phi}(k)\mathbf{P}^{\text{-}}(k)\mathbf{H}^{\mathrm{T}}(k)}{\mathbf{H}(k)\mathbf{P}^{\text{-}}(k)\mathbf{H}^{\mathrm{T}}(k) + \mathbf{R}(k)}, \tag{9}$$

where $\mathbf{R}(k)$ is the measurement error covariance matrix, and $\mathbf{P}^{\text{-}}(k)$ is the state prediction covariance defined as

$$\mathbf{P}^{\text{-}}(k) = \mathbf{\Phi}(k)\mathbf{P}(k-1)\mathbf{\Phi}(k)^{\mathrm{T}} + \mathbf{Q}(k), \tag{10}$$

where $\mathbf{Q}(k)$ is the model error covariance matrix, and estimation error covariance $\mathbf{P}(k)$ is updated as

$$\mathbf{P}(k) = [\mathbf{I} - \mathbf{K}(k)\mathbf{H}(k)]\mathbf{P}^{\text{-}}(k) \tag{11}$$

The following state vector is required to estimate a nth frequency component ω_{n}

$$\mathbf{x}(k) = \begin{bmatrix} x_{\mathrm{real}}(k) \\ x_{\mathrm{imag}}(k) \end{bmatrix} \tag{12}$$

where $x_{\mathrm{real}}(k)$ and $x_{\mathrm{imag}}(k)$ are the real and imaginary components of the signal that can be estimated by considering the following transition matrix

$$\mathbf{\Phi}(k) = \begin{bmatrix} \cos(T_{\mathrm{s}} \cdot \omega_{\mathrm{n}}) & \sin(T_{\mathrm{s}} \cdot \omega_{\mathrm{n}}) \\ \text{-}\sin(T_{\mathrm{s}} \cdot \omega_{\mathrm{n}}) & \cos(T_{\mathrm{s}} \cdot \omega_{\mathrm{n}}) \end{bmatrix} \tag{13}$$

where T_{s} is the sample time. Furthermore, the amplitude of the tracked frequency can be directly calculated at any time instant k from the estimated state variables as follows

$$A(k) = \sqrt{x^2_{\mathrm{real}}(k) + x^2_{\mathrm{imag}}(k)} \tag{14}$$

It is worth noticing that the first and second element of the state vector Eq. (12) consist of a frequency component and its derivative. Thus, the output $z(k)$ of the signal model Eq. (7) is formed from the real part of the signal components by using measurement matrix $\mathbf{H}(k) = [1\ 0]$. Moreover, as the covariance matrix is updated Eq. (11), the optimal Kalman gain $\mathbf{K}(k)$ has a time-varying nature. As proposed in (Bitmead et al., 1986), fixing the covariance matrix at $\mathbf{P}(k) = \alpha\mathbf{I}$ and choosing $\mathbf{R}_{1\mathrm{x}1} = r$ gives the steady-state values of the Kalman gain vector

$$\mathbf{K}(k) = \frac{\mathbf{\Phi}(k)\mathbf{H}^{\mathrm{T}}(k)}{\mathbf{H}(k)\mathbf{H}^{\mathrm{T}}(k) + \frac{r}{\alpha}}, \tag{15}$$

This expression gives a filter expression that is a fixed-coefficient state observer with predetermined stability characteristics (Kamwa et al., 2014), and the states can be straightforwardly estimated by using Eq. (8). Furthermore, this form provides a simple tuning rule for the gain: the gain depends only on the ratio r/α as the matrices $\mathbf{\Phi}(k)$ and $\mathbf{H}(k)$ are known. Thus, the choice of α directly influences the tracking and error covariance; for instance, a small value yields slow tracking and a small error covariance. Setting $\lambda = r/\alpha$ gives the opportunity to use only one design parameter in the Kalman gain.

2.2 Chirp Excitation Signal

As discussed in (Jenssen and Zarrop, 1994) and (Nevaranta et al., 2015b), in the case of a multi-sine excitation signal the state-space realization Eq. (12)and Eq. (13) can be modified so that more than one frequency component can be estimated at the same time by using the block-diagonal representation. However, this modification increases the computational burden, and the estimator is slightly slower as more states are estimated simultaneously at the same time instant k. When considering the chirp excitation signal, it can be expressed as sinusoid so that the frequency is time varying

$$r_{\mathrm{u}}(k) = A \cdot \cos(2 \cdot \pi \cdot f(t) \cdot t + \phi) \tag{16}$$

The time-varying frequency $f(t)$ can be expressed as

$$f(t) = \frac{m}{2}t + f_0 \tag{17}$$

where f_0 is the starting frequency of the chirp, and m is the rate of frequency increase over duration T

$$m = \frac{f_1 - f_0}{T} \tag{18}$$

Hence, the frequency is linearly swept from the starting frequency f_0 to the desired end frequency f_1. When considering the transition matrix Eq. (13) for tracking a single frequency component, the Kalman gain Eq. (15) is fixed. In the case of chirp, the swept sinusoid can be tracked with proposed fixed Kalman gain filter by updating Eq. (13) with the known time-varying frequency Eq. (17). In this case, the Kalman gains behave

sinusoidal as a function of frequency, because the transition matrix $\mathbf{\Phi}(k)$ is frequency dependent. Thus, depending of the frequency of the sinusoid to be tracked, the fixed Kalman gains are different. As a conclusion, depending on the Kalman filter configuration used, for instance Eq. (9) or Eq. (15), the frequency to be tracked must be considered in the Kalman gain update routine. In practice, the frequency of the swept sinusoid can also be estimated as proposed in (Bittanti and Savaresi, 2000) and the time-varying Kalman gain is updated with the estimated state instead of a priori known value.

3 Monitoring and Identification of a Mechanical System

From the viewpoint of system identification, the signal component representation with Kalman filter provides an opportunity to recursively estimate Fourier components of the signals depicted in Figure 1 in the form $\hat{Y}(e^{\mathrm{j}\omega},k)$, $\hat{U}(e^{\mathrm{j}\omega},k)$ and $\hat{R}_{\mathrm{u}}(e^{\mathrm{j}\omega},k)$. Thus, by writing the frequency response description

$$\hat{Y}(e^{\mathrm{j}\omega},k) = \hat{G}(e^{\mathrm{j}\omega},k)\hat{U}(e^{\mathrm{j}\omega},k) \tag{19}$$

the non-parametric system model $\hat{G}(e^{\mathrm{j}\omega},k)$ can be online identified in a phasor form from the corresponding states $x_{\mathrm{real}}(k)$ and $x_{\mathrm{imag}}(k)$ of the estimated signals. This allows to estimate the frequency response by a magnitude and phase as

$$|\hat{G}(e^{\mathrm{j}\omega},k)| = \sqrt{\mathrm{Re}[\hat{G}(e^{\mathrm{j}\omega},k)]^2 + \mathrm{Im}[\hat{G}(e^{\mathrm{j}\omega},k)]^2} \tag{20}$$

$$\hat{\phi}(e^{\mathrm{j}\omega},k) = \tan^{-1}\left(\frac{\mathrm{Im}[\hat{G}(e^{\mathrm{j}\omega},k)]}{\mathrm{Re}[\hat{G}(e^{\mathrm{j}\omega},k)]}\right) \tag{21}$$

The magnitude Eq. (20) is generally expressed in dB as $20 \cdot \log_{10}|\hat{G}(e^{\mathrm{j}\omega},k)|$. As a conclusion, the proposed method can be used to estimate frequency responses as Bode or Nyquist (polar) plots on a sample-by-sample basis. It should be noted, that the sample-by-sample recursive calculations are basic properties or options of other well-known online frequency domain identification methods, such as Sliding-DFT (Nevaranta et al., 2016) or Fourier transform regression (Holzel and Morelli, 2011). However, these methods are based on the utilization of a moving window to store predefined amount of samples, whereas the method proposed in this paper, the frequency response is processed online from the current values of the measured input-output signals by synchronizing the Kalman filter to the instantaneous frequency of the excitation signal. In other words, the frequency response estimate is obtained from the instantaneous states. However, the main drawback is the rapid changes in the excitation signal that can introduce transients to the system which can distorts the frequency response measurement, as the proposed Kalman filter method assumes a steady state response to a constant frequency harmonic signal from its definition (Goubej, 2015). Thus, a longer duration of the identification experiment is essential in order to obtain reliable results, and hence, a slow frequency sweeping is required.

In order to show the feasibility of the method, in this paper, the online-estimated frequency responses are analysed and validated by comparing the obtained magnitude and phase with the reference model. Moreover, the time-frequency presentation of signals with Kalman filter yields a non-parametric model in the form of $G(\mathrm{j}\omega)$ in the selected band of frequencies, thereby leading to an option to directly use this result with the known controller $C(\mathrm{j}\omega)$ to calculate loop transfer function $L(\mathrm{j}\omega) = C(\mathrm{j}\omega)\cdot G(\mathrm{j}\omega)$. Thus the result is also analysed with the Nyquist plot, and opportunities for loop-diagnostics purposes are discussed.

3.1 Two-Mass-System

In this paper, an experimental mechanical system with different mechanical configurations is considered to experimentally verify the identification method. The parameters presented in Table 1 are regarded as the reference system values for the experimental coupled belt drive system under study. First, the proposed identification method is studied by simulations by considering a closed-loop controlled two-mass system depicted in Figure 2 with both reference system A and B parameters from Table 1. The dynamics of the mechanical system in Figure 2 can be described by the following set of equations:

$$J_1\frac{d\Omega_1}{dt} = T_1 - T_{\mathrm{fr1}} + r_1 F \tag{22}$$

$$J_2\frac{d\Omega_2}{dt} = T_2 - T_{\mathrm{fr2}} - r_2 F \tag{23}$$

$$F = K(r_2\Omega_2 - r_1\Omega_1) + D(r_2\dot{\Omega}_2 - r_1\dot{\Omega}_1) \tag{24}$$

Equations (22) and (23) are the elementary dynamic equations for rotation, where $J_1 = J_{11} + J_{12}$ and J_2

Table 1: Parameters of reference systems

Parameters	Ref. system A	Ref. system B
K[N/m]	$5.75{\cdot}10^4$	$7.00{\cdot}10^4$
D[Ns/m]	120	100
J_1[kgm^2]	0.032	0.018
J_2[kgm^2]	0.032	0.032
f_{res}[Hz]	15.1	20.4
f_{ares}[Hz]	10.7	16.6

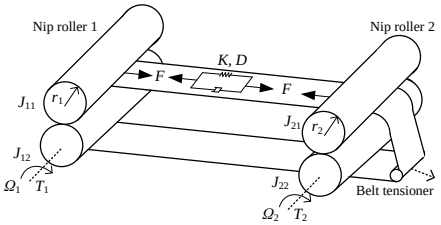

Figure 2: Coupled belt system consisting of nip rollers coupled by a flexible belt. A belt tensioner is used to set the tension in the system. The inertia ratio of the system can be adjusted by removing the upper rollers.

$= J_{21} + J_{22}$ represents the total moment of inertias of the nip rollers 1 and 2, Ω_1 and Ω_2 are the angular velocities of the rollers, T is the torque, T_{fr} is the frictional torque component, r is the roller radius, and F represents the tension force. The dynamics of the coupling is expressed by Eq. (24), where K is the spring constant, and D is the damping constant of the belt material. A more detailed discussion on the mechanical system considered in this paper can be found in (Nevaranta et al., 2015b).

The identification experiments are carried out so that the nip roller 2 is treated as a driven one, and the nip roller 1 is used as a load to set the tension of the belt. The angular velocity Ω_2 of the nip roller 2 is controlled with a PI-controller, whereas the nip roller 1 is controlled by a torque controller. Thus, the system is operated at the desired constant nonzero velocity, and the identification is carried out so that the excitation signal is added to the torque reference signal of nip roller 2 after the system has been stabilized to the desired velocity. The signals used in the identification are the torque input $u(k) = T_2$ and angular velocity $y(k) = \Omega_2$.

3.2 Frequency Response Estimation

The identification tests are performed so that a constant velocity profile 10 rad/s is used, and persistent excitation is superposed to the torque reference. A chirp signal is considered as an excitation signal, which is swept from 35 to 1.5 Hz during 17 s and the amplitude is chosen as 1 Nm. The controller $C(z)$ of the system is a low-bandwidth PI-controller with a proportional gain $K_{\text{p}} = 10$ 1/s and integration time $T_{\text{i}} = 0.1$ s. The feedback delay of 4 ms is considered in the simulations and assumed to be known in the estimation routine, and the Kalman filter tuning parameter is set $\lambda = 8$. In the simulations, white noise, zero mean, with a standard deviation 0.1 is added to the output signal $y(k)$. A direct identification method Eqs. (19)–(21) is considered, where input $u(k)$ and output $y(k)$ signals are used in the identification process. Obviously, the inherent problem of direct identification schemes arises as a result of correlation between the input and output signals used in the identification experiment, but as the low bandwidth controller is considered the direct identification is applicable for frequency response estimation (Villwock and Pacas, 2008). It is also remarked that, in practical applications several noise and disturbances sources can be found which influences the frequency response estimation. In this paper, the proposed identification method is further validated with an experimental test setup when disturbance sources such as field-bus delays, encoder noise, torque control of the frequency converters and friction influences to the estimation.

In Figure 3 a)–b) the directly online estimated frequency responses are shown for both reference systems A and B when noise is affecting the system output and also in the noise-free case. Moreover, in Figure 3 c)–e) the signals used in the identification experiment are evaluated by the residual $\epsilon(k) = z(k) - \mathbf{H}(k)\hat{x}$, and the Figure 3 f) shows the frequency contents of the swept excitation signal. It can be seen that the online estimated frequency response is in a satisfactory agreement with the reference systems. Especially when noise-free case is considered, the online-estimated results agree well with the reference systems, and only a small difference can be seen in the low-frequency band. For the noisy cases, the identified magnitude and phase responses are in a good correspondence with reference models, and the characteristics of the two-mass system are evident. It is pointed out that the noise included in the simulation is chosen so that it over-emphasizes disturbance in the anti-resonance region. Even assuming measurement disturbances, the resonance and anti-resonance frequencies are clearly visible from the online estimated frequency responses. Moreover, when evaluating the tracking properties of the proposed Kalman filter it can be noticed in Figure 3 c) that a good estimation accuracy is obtained as the residual between the excitation signal and estimation is low. In the noise-free case in Figure 3 d)–e), the residual remains low during the sweep, but as can be expected, the residuals are higher especially in the frequency region around the resonance frequencies. It should be noted that the quality of the obtained frequency response estimate depends on the amplitude chosen for the excitation signal, which is related to the signal-to-noise ratio similarly as in the case of other identification studies considering persistent excitation (Schoukens et al., 2012),(Schoukens et al., 2000).

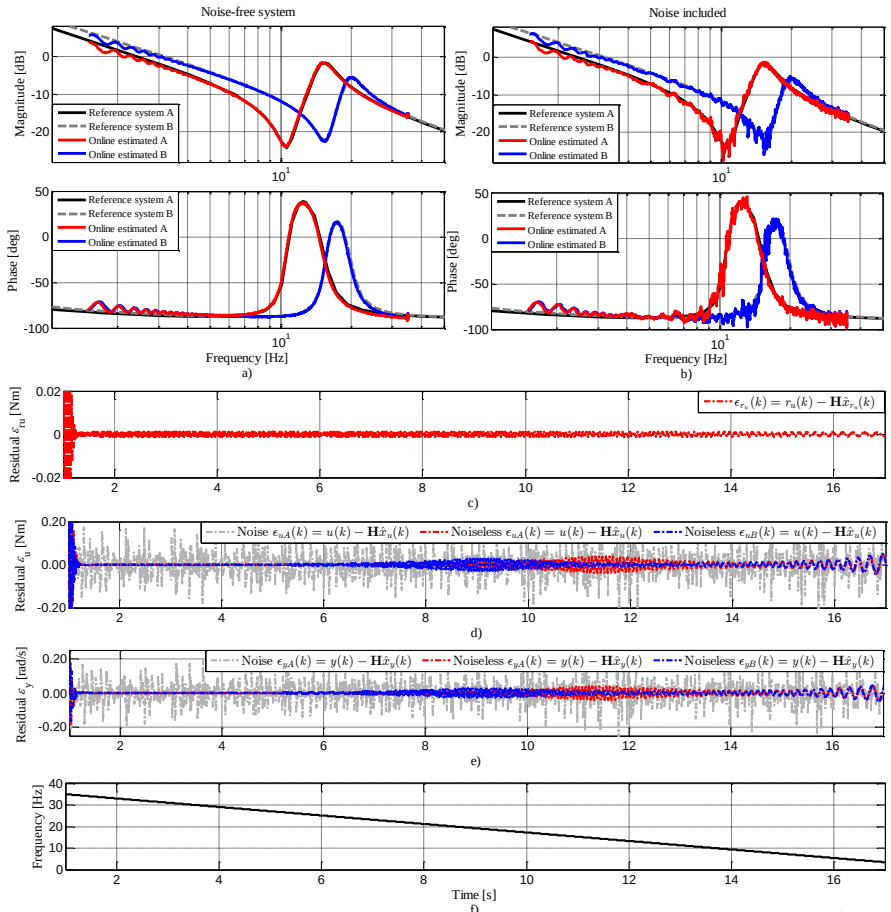

Figure 3: Online directly estimated open loop frequency responses for reference systems A and B a) in the case of a noise-free system and b) when noise is affecting the system output. The tracking properties of the Kalman filter are evaluated with residuals of the signals used in the identification: c) Residual of the excitation signal and estimation. d) Residual of the input signal and estimation. e) Residual of the output signal and estimation. f) Frequency contents of the excitation signal

The duration of the sweep and the selection of the Kalman gain is directly related to the tradeoff of the filter tracking and error properties. It is evident that the duration of the identification experiment related to the selection of the Kalman filter tuning parameter has an influence to the accuracy of the frequency response estimation. In Figure 4 the directly identified frequency responses are shown in the case of reference system A when the Kalman filter tuning parameter λ, the excitation signal amplitude A and duration T of the identification experiment (length of sweep) is varied. Figure 4 clearly shows that the accuracy of the estimated frequency response depends on the length of sweep chosen for the excitation signal, and obviously, the excitation signal amplitude should be chosen be as large as possible in order to achieve a good signal-to-noise ratio. Especially, it can be noticed in Figure 4 that when the sweep is fast, $T = 5s$, the identified responses deviates from the reference system even though the tuning parameter is varied. Moreover, this shows the the main disadvantage of the proposed identification method as a slow sweeping is required for precise

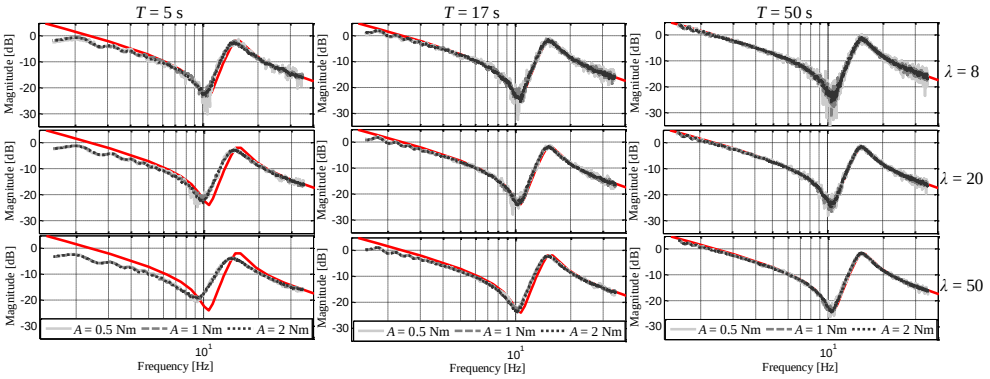

Figure 4: Online identified open loop frequency responses when the Kalman filter tuning parameter λ and amplitude A of the excitation signal and duration T of the identification experiment is varied. The red solid line represents the reference system A.

measurement in order to reduce errors and obtain accurate results, which prolongs the duration of the experiment. The proposed method for online frequency response estimation is further validated and discussed in the case of experimental results in Section 4.

3.3 Loop-transfer Function

When considering classical robustness margins or performance indicators, the controller design usually involves determination of parameters such as modulus M_m, gain G_m and phase P_m margins and cross-over frequency ω_c. In practical applications, it is usually desirable to determine the frequencies at which a given closed-loop system achieves a certain magnitude or phase. In particular, methods such as relay-experiment (de Arruda and Barros, 2003) can be regarded as a kind of frequency domain identification for control methods that utilizes only a few points of the frequency response of the loop transfer function to design, for instance, PID controllers. Similarly, the desired open-loop dynamics can be online shaped by considering for instance an adaptive structure (Balchen and Lie, 1987).

The open-loop transfer function $G(\mathrm{j}\omega)$ can be estimated with the proposed method on a sample-by-sample basis, which makes it possible to use the proposed method to calculate the loop transfer function in a real-time by using the known controller $C(\mathrm{j}\omega)$ to obtain $L(\mathrm{j}\omega)$. As the online identification method estimates instantaneous non-parametric model frequency-by-frequency, it also allows to determine rough estimates of M_m, P_m and ω_c during the identification experiment by considering different distances in the Nyquist plot. In this paper, the regions inside the unit circle of the Nyquist plot are determined as regions I, II, III and IV. Region I is located in the plane defined by the negative imaginary and real axes, and thus, this region determines the behaviour at low frequencies.

If the sweep starts exciting low frequencies, and thus at first, the critical frequency ω_c can be determined by calculating the distance of Nyquist curve to the origin frequency-by-frequency as follows

$$d_1(\omega) = |L(\mathrm{j}\omega)| = \sqrt{(0 - \mathrm{Re}[L(\mathrm{j}\omega)])^2 + (0 - \mathrm{Im}[L(\mathrm{j}\omega)])^2} \tag{25}$$

and finding the frequency at which the curve intersects the unit circle, thus $|L(\mathrm{j}\omega_\mathrm{c})| = 1$. After the estimated Nyquist curve has intersected the unit circle and the curve lies in the region I, the modulus and the phase margin can be roughly determined by estimating the distance of the curve to the critical point (-1,0j) by

$$d_2(\omega) = |1 + L(\mathrm{j}\omega)| = \sqrt{(-1 - \mathrm{Re}[L(\mathrm{j}\omega)])^2 + (0 - \mathrm{Im}[L(\mathrm{j}\omega)])^2} \tag{26}$$

By using the first value of this distance metric, $d_2(\omega_\mathrm{c})$, the phase margin can be obtained as

$$P_\mathrm{m} = \cos^{-1}\left(\frac{d_2(\omega_\mathrm{c}) - 2}{-2}\right) \tag{27}$$

The modulus margin can be estimated by finding the minimum distance of the curve in region I to the critical point, thus $M_\mathrm{m} = \min_{\omega} |1 + L(\mathrm{j}\omega)|$. Moreover, as the system under study is a controlled two-mass system, the estimation routine can be further extended to obtain mechanical parameters in region II, which is located in the plane defined by the negative imaginary and positive real axes. By considering the distance

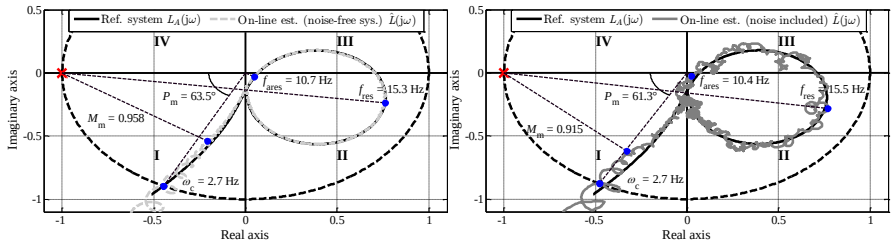

Figure 5: Frequency-by-frequency online-estimated Nyquist curves compared with the reference curve in the case of noise-free system and when the noise is affecting the system output. Equations (25)-(27) are used to determine controller performance parameters M_m, P_m and ω_c in region I. Moreover, the system parameters ω_{ares} and ω_{res} in region II are determined by calculating the corresponding distances Eqs. (25)–(26). The critical point (-1, j·0) is indicated by a red cross.

metrics Eqs. (25)–(26) the anti-resonance ω_{ares} and resonance ω_{res} frequencies can be determined in region II similarly as the margins. Hence, the anti-resonance frequency can be estimated in region II by finding the minimum distance to the origin $d_3(\omega_{ares}) = \min_{\omega} |L(j\omega)|$ calculating the distance of the curve similarly as in Eq. (25). Correspondingly, the resonance frequency can be estimated by finding the maximum distance of the curve to the critical point $d_4(\omega_{res}) = \max_{\omega} |1 + L(j\omega)|$ similarly as in Eq. (26).

In the Figure 5 the sample-by-sample online-estimated Nyquist curve is shown with the distance metrics Eqs. (26)–(25) that are used to calculate controller performance- and system-related parameters in the case of reference system A. The closed-loop controller has been designed so that $P_m = 63.5°$ and $f_c = 2.7$ Hz. Evidently, in the noise-free case the online-identified Nyquist curve is in a good correspondence with the reference loop transfer function, although small discrepancies can be noticed. The behaviour of the low frequencies is similar with the results in the Figure 3, which further shows that the largest estimation error is in the low frequency band, as expected. It is clear that this is partially due to the start of the chirp excitation, which causes a transient that can also be noticed from the Figure 3 at t = 5 s after the initialization. Naturally, the duration of the sweep and the selection of the Kalman gain have an effect on the frequency response estimation. For this purpose, the known limitation of Kalman filter is the tracking and error tradeoff based on the choice of the Kalman filter tuning parameter λ. Thus, choosing a value of the tuning parameter λ for the Kalman filter is a case-specific compromise, similarly as reported in (Kshirsagar et al., 2016).

In this paper, the rough control performance estimates in region I are only considered for illustrative purposes and to further demonstrate the possibilities of the identification method. It can be seen that the online estimated controller-behaviour-related parameters are close to the actual ones; nevertheless, it is pointed out that especially an erroneous estimate of the cross-point f_c directly influences to the estimate of P_m as can be noticed in the noisy case. It is clear that the emphasized estimation error in the low-frequency region influences these estimates. When considering the distances in region II, the estimated system parameters f_{ares} and f_{res} correspond well with the ones of reference model A illustrated in Table 1 in the case of both simulations. The estimation of these values are further discussed in Section 4.

For actual performance monitoring purposes, it could be more preferable to use a separate soft controller to perform the identification experiments in order to analyse the desired controller performance in region I. In practice, the proposed online distance metrics can be used for diagnostics purposes for instance by considering a predetermined safety limits in region I. Moreover, the loop-transfer function could be estimated directly from the closed-loop experiment (Barkley and Santi, 2009), (Bhardwaj et al., 2016). These issues will be considered in the future research, and thus not further discussed in this work, where the main focus is to analyse and validate the feasibility of the proposed method for frequency response estimation.

4 Experimental Results

The proposed online identification routine is validated with the experimental two-mass-system used in (Nevaranta et al., 2015b) and depicted in Figure 6. The rollers are driven by frequency-converter-supplied permanent magnet synchronous motors (PMSM), and a

programmable logic controller (PLC) is used for data acquisition and to implement the excitation signals, PI controller, and references. It is pointed out that now the experimental system includes a belt-tensioner, which, in practice, changes the system dynamics over to a three-mass-system. However, in this paper, the frequency region around the dominant resonance frequency is considered in the online identification, which usually sufficiently reflects dominant behaviour of the real system. The tests are performed so that the same PI-controller parameters are considered as in the simulations, and also the chirp excitation signal is kept same, thus swept from 35 Hz to 1.5 Hz during s 17 s interval. In addition, to further verify the online identification method, the system dynamics of the experimental test setup is varied by changing the belt material and the inertia ratio of the system from 1 to 0.56. The results in Figure 8 have been obtained by using an experimentally chosen Kalman filter tuning parameter $\lambda = 8$.

Moreover, in order to validate the rough online estimates of the anti-resonance f_{ares} and resonance f_{res} the experimental system is offline identified by considering the open-loop identification method proposed in (Villwock and Pacas, 2008). A PRBS is used to excite the system, and the experimental frequency response estimate $G_{\text{e}}(\text{j}\omega)$ is obtained by Welch method. Then, the calculation of the mechanical parameters of the analytical frequency response function $G_{\text{model}}(\text{j}\omega)$ of the reference two-mass system is accomplished on the basis of the M frequency response data points, and the best fit is iteratively searched by minimizing the error function

$$J(\boldsymbol{\vartheta}) = \sum_{i=1}^{M} |G_{\text{e}}(\text{j}\omega_i) - G_{\text{model}}(\text{j}\omega_i, \boldsymbol{\vartheta})|^2 \qquad (28)$$

where $G_{\text{e}}(\text{j}\omega_i)$ are the experimental frequency response data and $G_{\text{model}}(\text{j}\omega_i, \boldsymbol{\vartheta})$ is the analytical model function with the parameter vector $\boldsymbol{\vartheta} = [J_1, J_2, K, D]$. In the parameter estimation, the reference model parameters of Table 1 are used in the initialization, thus in the first iteration.

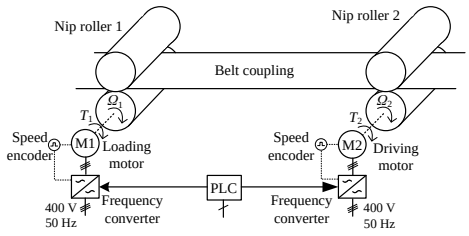

Figure 6: Electromechanical system used for experimental verification.

The offline identification experiments are carried out so that the PRBS is generated by a seventeen-cell shift register with values 2.1 Nm and -2.1 Nm (the rated torque being 11.55 Nm). The sampling of the data acquisition is set to 2 ms. In Figure 7, the online-estimated frequency responses are compared with the offline post-processed ones for both system configurations: a) reference system A and b) reference system B, respectively. Moreover, the offline post-processed frequency responses are compared to the ones calculated by using the identified parameters Eq. (28).

The characteristics of the three-mass-system are clearly visible in the offline frequency responses, and when the mechanical configuration is changed over from reference system A to B, the change of the first resonance is evident. This change can also be seen in the online-estimated frequency response results. The obtained results clearly show a similar behaviour, and the dynamics of two-mass system are seen in the online-estimated amplitude and phase responses in the selected band of frequencies. Again, it is worth remarking that the offline post-processed frequency response is estimated applying the whole data of the identification experiment using the PRBS excitation signal, and correspondingly, the online ones are obtained on a sample-by-sample basis from the swept excitation; and thus, these results are not directly comparable. Nevertheless, the offline- and online estimated frequency responses are in a good agreement, which clearly indicates that the proposed identification method yields accurate results.

With the results of the parameter-fitting for the corresponding mechanical parameters, the resonance and the anti-resonance frequencies of the two-mass system approximation can be calculated. In Table 2, the estimated mechanical parameters for the both experimental system configurations are shown. The system change can also be seen in the estimated parameters, and especially, the effect of the change in the inertia ratio as the resonance and anti-resonance of the system changes. It should be noted that a two-mass-system parameter-fitting is considered for the offline identified frequency responses that have three-mass system characteristics, and thus, the mechanical parameter estimation results cannot be directly compared to the initial assumption of the system dynamics. However, the offline-estimated resonances $\hat{f}_{\text{res}}$ and anti-resonances $\hat{f}_{\text{ares}}$ are used as benchmark values to validate online estimated ones.

In Figure 8, the frequency-by-frequency online-estimated Nyquist curves are compared with the offline post-processed ones, and the proposed online distance

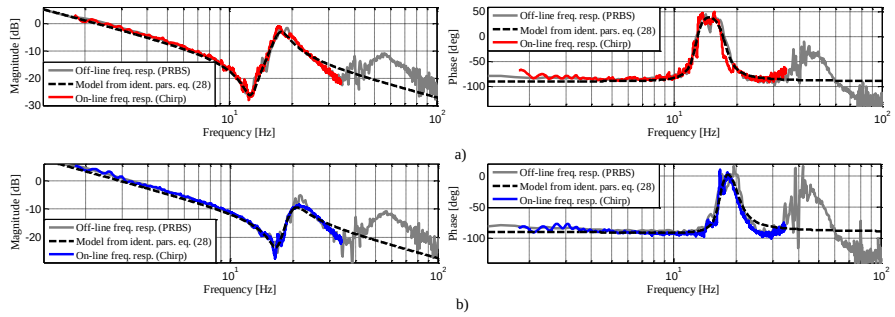

Figure 7: Online-estimated frequency responses Eqs. (20)-(21) compared with the offline post-processed frequency response Eq. (1) by using signals $u(k)$ and $y(k)$ in the identification. a) Experimental system configuration correspond to reference system A and b) reference system B, respectively.

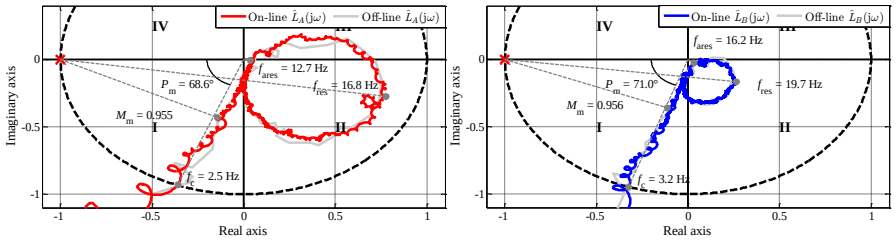

Figure 8: Online-estimated Nyquist curve compared with the offline post-processed one. The system is changed over from reference system A (left Fig.) to B (right Fig.) and equations (25)–(27) are used to determine controller performance parameters M_m, P_m and f_c in region I. Moreover, the system parameters f_ares and f_res in region II are determined by calculating the corresponding distances, Eqs. (25)–(26).

metrics are used to calculate the controller performance and system parameters. Evidently, the offline- and online-identified Nyquist curves are in a good correspondence although small discrepancies can be noticed. Moreover, the system change can be clearly noticed as the size of the resonance loop changes. It should be noted, that the distance metrics in region I are problematic as the largest estimation error is expected in the low frequency region, and the estimated values can be only used as rough estimates of the controller performance during the identification experiment. Again, it is pointed out that these values are considered for illustrative purposes only in order to further demonstrate the prospects of the proposed identification method. When focusing on the online-estimated resonance and anti-resonance values in Figure 8, it can be noticed that these values are close to the offline-estimated ones shown in Table 2, thus indicating that instantaneous estimates give reasonable results.

In Figure 8 it is clear that, the duration of the sweep and the selection of the Kalman gain has an effect on the frequency response estimation. In order to further validate the online-estimated results, the experimental system configuration B is identified using three different experimental data sets, and the proposed distance metrics are tested by varying the Kalman filter tuning parameter. In Figure 9, the estimated values obtained from the identification experiments are shown as a function α. It can be seen that similar values of f_{res} and f_{ares} can be estimated by using different values in the Kalman filter gain. Obviously, this result also depends on the amplitude chosen for the excitation signal, which is related to the signal-to-noise ratio, but it clearly shows instantaneous values can be used to obtain reasonable estimates. This can be also noticed from the minimum distance estimation to critical point. Thus, these results indicate that the proposed online identification method can be used for diagnostics purposes for instance by considering different fault classifiers and/or combination rules. Moreover, the results show the problem of the low-frequency region identification as a larger deviation in the estimated P_{m} and f_{c} parameters can be noticed. These values do not explicitly describe controller-performance-related behaviour. However, as shown in (Ferretti et al., 2003), a rough estimate of f_{c} can be obtained similarly during the commissioning state of a PID-controlled two-mass system by using a chirp excitation signal, and successfully used for controller design validation.

Table 2: Offline-estimated parameters for different system configurations

Parameters	System conf. A	System conf. B
$\hat{K}$[N/m]	$7.51{\cdot}10^4$	$8.70{\cdot}10^4$
$\hat{D}$[Ns/m]	140.1	92.7
$\hat{J}_1$[kgm^2]	0.036	0.037
$\hat{J}_2$[kgm^2]	0.033	0.016
$\hat{f}_{\text{res}}$[Hz]	17.5	20.1
$\hat{f}_{\text{ares}}$[Hz]	12.7	16.7

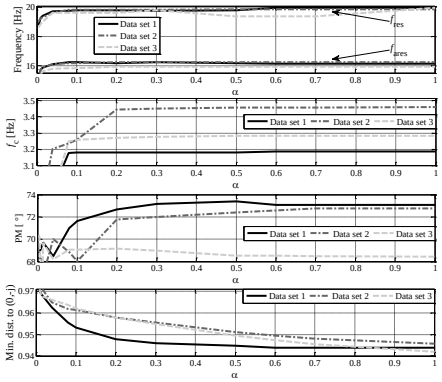

Figure 9: Estimated system and performance parameters as a function of the Kalman filter tuning parameter α ($r = 1$). Data sets 1–2 include chirp with $f_0 = 35$ Hz to $f_0 = 1.5$ Hz and a data set 3 $f_0 = 50$ Hz to $f_0 = 1.5$ Hz during 17 s.

4.1 Supporting results and discussion

The main objective of this paper is to propose a nonparametric online frequency response estimation method that is suitable for tracking of a selected band of frequencies, with a specific objective to identify a predefined frequency band around the first resonance frequency of the system. Figure 7 shows that the offline-identified frequency response clearly indicates a three-mass system dynamics.

To further validate this observation, in Figure 10, the experimental system configuration A is also identified with a chirp excitation signal, which is swept from 100 Hz to 1.5 Hz (during 17 s) and compared with the results shown in Figure 7 a). When the frequency band of the chirp excitation signal is extended, the dynamics of three-mass system is clearly noticeable in the online-estimated frequency response. This result further indicates the feasibility of the proposed identification approach, but also shows that the Kalman filter tuning parameter should be preferably chosen differently for different frequency regions. This issue is also considered in the future research.

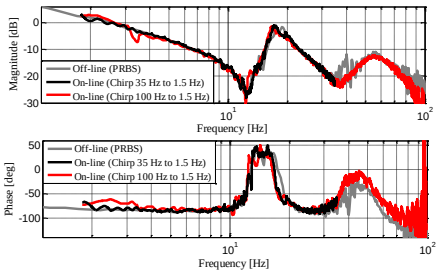

Figure 10: Online-estimated frequency responses compared with the offline post-processed frequency response. The Kalman filter tuning parameter is set $\lambda = 8$.

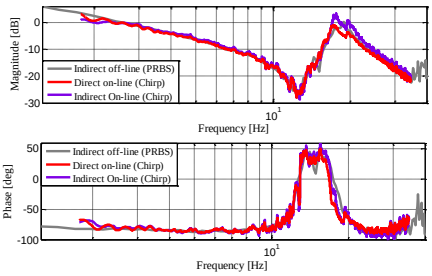

Figure 11: Indirectly estimated online frequency response compared to the offline post-processed frequency response Eq. (6) by using the signals $r_u(k)$ and $y(k)$ and known controller $G(z)$ in the identification. The directly online-estimated frequency response is also shown.

As discussed in Section 2, the open-loop transfer function can be estimated indirectly from a closed-loop identification experiment by using the excitation signal and the output signal in the identification routine and by considering the relation of the signals Eq. (5). In Figure 11, the indirectly estimated open-loop offline and online frequency responses are shown. The results confirm the remarks in previous results about the good correspondence between the off-line and online estimated frequency responses. More importantly, by comparing the directly and indirectly obtained results in Figures 11, it can be seen that the obtained open-loop models are rather similar with only minor noticeable differences. These results clearly indicate that the proposed non-parametric online identification routine supports the well-established frequency domain closed-loop identification theories (Heath, 2001), and thus, can be applied accordingly to determine the open-loop frequency response from closed-loop experiments. Furthermore, in the case of indirect identification, the proposed method gives more design freedom in the parametrization of Kalman filter as the excitation signal used in the identification is known in advance.

In this paper, the experimental results clearly validate the proposed methodology and effectiveness of using online Kalman filters for frequency response analysis. The known limitation of the Kalman filter is its convergence time and tracking tradeoff with respect on the choice of tuning parameters. This limitation requires the frequency sweep to be slow. However, usually in the case of chirp-excitation-based identification, the duration of the sweep must be designed long in order to reduce errors and obtain accurate results (Östring et al., 2001). A second drawback can be found when considering identification of systems with nonlinear dynamics. The chirp signal can have a disturbing effect, because a number of other spectral lines are also excited with the frequency lines of interest. Despite these limitations, the chirp-excitation-based offline identification is widely applied for instance to the identification of the flexibilities of nonlinear industrial robot manipulators (Östring et al., 2003), (Saupe and Knoblach, 2015).

5 Conclusions

This paper presented an online non-parametric approach that is based on a time-frequency presentation of signals in order to estimate a frequency response of a closed-loop controlled servomechanism in a computationally efficient manner. The method is based on a fixed-coefficient non-parametric Kalman filter, which is updated with the known frequency of the chirp excitation signal. The results from the simulations and experimental tests show that the approach can be used to achieve reasonable estimates of the frequency responses in real time on a sample-by-sample basis. The online estimated frequency responses during operation were compared with the corresponding frequency responses obtained by off-line identification using the whole data of the identification experiment collected prior to the estimation. The results show acceptable agreement, thus indicating that the proposed method is suitable for the online frequency-domain nonparametric identification of a mechanical system. Moreover, it was experimentally validated that the method is feasible to detect system changes for diagnostics purposes.

As the deterioration of mechanical parts over time or other unexpected changes in the system dynam-

ics may lead to the degradation of the control performance or cause unexpected interruptions, it is important to detect the system changes as proactive maintenance before they lead to performance degradation. The future work will focus on the performance assessment and diagnostics opportunities of the identification method and the option to diagnose mechanical faults e.g. changes in the resonances resulting from deterioration.

References

de Arruda, G. and Barros, P. Relay-based closed loop trasfer function frequency points estimation. *Automatica*, 2003. 39(2):309–315. doi:10.1016/S0005-1098(02)00205-4.

Balchen, J. and Lie, B. An adaptive controller based upon continous estimation of the closed loop frequency response. *Modeling, Identification and Control*, 1987. 8(4):223–240. doi:10.4173/mic.1987.4.3.

Barkley, A. and Santi, E. Improved online identification of a dc-dc converter and its control loop gain using cross-correlation methods. *IEEE Trans. on Power. Elect.*, 2009. 24(8):2021–2031. doi:10.1109/TPEL.2009.2020588.

Beineke, S., Wertz, H., Schütte, F., Grotstollen, H., and Fröhleke, N. Identification of nonlinear two-mass systems for self-commissioning speed control of electrical drives. *in Proc. IEEE IECON*, 1998. pages 2251–2256. doi:10.1109/IECON.1998.724071.

Bhardwaj, M., Choudhury, S., Poley, R., and Akin, B. Online frequency response analysis: A poweful plug-in tool for compensation design and health assessment of digitally controlled power controllers. *IEEE Trans. Ind. Appl.*, 2016. 00(99):1–10. doi:0.1109/TIA.2016.2522951.

Bitmead, R., Tsoi, A. C., and Parker, P. J. A kalman filtering approach to short-time fourier analysis. *IEEE Trans. Acoust., Speech, Signal Process*, 1986. 34(6):1493–1501. doi:10.1109/TASSP.1986.1164989.

Bittanti, S. and Savaresi, S. M. On the parameterization and design of an extended kalman filter frequency tracker. *EEE Trans. Aut. Cont.)*, 2000. 45(9):1718–1724. doi:10.1109/9.880631.

Duda, K. Accurate, guaranteed stable, sliding discrete fourier transform. *IEEE Signal Processing Magazine,*, 2010. 27(6):124–127. doi:10.1109/MSP.2010.938088.

Ferretti, G., Magnani, G., and Rocco, P. Load behavior concerned pid control for two-mass servo systems. *In Proc. of IEEE/ASEM Int. Conf. on Adv. Intelligent Mechatronics*, 2003. pages 821–826. doi:10.1109/AIM.2003.1225448.

Goubej, M. Kalman filter based observer design for real-time frequency identification in motion control systems. *in Proc. 20th Conf. on Process Control*, 2015. pages 296–301. doi:10.1109/PC.2015.7169979.

Goubej, M., Krejčí, A., and Schlegel, M. Robust frequency identification of oscillatory electromechanical systems. *in Proc. 18th Conf. on Process Control*, 2013. pages 79–84. doi:10.1109/PC.2013.6581387.

Heath, W. Bias of indirect non-parametric transfer function estimates for plants in closed loop. *Automatica*, 2001. 37(10):1529–1540. doi:10.1016/S0005-1098(01)00105-48.

Holzel, M. and Morelli, E. Real-time frequency response estimation from flight data. *in Proc. AIAA Atmospheric Flight Mechanics Conference*, 2011. pages 1–26. doi:10.2514/6.2011-6358.

Jenssen, A. and Zarrop, M. Frequency domain change detection in closed loop. *in Proc. Int. Conf. in Control*, 1994. pages 676–680. doi:10.1049/cp:19940213.

Kamwa, I., Samantaray, S. R., and Joos, G. Wide frequency range adaptive phasor and frequency pmu algorithms. *IEEE Trans. Smart Grid.*, 2014. 5(2):569–579. doi:10.1109/TSG.2013.2264536.

Kshirsagar, P., Juang, D., and Zhang, Z. Implementation and evaluation of online system identification of electromechanical systems using adaptive filters. *IEEE Trans. Ind. Appl.*, 2016. 00(99):1–9. doi:10.1109/TIA.2016.2515994.

Kurita, Y., Hashimoto, T., and Ishida, Y. An application of time delay estimation by anns to frequency domain i-pd controller. *in Proc. Int. Joint Conf. on Neural Networks*, 1999. pages 2164–2167. doi:10.1109/IJCNN.1999.832723.

LaMaire, R., Valavani, L., Athans, M., and Gunter, S. A frequency-domain estimator for use in adaptive control systems. *in Proc. American Control Conf.*, 1987. pages 238–244.

Ljung, L. Perspectives on system identification. *Annual Reviews in Control*, 2010. 34(1):1–12. doi:10.1016/j.arcontrol.2009.12.001.

Nevaranta, N., Derammelaere, S., Parkkinen, J., Vervisch, B., Lindh, T., Stockman, K., Pyrhönen,

O., and Pyrhönen, J. Online identification of a mechanical system in frequency domain using sliding dft. *IEEE Trans. Ind. Electron.*, 2016. 63(9):5712–5723. doi:10.1109/TIE.2016.2574303.

Nevaranta, N., Parkkinen, J., Niemelä, M., Lindh, T., Pyrhönen, O., and Pyrhönen, J. Recursive identification of linear tooth belt-drive system. *in Proc. EPE*, 2014. pages 1–8. doi:10.1109/EPE.2014.6910904.

Nevaranta, N., Parkkinen, J., Niemelä, M., Lindh, T., Pyrhönen, O., and Pyrhönen, J. Online estimation of linear tooth-belt drive system parameters. *IEEE Trans. Ind. Electron*, 2015a. 62(11):7214–7223. doi:10.1109/TIE.2015.2432103.

Nevaranta, N., Parkkinen, J., Niemelä, M., Lindh, T., Pyrhönen, O., and Pyrhönen, J. Online Identification of a Mechanical System in the Frequency Domain with Short-Time DFT. *Modeling, Identification and Control*, 2015b. 36(3):157–165. doi:10.4173/mic.2015.3.3.

Olivier, P. D. Online system identification using laguerre series. *in Proc. IEE Control Theory and Application*, 1994. 141(4):249–254. doi:10.1049/ip-cta:19941239.

Östring, M., Gunnarsson, S., and Norrlöf, M. Closed loop identification of the physical parameters of an industrial robot. *In Proc. of 32th Int. Symp. on Robotics*, 2001. pages 1–20.

Östring, M., Gunnarsson, S., and Norrlöf, M. Closed-loop identification of an industrial robot containing flexibilities. *Control Engineering Practice*, 2003. 11(3):291–300. doi:10.1016/S0967-0661(02)00114-4.

Parker, P. and Bitmead, R. Adaptive frequency response identification. *in Proc. 28th Conf. on Decision and Control*, 1987. pages 348–353. doi:10.1109/CDC.1987.272820.

Perdomo, M., Pacas, M., Eutebach, T., and Immel, J. Identification of variable mechanical parameters using extended kalman filters. *in 9th IEEE Int. Symp. on Diagnostics for Electric Machines, Power Electronics and Drives (SPEMPED)*, 2013. pages 377–383. doi:10.1109/DEMPED.2013.6645743.

Saarakkala, S. and Hinkkanen, M. Identification of two-mass mechanical systems using torque excitation: Design and experimental evaluation. *IEEE Trans. Ind. Appl.*, 2015. 51(5):4180–4189. doi:10.1109/TIA.2015.2416128.

Saupe, F. and Knoblach, A. Experimental determination of frequency response function estimates for flexible joint industrial manipulators with serial kinematics. *Mechanical Systems and Signal Processing*, 2015. 52(4):60–72. doi:10.1016/j.ymssp.2014.08.011.

Schoukens, J., Pintelon, R., and Rolain, Y. Broadband versus stepped sine frf measurements. *IEEE Trans. Instr. Meas.*, 2000. 49(1):275–278. doi:10.1109/19.843063.

Schoukens, J., Vandersteen, G., Rolain, Y., and Pintelon, R. Frequency response function measurements using concatenated subrecords with arbitrary length. *IEEE Trans. Instr. Meas.*, 2012. 61(10):2682–2688. doi:10.1109/TIM.2012.2196400.

Schutte, F., Beineke, S., Rolfsmeir, A., and Grotstollen, H. Online identification of mechanical parameters using extended kalman filters. *in Conf. Rec. IEEE-IAS Annual Meeting*, 1997. pages 501–508. doi:10.1109/IAS.1997.643069.

Villwock, S. and Pacas, M. Application of the welch-method for the identification of two- and three-mass-systems. *IEEE Trans. Ind. Electron*, 2008. 55(1):457–466. doi:10.1109/TIE.2007.909753.

Yen, G. G. Frequency-domain vibration control using adaptive neural network. *in Proc. Int. Joint Conf. on Neural Networks*, 1997. pages 806–810. doi:10.1109/ICNN.1997.616126.

ACTA UNIVERSITATIS LAPPEENRANTAENSIS

675. MIELONEN, KATRIINA. The effect of cationic-anionic polyelectrolyte multilayer surface treatment on inkjet ink spreading and print quality. 2015. Diss.

676. OMAJENE, JOSHUA. Underwater remote welding technology for offshore structures. 2015. Diss.

677. NUUTINEN, PASI. Power electronic converters in low-voltage direct current distribution – analysis and implementation. 2015. Diss.

678. RUSATSI, DENIS. Bayesian analysis of SEIR epidemic models. 2015. Diss.

679. STRAND, ELSI. Enhancement of ultrafiltration process by pretreatment in recovery of hemicelluloses from wood extracts. 2016. Diss.

680. TANNINEN, PANU. Press forming of paperboard – advancement of converting tools and process control. 2015. Diss.

681. VALTONEN, PETRI. Distributed energy resources in an electricity retailer's short-term profit optimization. 2015. Diss.

682. FORSSTRÖM-TUOMINEN, HEIDI. Collectiveness within start up-teams – leading the way to initiating and managing collective pursuit of opportunities in organizational contexts. 2015. Diss.

683. MAGUYA, ALMASI. Use of airborne laser scanner data in demanding forest conditions. 2015. Diss.

684. PEIPPO, JUHA. A modified nominal stress method for fatigue assessment of steel plates with thermally cut edges. 2015. Diss.

685. MURASHKO, KIRILL. Thermal modelling of commercial lithium-ion batteries. 2016. Diss.

686. KÄRKKÄINEN, TOMMI. Observations of acoustic emission in power semiconductors. 2016. Diss.

687. KURVINEN, EMIL. Design and simulation of high-speed rotating electrical machinery. 2016. Diss.

688. RANTAMÄKI, JUKKA. Utilization of statistical methods for management in the forest industry. 2016. Diss.

689. PANOVA, YULIA. Public-private partnership investments in dry ports – Russian logistics markets and risks. 2016. Diss.

690. BAHARUDIN, EZRAL. Real-time simulation of multibody systems with applications for working mobile vehicles. 2016. Diss.

691. MARTIKAINEN, SOILI. Development and effect analysis of the Asteri consultative auditing process – safety and security management in educational institutions. 2016. Diss.

692. TORVINEN, PEKKA. Catching up with competitiveness in emerging markets – An analysis of the role of the firm's technology management strategies. 2016. Diss.

693. NORONTAUS, ANNUKKA. Oppisopimuskoulutus yritysten tuottamana koulutuspalveluna: tavoitteista vaikutuksiin. 2016. Diss.

694. HALMINEN, OSKARI. Multibody models for examination of touchdown bearing systems. 2016. Diss.

695. TALONPOIKA, ANNA-MARIA. Financial working capital – management and measurement. 2016. Diss.

696. INKINEN, HENRI. Intellectual capital, knowledge management practices and firm performance. 2016. Diss.

697. YANG, XIAOCHEN. Development of a welding production quality control and management system model for China. 2016. Diss.

698. LEMINEN, VILLE. Leak-proof heat sealing of press-formed paperboard trays. 2016. Diss.

699. LAAKSONEN, LAURI. Spectral retinal image processing and analysis for ophthalmology. 2016. Diss.

700. OINONEN, MINNA. Management of customer co-development in business-to-business markets. 2016. Diss.

701. ALATALO, SARA-MAARIA. Hydrothermal carbonization in the synthesis of sustainable porous carbon materials. 2016. Diss.

702. UZHEGOV, NIKITA. Design and material selection of high-speed rotating electrical machines. 2016. Diss.

703. RICHTER, CHRIS. Digital collaborations and entrepreneurship – the role of shareconomy and crowdsourcing in the era of smart city. 2016. Diss.

704. JAFARI, SHILA. Investigation of adsorption of dyes onto modified titanium dioxide. 2016. Diss.

705. PATEL, YOGINI. Computational modelling of non-equilibrium condensing steam flows in low-pressure steam turbines. 2016. Diss.

706. LEVCHUK, IRINA. Titanium dioxide based nanomaterials for photocatalytic water treatment. 2016. Diss.

707. AMOUR, IDRISSA. Variational ensemble kalman filtering applied to data assimilation problems in computational fluid dynamics. 2016. Diss.

708. SHESTAKOVA, MARINA. Ultrasound-assisted electrochemical treatment of wastewaters containing organic pollutants by using novel Ti/Ta2O5-SnO2 electrodes. 2016. Diss.

709. OLEKSIIENKO, OLGA. Physico-chemical properties of sol-gel synthesized titanosilicates for the uptake of radionuclides from aqueous solutions. 2016. Diss.

710. PATALA, SAMULI. Advancing sustainability-oriented innovations in industrial markets. 2016. Diss.

711. KUORIKOSKI, TERO. Kohti resonoivaa urheilujohtamista – Tavoitteen muodostuminen urheilun kentässä. 2016. Diss.

712. LAHTELA, VILLE. Improving the properties of solid Scots pine (Pinus sylvestris) wood by using modification technology and agents. 2016. Diss.